

**BORANG PENGESAHAN  
LAPORAN AKHIR PENYELIDIKAN**

TAJUK PROJEK : CLASSIFICATION OF FILLED JOINT BASED ON THE  
CHARACTERISTICS OF ITS CONSTITUTIVE COMPONENTS

Saya MOHD FOR MOHD AMIN  
(HURUF BESAR)

Mengaku membenarkan **Laporan Akhir Penyelidikan** ini disimpan di Perpustakaan Universiti Teknologi Malaysia dengan syarat-syarat kegunaan seperti berikut :

1. Laporan Akhir Penyelidikan ini adalah hakmilik Universiti Teknologi Malaysia.
2. Perpustakaan Universiti Teknologi Malaysia dibenarkan membuat salinan untuk tujuan rujukan sahaja.
3. Perpustakaan dibenarkan membuat penjualan salinan Laporan Akhir Penyelidikan ini bagi kategori TIDAK TERHAD.
4. \* Sila tandakan (/)

- |                          |              |   |
|--------------------------|--------------|---|
| <input type="checkbox"/> | SULIT        | (Mengandungi maklumat yang berdarjah keselamatan atau Kepentingan Malaysia seperti yang termaktub di dalam AKTA RAHSIA RASMI 1972). |
| <input type="checkbox"/> | TERHAD       | (Mengandungi maklumat TERHAD yang telah ditentukan oleh Organisasi/badan di mana penyelidikan dijalankan).                          |
| <input type="checkbox"/> | TIDAK TERHAD |   |

TANDATANGAN KETUA PENYELIDIK

**MOHD. FOR BIN MOHD. AMIN**  
Pensyarah Kanan  
Jabatan Geoteknik & Pengangkutan  
Fakulti Kejuruteraan Awan  
Universiti Teknologi Malaysia



Nama & Cop Ketua Penyelidik

Tarikh : 26.02.2007

**CATATAN :** \*Jika Laporan Akhir Penyelidikan ini SULIT atau TERHAD, sila lampirkan surat daripada pihak berkuasa/organisasi berkenaan dengan menyatakan sekali sebab dan tempoh laporan ini perlu dikelaskan sebagai SULIT dan TERHAD.

**CLASSIFICATION OF FILLED JOINT BASED ON THE  
CHARACTERISTICS OF ITS CONSTITUTIVE COMPONENTS**

**(PENGKELASAN KEKAR BERINTI BERDASARKAN KEPADA SIFAT-  
SIFAT KOMPONEN UTAMANYA)**

**MOHD FOR MOHD AMIN  
EDY TONIZAM MOHAMMAD  
ASSOC. PROF. IR AZMAN BIN KASSIM  
ONG HENG YAU**

**PUSAT PENGURUSAN PENYELIDIKAN  
UNIVERSITI TEKNOLOGI MALAYSIA**

**2007**

**CLASSIFICATION OF FILLED JOINT BASED ON THE  
CHARACTERISTICS OF ITS CONSTITUTIVE COMPONENTS**

**(PENGKELASAN KEKAR BERINTI BERDASARKAN KEPADA SIFAT-  
SIFAT KOMPONEN UTAMANYA)**

**MOHD FOR MOHD AMIN  
EDY TONIZAM MOHAMMAD  
ASSOC. PROF. IR AZMAN BIN KASSIM  
ONG HENG YAU**

**RESEARCH VOTE NO:  
71825**

**Jabatan Geoteknik & Pengangkutan  
Fakulti Kejuruteraan Awam  
Universiti Teknologi Malaysia**

**2007**

To my beloved family

## CLASSIFICATION OF FILLED JOINT BASED ON THE CHARACTERISTICS OF ITS CONSTITUTIVE COMPONENTS

(Keywords: Filled joint, behaviour, components, field and laboratory assessments)

Filled joints in rock mass pose a number of constructional problems. When filled joints are reckoned to be critical to an engineering structure, their behaviours are often studied using expensive *in-situ* testing and complex full-scale physical modelling. This is because sampling of an undisturbed filled joint is almost impossible to undertake. As such, a means of anticipating the behaviour and characteristics of this critical geological discontinuity is important. One method to predict the behaviour of filled joint is through systematic classification based on its essential components, particularly those features that control the behaviour of the joint under shear and compressive load.

Exposed filled joints in granite rock in Lahat, Perak, have been selected for the field study. The field assessments indicate there are several components of filled joint that exhibit certain geological and mechanical characteristics which can be identified and assessed in the field and laboratory. For the infilling material, the essential features include *thickness*, *weathering grade* and *texture*. For the host joint blocks, the features include *texture* and *roughness* of the joint surface and *weathering degree* of the blocks. The weathering grade of the infill and joint blocks are geological characteristics that can be graded according to the standard classification system. The samples of infilling were further evaluated in the laboratory using index and characterisation tests like sieving, compression and shear tests.

This study has shown that there are several essential components of filled joint that can be used to predict its behaviour. These components can be easily characterised and evaluated in the field and laboratory. The characteristics of the infilling material and roughness of joint surface are among the features that control the behaviour of filled joint, and subsequently can be used as classification index for predicting the joint behaviour.

### Key researchers:

Mr. Mohd For bin Mohd Amin  
Mr. Edy Tonizam bin Mohammad  
Assoc. Prof. Ir Azman bin Kassim  
Ong Heng Yau

**E-mail :** mohdfor@yahoo.com  
**Tel. No. :** 07-5531726  
**Vote No. :** 71825

## **PENGGELASAN KEKAR BERINTI BERDASARKAN KEPADA SIFAT-SIFAT KOMPONEN UTAMANYA**

*(Katakunci: Kekar berinti, tingkahlaku, komponen, penilaian di tapak dan makmal)*

Kekar berinti yang wujud di dalam massa batuan boleh menimbulkan pelbagai masalah dalam bidang pembinaan. Jika kekar berinti diramalkan kritikal terhadap sesuatu struktur binaan, tingkahlaku kekar tersebut selalunya dikaji dengan menggunakan kaedah ujian di tapak dan model fizikal skala besar yang kompleks dan mahal. Ini kerana proses perolehan sampel kekar berinti yang tak cacat merupakan sesuatu yang amat sukar untuk dilaksanakan. Oleh yang demikian, satu kaedah bagi meramalkan tingkahlaku ketakseleran geologi yang kritikal ini amat penting diwujudkan. Pengkelasan secara sistematik bagi komponen-komponen utama kekar berinti merupa satu pendekatan yang sesuai bagi tujuan ini terutamanya, komponen yang mempengaruhi kelakuan kekar ini di bawah pengaruh beban ricih dan mampatan.

Beberapa singkapan kekar berinti yang wujud di dalam batuan granit di kawasan Lahat, Perak, telah dipilih untuk tujuan kajian di tapak. Penilaian di lapangan menunjukkan terdapat beberapa komponen kekar berinti yang memperlihatkan ciri-ciri geologi dan mekanikal tertentu yang boleh dikenalpasti dan dinilai di lapangan dan juga di makmal. Bagi bahan intinya, sifat-sifat yang berkaitan termasuk *ketebalan*, *gred perluluhawaan* dan *tekstur*. Bagi blok kekar pula, ciri penting termasuk *tekstur* dan *kekasaran* permukaan kekar dan *tahap perluluhawaan* blok tersebut. Gred perluluhawaan inti dan blok kekar dan adalah sifat-sifat geologi yang boleh digredkan mengikut sistem pengkelasan piawai. Sampel inti kekar yang diperolehi telah diuji secara lebih terperinci di makmal menggunakan ujikaji indeks dan pencirian seperti ujian ayakan, mampatan dan ricih.

Kajian ini menunjukkan wujud beberapa komponen kekar berinti yang boleh digunakan bagi meramalkan kelakuannya. Komponen-komponen in mudah untuk dicirikan dan dinilai di lapangan dan di makmal. Sifat-sifat bahan inti dan kekasaran permukaan kekar adalah antara komponen yang amat mempengaruhi kelakuan kekar berinti, dan seterusnya boleh digunakan sebagai indeks pengkelasan bagi meramalkan kelakuan kekar.

### **Penyelidik utama:**

En. Mohd For bin Mohd Amin  
En. Edy Tonizam bin Mohammad  
PM Ir Azman bin Kassim  
Ong Heng Yau

**E-mail :** mohdfor@yahoo.com  
**Tel. No. :** 07-5531726  
**Vot No. :** 71825

## TABLE OF CONTENTS

<b>CHAPTER</b>	<b>TITLE</b>	<b>PAGE</b>
	<b>TITLE</b>	i
	<b>DEDICATION</b>	ii
	<b>ABSTRACT</b>	iii
	<b>ABSTRAK</b>	iv
	<b>TABLE OF CONTENTS</b>	v
	<b>LIST OF TABLES</b>	viii
	<b>LIST OF FIGURES</b>	ix
	<b>LIST OF SYMBOLS</b>	xii
	<b>LIST OF APPENDICES</b>	xiv
<b>1</b>	<b>INTRODUCTION</b>	
	1.1 Introduction	1
	1.2 Background Problems	3
	1.3 Objectives of Study	3
	1.4 Significance of Study	4
	1.5 Scopes of Study	4
	1.6 Organisation of Thesis	5
<b>2</b>	<b>LITERATURE REVIEW</b>	
	2.1 Introduction	6
	2.2 Joint	7
	2.2.1 Filled Joints	9
	2.3 Filled Joint Elements	11
	2.3.1 Material of Infilling	11

2.3.2	Particle Shape of Infill Material	13
2.3.3	Thickness of Infilling	14
2.3.4	Particle Size Distribution	18
2.3.5	Surface Roughness	19
<b>3</b>	<b>RESEARCH METHODOLOGY</b>	
3.1	Introduction	22
3.2	Field Study	23
3.3	Sample Preparation	27
3.3.1	Infill	27
3.3.2	Artificial Joint Block	28
3.4	Preliminary Tests	28
3.4.1	Static Compression Test	29
3.4.2	Uniaxial Compression Test	30
3.4.3	Direct Shear Test on Infill Material	32
3.4.4	Direct Shear Test on Joint-Infill Boundary	33
3.5	Field and Laboratory Test Equipment	34
3.5.1	Uniaxial Compression Machine	35
<b>4</b>	<b>RESULT AND ANALYSIS</b>	
4.1	Introduction	36
4.2	Field Investigation	36
4.2.1	Schmidt Hammer Test	38
4.2.2	Joint Roughness Coefficient	39
4.3	Preliminary Tests	40
4.3.1	Particle Size Distribution and Specific Gravity	40
4.3.2	Static Compression Test	43
4.3.3	Uniaxial Compression Test	45
4.3.4	Direct Shear Test on Infill Material	53
4.3.5	Direct Shear Test on Joint-Infill Boundary	59



<b>5</b>	<b>CONCLUSIONS AND RECOMMENDATIONS</b>	
	5.1 Introduction	64
	5.2 Conclusions	65
	5.3 Recommendations	66
	<b>REFERENCES</b>	67
	<b>APPENDICES A-M</b>	75

**LIST OF TABLES**

<b>TABLE NO.</b>	<b>TITLE</b>	<b>PAGE</b>
2.1	Classification of joint filler by origin	10
4.1	JCS at different parts of joint system	38
4.2	Particle size and content of infill sample	41
4.3	Density of infill before and after static compression test	44
4.4	UCS and E Values of rock specimens	51
4.5	Settlement of infill sample at different stages	58
4.6	Shear characteristics of infill with and without preloading	58

## LIST OF APPENDICES

<b>APPENDIX</b>	<b>TITLE</b>	<b>PAGE</b>
A	Probable weathering stages of filled joint in granite	75
B	Comparison of uniaxial compressive and uniaxial tensile strengths of rocks	78
C	Corrections for reducing measured Schmidt hammer rebound (R) when the hammer is not used vertically downwards	79
D	Weathering grade and rock properties	80
E	Strength classification based on point load index; Unconfined compressive strength of the main rock types; Categorization and description of rock based on its uniaxial compressive strength	81
F	Data of Rebound hammer test	83
G	Calculation of surface roughness	84
H	Specific gravity of infill particles	89
I	Result of Static Compression Test	91
J	Data of preliminary test (direct shear test on preloaded infill material alone)	93
K	Data of preliminary test (direct shear test on non-preloaded infill material alone)	97
L	Data of preliminary test (direct shear test on smooth joint-infill boundary)	100
M	Data of preliminary test (direct shear test on rough joint-infill boundary)	102

## LIST OF FIGURES

<b>FIGURE NO.</b>	<b>TITLE</b>	<b>PAGE</b>
2.1	Layers and movement of grains of infill	15
2.2	Four categories of discontinuity filling thickness	16
2.3	Grain arrangement in	
	(a) coarse-grained sample	18
	(b) fine-Grained sample	18
2.4	Typical roughness profiles and suggested nomenclature	20
2.5	Condition at joint wall-infill interface for granular infill at	
	(a) rough joint surface, and (b) smooth joint surface	21
3.1	Site location map	24
3.2	Highly jointed granite outcrop selected for the field study	25
3.3	Filled-joint system, infill sandwiched between two joint blocks	25
3.4	Measuring of Joint Surface Roughness	26
3.5	(a) Concrete block with saw-toothed surface	28
	(b) Schematic diagram of saw-toothed surface	28
3.6	Schematic diagram of static compression test	30
3.7	Model of specimen tested In uniaxial compression test,	
	(a) Intact Rock, (b) Matched Joint, (c) Mis-matched Joint,	
	(d) Filled Joint (t = 10mm) and (e) Filled Joint (t = 20mm)	31
3.8	UCT test specimens	31
3.9	Direct shear test for the investigation of shear strength of joint-infill boundary for	
	(a) Smooth joint	34
	(b) Rough joint	34

3.10	MaTest 500 compression machine used in UCT	35
4.1	Filled joint system with no banding of weathering grade across the infill and joint blocks	37
4.2	Joint surface profiles (a) JRC = 14.1 and (b) JRC = 4.7	39
4.3	PSD curve of infill material	41
4.4	Infill sample divided according to the grain size	42
4.5	Compressibility vs. infill thickness graph	43
4.6	Compressibility vs. normal stress graph	44
4.7	Stress-strain relationship of intact rocks	46
4.8	Stress-strain relationship of matched-joints	46
4.9	Stress-strain relationship of mismatched-joints	47
4.10	Stress-strain relationship of filled joint (10mm infill)	49
4.11	Stress-strain relationship of filled joint (20mm infill)	50
4.12	Stress-strain relationship of different rock specimens	50
4.13	Particle size distribution of infill material after UCT	52
4.14	Shear stress versus displacement, for infill with preloading, under normal stress of	
	(a) 133 kPa	53
	(b) 264 kPa	54
4.15	Shear stress versus displacement, for infill without preloading, under normal stress of	
	(a) 133 kPa	55
	(b) 264 kPa	55
4.16	Shear stress versus displacement, for infill samples with and without preloading	56
4.17	Normal versus shear displacement, for infill sample with and without preloading	57
4.18	Shear stress versus displacement, for smooth soil-rock contact	59
4.19	Shear stress versus displacement, for rough soil-rock contact	60
4.20	Shear stress (at 10 mm shear displacement) versus normal shear stress, for smooth and rough joint-infill contact	61

4.21	Normal versus shear displacement, for shearing of different joint-infill boundaries	62
------	---	----

## LIST OF SYMBOLS

$\Delta_x$	-	Shear displacement
$\Delta_y$	-	Vertical displacement
$\sigma_p$	-	Shear stress
$\sigma_n$	-	Normal stress
$\sigma_c$	-	Unconfined compression strength
$\phi$	-	Basic friction angle
$\tau$	-	Peak shear strength
$\gamma$	-	Dry density of rock
$c$	-	Coefficient of cohesion
IA	-	Infill material alone, with normal stress of 133 kPa
IB	-	Infill material alone, with normal stress of 264 kPa
IC	-	Infill material alone, with normal stress of 396 kPa
JRC	-	Joint roughness coefficient
PSD	-	Particle size distribution
R	-	Rebound number
RUA	-	Rough unfilled joint, with normal stress of 133 kPa
RUB	-	Rough unfilled joint, with normal stress of 264 kPa
RUC	-	Rough unfilled joint, with normal stress of 396 kPa
RFA	-	Rough filled joint, with normal stress of 133 kPa
RFB	-	Rough filled joint, with normal stress of 264 kPa
RFC	-	Rough filled joint, with normal stress of 396 kPa
SFA	-	Smooth filled joint, with normal stress of 133 kPa
SFB	-	Smooth filled joint, with normal stress of 264 kPa
SFC	-	Smooth filled joint, with normal stress of 396 kPa
SUA	-	Smooth unfilled joint, with normal stress of 133 kPa

SUB	-	Smooth unfilled joint, with normal stress of 264 kPa
SUC	-	Smooth unfilled joint, with normal stress of 396 kPa
TFA	-	Smooth joint filled with very thin infill, with normal stress of 133 kPa
TFB	-	Smooth joint filled with very thin infill, with normal stress of 264 kPa
TFC	-	Smooth joint filled with very thin infill, with normal stress of 396 kPa
UCT	-	Uniaxial compression test
XIA	-	Non-preloaded infill material alone, with normal stress of 133 kPa
XIB	-	Non-preloaded infill material alone, with normal stress of 264 kPa



## **CHAPTER 1**

### **INTRODUCTION**

#### **1.1 Introduction**

Geological processes and tectonic movements tend to create various geological discontinuities in rock masses such as fault and joint. Due to the presence of these discontinuities, rock masses are often weak, anisotropic and inhomogeneous. Consequently, excavation work in a rock mass can be subjected to various problems, particularly in terms of stability. Among these discontinuities, joints are the common weakness planes in rock outcrops, particularly in intrusive igneous rock like granite.

In tropical countries, high temperature and rate of rainfall help to induce a desirable environment for continuous and intensive weathering of rock. Weathering can affect both the surface and interior part of a rock mass. Joints (secondary permeability) allow water and other weathering agents to penetrate into the rock. Upon weathering, the material of the joint surface is being disintegrated and decomposed to form a completely weathered (CW) material which is much weaker than the host rock. This leads to the accumulation of weak infill material in the joint aperture, or in other words, a completely weathered material is being “sandwiched” in between the unweathered joint blocks. Filling of a joint aperture can also occur by

*in-situ* deposition. It involves in-wash of CW surface materials into the originally open joint (in this case the infill material is not due to gradual weathering of the host rock). Both weathering of the joint surface and the *in-situ* deposition in the joint aperture are the processes that lead to the formation of the most critical geological discontinuity in rock, namely filled joint.

The presence of weathered material in joint aperture induces a high degree of inhomogeneity into this weakness plane and leads to the unique behaviours of filled joint. Normally, materials that fill the joint apertures are highly weathered rock of grade V (completely weathered rock) and grade VI (residual soils). The infilling material is often more compressible and crushable than intact rocks. The varying particle size, shape and mineral composition induce significant variations in the infill material. Together with the weathered joint surface, the nature of contact between the interfacing joint surfaces and the nature of the infill create a very complex deformational behaviour of filled joints as compared to unfilled (clean) joint.

Filled joint often exhibits high deformability and low shear strength when subjected to loading. These characteristics are unfavourable for any civil engineering constructions particularly when it involves excavation of rock mass. They may induce instability into excavated surfaces such as rock slopes and tunnel walls. Therefore, the properties and behaviours of filled joints must be understood and appropriately interpreted to ensure adequate information is available for the design and construction of structure in rock mass that exhibits filled joints. In summary, filled joint is not only a critical discontinuity in rock, but also a complex geological structure to be modeled and studied under laboratory conditions.

## 1.2 Problem Background

Being the most critical discontinuity in rock masses, filled joints display behaviour that are critical to engineering constructions. Specifically, its deformability, compressibility and shear behaviours are thought to be detrimental to the stability of any excavation in rock. In addition, each constitutive component of filled joint, such as joint surface, infill material and joint blocks, displays its own discrete characteristics. Each characteristic of the constitutive component contributes to the behaviours of filled joint, interactively. Therefore, sufficient knowledge on the characteristics of each relevant component is essential to understand the overall behaviours of filled joint under loading.

Due to its uniqueness and complexity, detailed study must be carried out on this critical discontinuity. *In-situ* testing, full-scale laboratory modeling and computer simulation are often used to study verify its behaviour. However, these methods are relatively expensive and complex to undertake. Moreover, sampling of undisturbed filled joint for laboratory testing is almost impossible to be conducted. Therefore, an appropriate method in interpreting the behaviour and criticality of filled joint is essential. This method should be suitable to characterise the filled joint, specifically its characteristics that are relevant in predicting its behaviour. These characteristics must be those properties that can be easily measured and evaluated using relatively simple laboratory and field tests.

## 1.3 Objectives of Study

This study is undertaken in order to achieve the following main objectives:

1. To identify and to select the constitutive components of filled joint which control its behaviour under loading.

2. To assess the relevant characteristics of the selected components and to evaluate their degree of significance in controlling the joint behaviour.
3. To use the selected components and their respective characteristics as parameters for classifying and for predicting the behaviour of filled joint.

#### **1.4 Significance of Study**

The behaviour of filled joint specifically under shear and compressive load is significantly affected by its constitutive components, which include type of infill, surface of joint blocks and thickness of infill. By verifying the interacting effect between these components, a general behaviour of filled joint can be established. The general behaviour may serve as guidelines in predicting and evaluating the level of criticality of filled joint on any excavated surface in rock.

#### **1.5 Scopes of Study**

The scopes of this study, among others, cover the following aspects:

1. A filled joint resulting from *in-situ* deposition and with granular, granite residual soils as infilling.
2. Characteristics of filled joint components selected for study are thickness of the infill, type of infill and roughness of joint surface.

3. Laboratory tests were carried out on model of filled joint consisting of cast concrete as joint block (flat surface and saw-toothed surface) and granular granite residual soil as infill material.
4. Model filled joint were subjected to compressive and shear load to obtain the general deformation behaviour of the respective components.

## **1.6 Organisation of Report**

This report consists of five chapters. Introduction, problem background, objectives and scopes of study and its significance are outlined in Chapter 1. Chapter 2 comprises some important theories and past researches about filled joint. Chapter 3 focuses on the methodology of this research, which includes field study and laboratory assessments. The test results and analysis of data are discussed in Chapter 4. Finally, Chapter 5 summarises the research findings and recommendations for further study.

## **CHAPTER 2**

### **LITERATURE REVIEW**

#### **2.1 Introduction**

Rock mass is an inhomogeneous and anisotropic material. It is formed by intact rock substance and very often disrupted by different types of discontinuities such as joints, bedding planes, cleavage and fractures, formed either by tectonic deformation, sedimentation or weathering process (Wan Mohd Kamil, 2002). The strength of rock mass does not normally depend on its material characteristics, but on the strength of the discontinuities in it. Unfortunately, these discontinuities are often weaker than the rock. Therefore, the strength and characteristics of discontinuities must be studied to interpret the stability of the rock mass involved. Among that, filled joints are likely to be the weakest elements of any rock mass in which they occur and to exert a significant influence of its behaviour (de Toledo and de Freitas, 1993).

In the field of rock engineering, certain important characteristics of filled joints can be interpreted through laboratory tests on simulated and artificial joints model. Many elements of a filled joint can be analyzed to estimate its behaviours under different

conditions. Throughout the years, quite a number of researches have been carried out to study various characteristics of filled joints, they include authors like de Toledo and de Freitas (1993 and 1995), Phien-Wej *et al.* (1990), Pereira (1990), Papaliangas *et al.* (1993) and Ladanyi and Archambault (1977).

The outcomes of these studies have contributed significantly towards the understanding of the behaviour and characteristics of filled joint, particularly the effect of this discrete discontinuity on the deformational behaviour of rock mass. This understanding is vital in assessing and predicting potential slope failure or rock sliding, which is mostly related to planar weaknesses, like filled joint (Waltham, 2002).

## **2.2 Joint**

Price (1966) described joints as cracks and fractures in rock along which there has been extremely little or no movement. In geological terms, the word “joint” is frequently treated as an omnibus term and has been used to describe structures that vary widely in character. They have occurred and are present within all types of rock (Bell, 1983). Hence, joints are often encountered during excavation of any rock masses.

Since earlier days, the formation and origin of joints have attracted many researchers' interest. Many types of forces have been advocated to account for the formation of joints, which include torsion, compression and shear, tension and also fatigue phenomenon. Price (1966) suggested that the majority of joints are post-compressional structures, formed as a result of the dissipation of residual stress after folding has occurred.

Rock masses are continually affected and modified by weathering and erosion.

Mechanical weathering, or disintegration, breaks down rock mass into smaller blocks by physical interaction (friction between rock and water, wind, raindrop, etc.) and the action of temperature.

Beavis (1992) explained that joints develop through different processes in different rock masses. Igneous rock is formed when the hot lava (from the inner of earth) cools down and solidifies (when it flows to the outer surface of earth). However, hot lava continues to flow upwards to the surface. The up-pushing lava tends to crack the rock solid above and creates fracture or joints in it. Joints may also develop in igneous rock due to the shrinkage of rock mass when magma cools down. In sedimentary rocks, joints develop when the rocks shrink, due to the drying process of rocks. In summary, joint, as other types of fractures, are formed as a result of different processes, such as mineralization, metamorphism, crushing, brecciation, mylonitization, metasomatic replacement, etc. (Chernyshev and Dearman, 1991).

Ladanyi and Archambault (1977) categorized joints into four classes to ease studies of joints:

- i) Clean
- ii) Coated
- iii) Filled with clay-like infilling
- iv) Filled with sand-like infilling



### 2.2.1 Filled Joints

Filled joints possess very unique characteristics. However, some of them resemble the properties of an unfilled joint or fracture. It is believed that filled joints develop gradually from unfilled joints, so as to maintain their certain behaviours and characteristics.

Generally, there are two types filled joints based on the origin of the infill. Infill within the apertures of joints may result from continuous weathering of joint surface, or *in-situ* deposition of ground surface materials from the nearby area.

Mohd Amin *et al.* (2000) briefly described the formation of filled joint in granite through continuous weathering (see Appendix A). Joints or fractures are discontinuities (weak plane) that are permeable. Water will penetrate through joint surface, and cause weathering to happen. The least stable feldspars at joint surfaces will firstly be broken down during weathering. Further weathering can be noticed by the penetration of discolouration inwards from the joint surfaces. Hydrolysis of feldspars and mica eventually increases the volume of the rock material. Expansion of joint block tends to push and press the opposite joint surfaces together. When compressed, the joint surfaces will crack and break down into small pieces. Consequently, joint surfaces open up and fresh rock (initially deep inside the joint) exposed, and subjected to continuous weathering. The torn pieces from the weathered joint surfaces, form the infilling between the joint apertures. As they are of smaller pieces, they possess greater effective surface for weathering. Therefore, the infillings of a filled joint is often of highly weathered materials (grade V or residual soil).

Beavis (1992) explained that weathering and the releasing of load above rock due to erosion would lead to the forming of an opened joint. These joint openings, might be clean without infillings, or filled with secondary minerals. These minerals could have been caused by hydrothermal changes or transportation, or weathering. Wide opened joints near to the surface of earth may contain infillings deposited from the earth surface. Chernyshev and Dearman (1991) drew up a classification chart of joint filler, based on its mode of deposition (see Table 2.1)

**Table 2.1:** Classification of joint filler by origin (after Chernyshev and Dearman, 1991).

<b>Deposition of fracture filler</b>	<b>Description of filler based on material</b>	<b>Composition and properties of fracture filler</b>
Chemical or physico-chemical	Magmatic Hydrothermal and pneumatolytic Hypergene Artificial	Rock healing fracture solidly Rock healing fracture Colloidal formations which cause fracture narrowing or healing Chemical grout infilling fracture
Mechanical	Tectonic  Hypergene  Artificial	Mylonite, fault breccia. Compact, impervious, low-strength, slightly compressed Clastic or clay, loose rocks. Impervious, low-strength, compressed Cement grout infilling fracture
Organic	Phytogenic  Zoogenic	Plant roots, rotting residues. Permeable medium, facilitates weathering Organic residues and rotting products washed into fractures. Weakens rock mass and facilitates weathering

## 2.3 Filled Joint Elements

Filled joints pose very unique and complex behaviours due to their components are made up of materials of different properties. There are numbers of components having significant influence on their characteristics. These components are to be studied individually to enable the interpretation of their interactive effect on a filled joint's behaviours to be made. Over the years, numbers of studies on filled joints have been carried out. Generally, certain joint elements have been recognized as having significant influence on joint behaviours, such as the material of infillings, the thickness of infillings and the contact condition between joint block and infillings. Changes in these elements directly lead to alteration of joint properties.

### 2.3.1 Material of Infilling

In filled joint, the physical and mineralogical properties of the material separating the joint walls are the primary concern in determining its shear strength and deformational characteristics. Filling materials vary greatly in their mechanical characteristics, from very soft to very hard and strong (Franklin and Dusseault, 1989).

Tulinov and Molokov (1971) defined five types of filling material according to the genesis:

- i) Loose material of tectonic crushed zones
- ii) Products of decompression and weathering of joint walls
- iii) Soils of the shear zones of rock slides

- iv) Filling material of karst cavities, which has been formed by leaching carbonaceous rocks and then shifted by the ground water flow
- v) Filling material of joints and cavities brought from the surface; or it may be of a mixed origin

Brekke and Howard (1972), on the other hand, distinguished seven major groups of joints / infilling materials according to their strength:

- i) Healed joints
- ii) Clean discontinuities
- iii) Calcite fillings
- iv) Coatings / fillings with chlorite, talc and graphite
- v) Inactive clay
- vi) Swelling clay
- vii) Material that has been altered to a more cohesionless material (sand-like)

The main difference between sand and clay is their permeability. Clay is considered soil of very low or non-permeability while sand is a highly permeable soil. The low permeability increases the effect of pore water pressure on the strength of soils. In low permeable soil, water is trapped inside the pores when the soil is compacted. Contrary, in highly permeable soil, like sand, pore water is drained out of soil immediately once the soil is loaded and does not influence to the strength of sand. Cheng and Evett (1987) described that, since the shear strength of most cohesionless soils is resulted from the interlocking between grains, values of friction angle differ little whether the soil is wet or dry. This clearly explains that moisture content display very small effect on the shear strength of cohesionless soil.

Mohd Amin and Awang (2002) carried out uniaxial compression test on modeled filled joints and found that a significant reduction in joint stiffness and Young's modulus (about 20 times smaller) may occur when weak material, like CW granite, is present in joint aperture. This is due to the high axial-strain and low Young's modulus exhibited by the infill material. The series of tests conducted strongly indicated the effect of infilling on the compressibility of joint.

### **2.3.2 Particle Shape of Infill Material**

Particle shape has a pronounced effect on properties of soil, such as, void ratio, compressibility, crushability, etc. Varying particle shapes can lead to drastically different engineering properties even on granular soils at the same relative density (Holubec and D'Appolonia, 1973).

Generally, particle shape is defined by its angularity/roundness and sphericity. Sphericity is the ratio of the surface area of a sphere having the same volume as the particle to the surface area of the particle, while angularity is a measure of the curvature of the corners to the average curvature of the particle (Holubec and D'Appolonia, 1973). Judging from the aspect of angularity, particle shape can be divided into five main categories, which are angular, sub-angular, sub-rounded, rounded and well rounded (Franklin and Dusseault, 1989).

Holubec and D'Appolonia (1973) studied the effect of particle shape on the engineering properties of granular soils. With the increase in particle angularity, the maximum and minimum void ratio of a soil is found to be increasing. The shear strength

or the friction angle is found to be greater for soils with more angular particles (also proven by Koerner, 1970). It is because the angularity provides interlocking effect between grains, thus increasing the resistance to shear. Whenever a grain is considered to be a polygon of a finite number of sides (high angularity), the concept of rolling friction is no more valid and is to be replaced by overturning friction (Pereira, 1990). Besides, the more angular the particles are, the greater the failure strain for a given relative density will be. Tests carried out showed that crushed stone with angular particles has greater elastic and permanent deformations than crushed gravel composed of rounded particles (Haynes, 1966; Dunlap, 1966; Holubec, 1969). Particle angularity is also proven to contribute to the resistance to the dynamic penetration of soils. However, angular particles are found to be more crushable than the spherical grains (Feda, 2002).

### **2.3.3 Thickness of Infilling**

Thickness of infilling layer has significant influence on filled joint's strength. The range of infill thickness with regard to the particle size limits the type of movement of the filler particles. Pereira (1990) studied the movement of grains in a filler of thickness twice greater than the grains size (see Figure 2.1). When sheared, grains with contact to the flat and planar joint surface tend to roll. However, grains on the other side may block the rolling motion and force it into sliding motion. In the middle of infill layer (soil-to-soil contact), each grain moves over one or more grains to occupy the voids next to them.

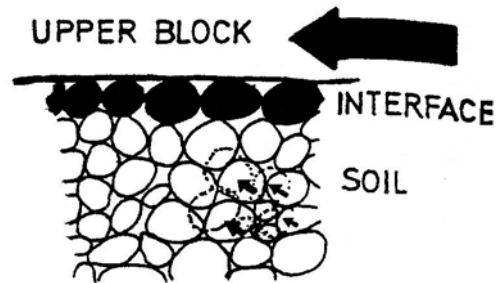


**Figure 2.1:** Layers and movement of grains of infill (after Pereira, 1990)

At the same time, it can be expected that when the filler is a-grain-thick, contact of grains to flat surface on both sides allow a rolling motion to take place, imposing only a low rolling friction rather than the high sliding friction.

Barton (1974) idealized four hypothetical thickness of clay filling in a rough, undulating joint (Figure 2.2). The shear characteristics of these filled joints can be briefly described as below:

- A) Almost immediate rock/rock asperity contact. Shear strength will be very little different from the unfilled strength because the rock/rock contact area at peak strength is always small. Dilation due to rock/rock contact will cause negative pore pressures to be developed in filling if shearing rate is fast.
- B) Similar to A, but a larger displacement is required to reach peak shear strength. Reduced dilation reduces tendency for negative pore pressures.
- C) No rock/rock contact occurs anywhere, but there will be a build up of stress in the filling where the adjacent rock asperities come closer together. Greater shear strength obtained if shearing rate is slow. Low shearing rate allows drainage to

occur, avoiding the increase in pore pressure that can reduce the effective stress on the filling.

- D) The influence of the rock walls will disappear, as the infillings are several times thicker than the asperity amplitude. If the filling is uniformly graded and mostly clay or silt, the shear strength behaviour can be estimated by basic soil mechanics principles.

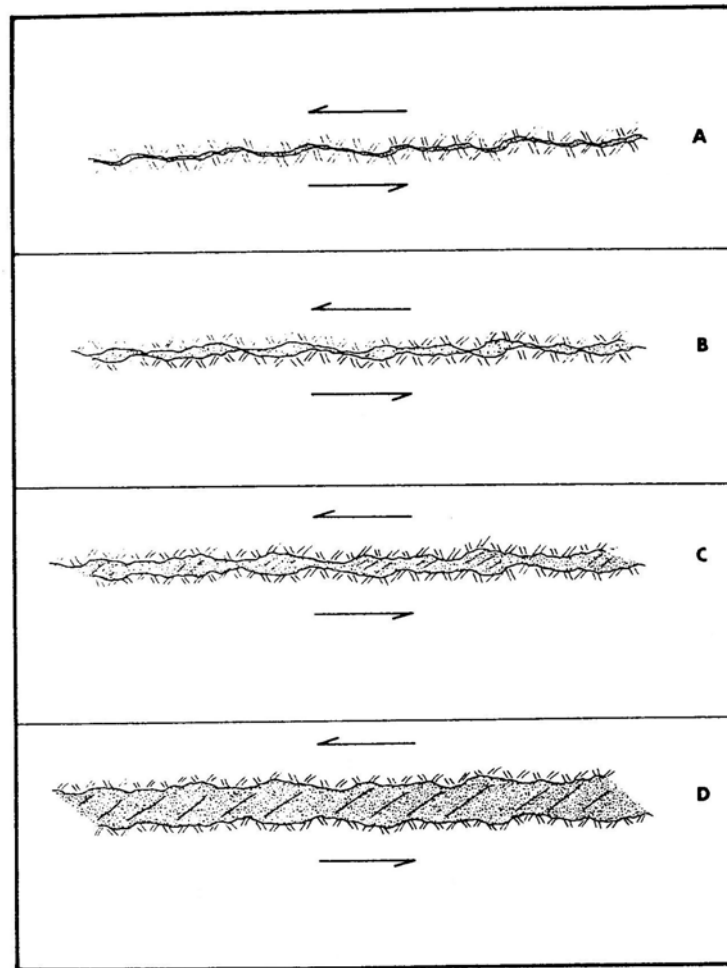


**Figure 2.2:** Four categories of discontinuity filling thickness (after Barton, 1974)



Over the years, many researchers have done their studies on the effect of infill thickness to the strength of the joint systems. Majority of them have shown that when the infill layer is thicker, the joint system is weaker. Aora and Trivedi (1992) found out that for filled joint with thicker infilling, its uniaxial compressive strength is relatively smaller than the unfilled one. Through triaxial test on filled joint, Sinha and Singh (2000) proved the weakening of joint system by the increasing infill thickness.

Lama (1978) on the other hand, analyzed the shear strength of rough joint with clayey materials, by Regression Method. Likewise, he proved that when the thickness of infill increases, the shear strength of the joint system decreases. Adding to that, his study suggested that the minimum shear strength of the joint system is of the filler alone. This means, when the infill is very thick, the shear strength of joint is equal to the shear strength of the filling material alone. Phien-Wej et al. (1990, 1991) supported this argument by proving that when the thickness of clay layer in filled joint approaches twice of the roughness amplitude or asperities of the joint surface, the shear strength of the joint system will reach its minimum, which is of the filler alone. However, for a flat planar joint filled with granular material, its shear strength is similar to the shear strength of the filler alone at any infill thickness.

However, there are other authors who postulated a different and extended interpretation. For example, Papaliangas *et al.* (1990) advocated that the infill/rock wall interface might have less shear resistance compared to the infill material, highlighting the probability that the shear strength of the filled joint might be lower than the shear strength of the infill material alone. Adding to it, they found that when the infill thickness increases, greater shear displacement is to be achieved in order to reach the peak shear strength.

### 2.3.4 Particle Size Distribution

Particle size distribution (PSD) is the content of grain of different sizes in a soil sample. It is an important parameter for classifying granular and relative coarse soil sample. It describes soil sample physically, from which, subsequently, the physical and mechanical behaviour of the sample can be interpreted.

Generally, potential crushing of mineral grain increases with the grain size (Hardin, 1985; Ong, 2000). Contact area between coarser grains is smaller, compared to finer grain (see Figure 2.3). Therefore, when loaded or stressed, the effective stress on each grain is much larger, resulting in greater crushing of grains. Fedra (1971) proved that poorly graded sample with high content of voids is more crushable than the well graded sample.

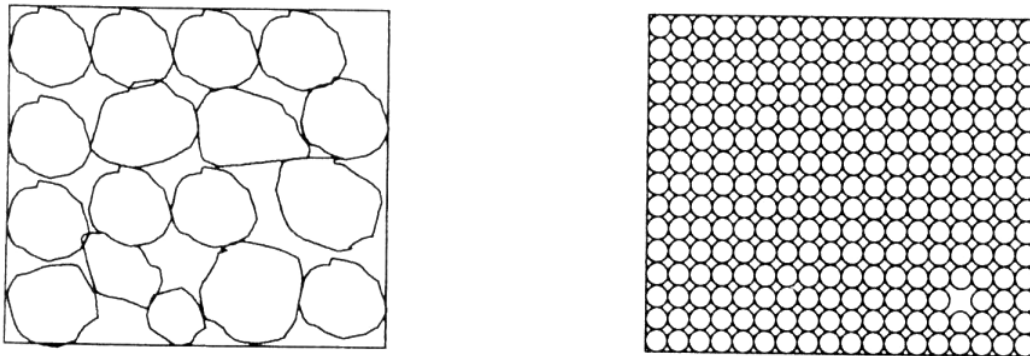


**Figure 2.3:** Grain arrangement in (a) coarse-grained sample (b) fine-grained sample (After Ong, 2000)

Farmer and Attewell (1973) proved that, apart from the crushability, compressibility of a soil sample also increases with its grain size. The presence of large amount of voids in coarse-grained sample allows more particle rearrangement to take

place. Compression comes mostly from the rearrangement of grain particles to fill the voids within.

### **2.3.5 Surface Roughness**

Surface roughness is a measure of the inherent surface unevenness and waviness of the discontinuity relative to its mean plane (Brady and Brown, 1985). It is a major factor determining the shear strength of a joint. The nature of the opposing joint surfaces influences the behaviour of rock mass as the smoother they are, the easier movement can take place along them (Bell, 1983).

Figure 2.4 shows the typical joint roughness profiles and nomenclature suggested by Barton (1978). It is recognized that the shear strength generated from the joint surface decreases from the upper roughness to the lower one.

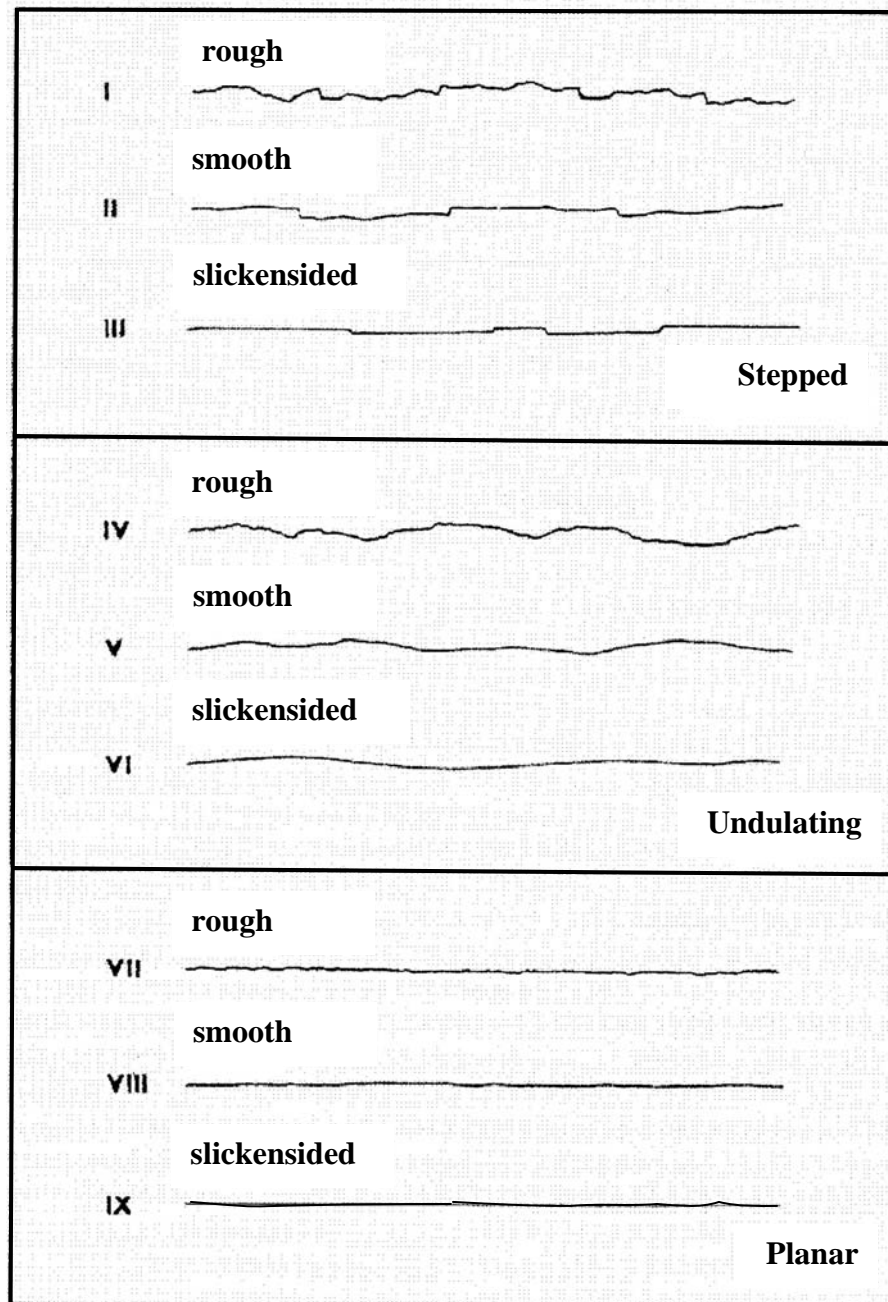


**Figure 2.4:** Typical roughness profiles and suggested nomenclature (after Barton, 1978)

In filled joint, the effect of surface roughness to the shear strength is reduced by the presence of infill material. However, when the infill thickness is within the interfering zone, joint surface roughness still contributes significantly to the joint shear strength.

The movement of infill grains at the interface layer is greatly influenced by the boundary effect (the infill-joint wall contact condition). The boundary effect is even more significant on granular infill. With reference to Figure 2.5(a), if the joint surface is rougher than the infill grain, it will hold the particles to position. Failure of joint will happen only if the stress applied overcomes the sliding friction of the infill. However, on a smooth joint surface, infill grains are not retained from movement. Infill particles are allowed to rotate for particles rearrangement to take place. A much lower resistance is to be overcome for grains to rotate than to slide. Therefore, the shear strength of a smooth filled joint is relatively low, resulted by the rolling friction at the infill-wall interface rather than sliding friction (Pereira, 1990 and de Toledo and de Freitas, 1993).

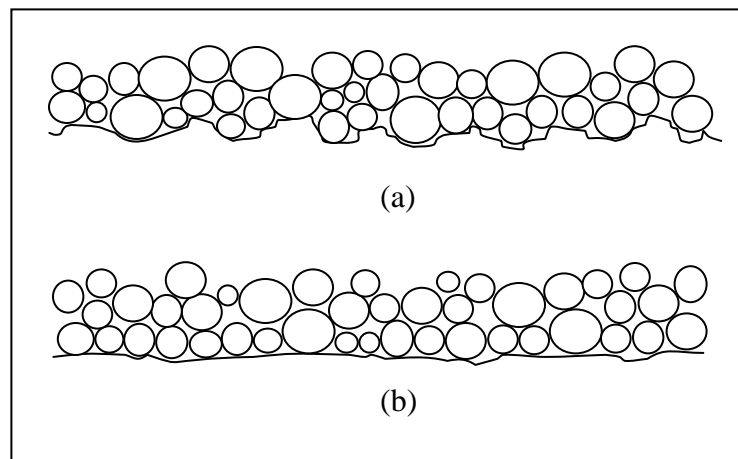


**Figure 2.5:** Condition at joint wall-infill interface for granular infill at (a) rough joint surface, and (b) smooth joint surface (after de Toledo and de Freitas, 1993)

## CHAPTER 3

### RESEARCH METHODOLOGY

#### 3.1 Introduction

This chapter highlights the various field study and preliminary laboratory tests in order to obtain a representative physical model of filled joint to be used in the main testing program. Actual conditions of filled joint in the field were observed and certain properties of filled joint were tested *in-situ*. A number of physical tests on the infill material were also carried out in the lab mainly to understand its characteristic before being modeled in the main tests. The properties of filled joint, which could not be assessed in the field, were accordingly simulated and modeled in the laboratory based on field data. The main testing programme carried out in laboratory was direct shear test. A large shear box apparatus was designed and used to shear the joint specimen up to 25 mm. Different joint surface textures, infill thickness, and normal stress were modeled on artificial filled joint model. The shear strength and vertical movement of joint during shear were studied.

### 3.2 Field Study

Field study was carried out on an outcrop of filled joint in granite rock. The site is located at Lahat, along Ipoh-Lumut trunk road, about 10 km south west of Ipoh (see Figure 3.1 and Figure 3.2). This filled joint was resulted by the in-situ deposition of surface material into the joint apertures. The infill material comprised of mainly decomposed weathered granite (see Section 2.4).

The relevant components of filled joint that contribute to its behaviours were identified and accordingly evaluated using index test and visual assessment (see Figure 3.3). These components included infill thickness, joint surface roughness, weathering condition of joint, joint surface hardness. Rebound number (Schmidt Hammer Test) was taken at different parts of the joint block (i.e. fresh rock, weathered rock and surfaces of joint apertures). The rebound numbers obtained were corrected according to the direction of Schmidt hammer when in use, as suggested by Brown (1981) (see Appendix C). The unconfined compression strength (UCS) of rock surface was then calculated by using Equation 3.1 (Miller 1965).

$$\log_{10}(\sigma_c) = 0.00088\gamma R + 1.01 \quad \dots\dots(3.1)$$

- where  $(\sigma_c)$  = Unconfined compression strength of surface ( $\text{MN/m}^2$ )  
 $\gamma$  = Dry density of rock ( $\text{kN/m}^3$ ) (26 for granite) (Daly, *et al.*, 1966; Waltham, 2002)  
 R = Rebound number

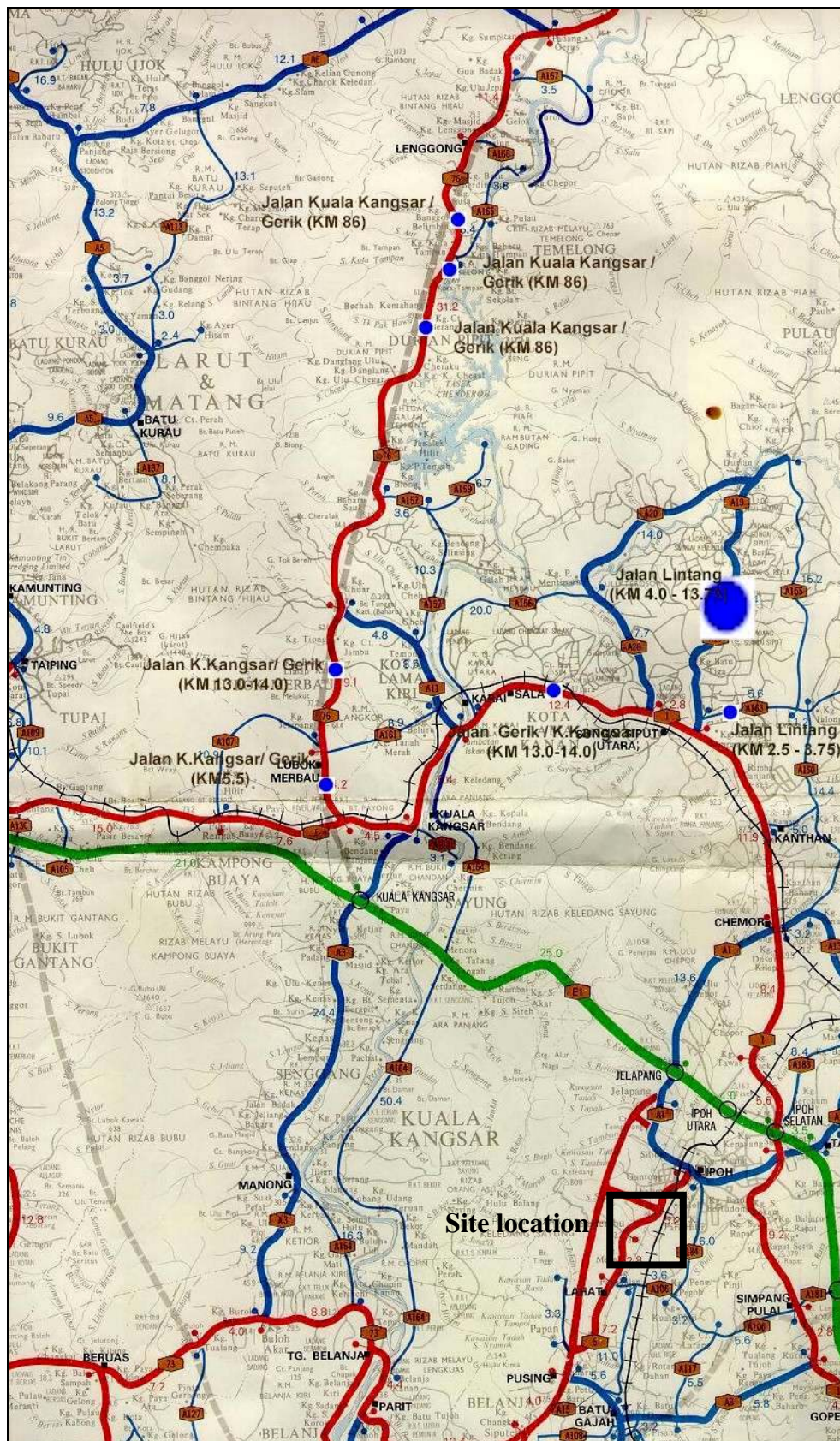
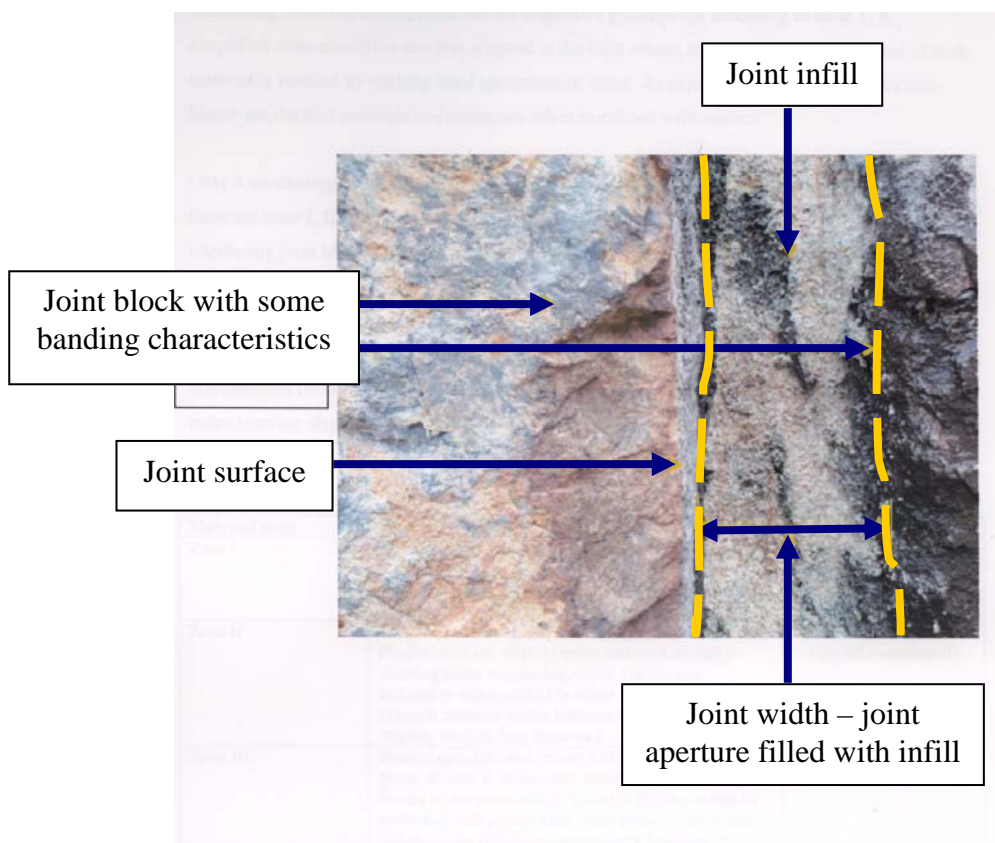


Figure 3.1: Site location map





**Figure 3.2:** Highly jointed granite outcrop selected for the field study



**Figure 3.3:** Filled-joint system, infill sandwiched between two joint blocks

Basic concept of Franklin and Dusseault (1989) was modified and adopted in measuring *in-situ* Joint Roughness Coefficient (JRC) of the filled joint. A straightedge steel ruler (100 cm length) was placed on the joint surface and photos were taken with the ruler, joint surface and the shadow of ruler on joint surface clearly shown (see Figure 3.4). As the photos were taken in the afternoon, the shadow of ruler on the joint surface reflects the exact surface roughness. From the photo, the shadow of ruler on joint was traced onto graph paper.



**Figure 3.4:** Measuring of JRC

The Centre Line Average (CLA) method by Tse and Cruden (1979) was adopted in calculating the joint roughness. The edge of ruler was taken as a reference plane to measure the asperities amplitude. The central plane of the asperities was determined and relative asperities heights relative to the centerline were measured. Equation 3.2 and 3.3 were used to calculate the JRC.

$$\begin{aligned}
 CLA &= \frac{1}{L} \int_{x=0}^{x=L} |y| dx \\
 &\approx \frac{1}{N} \sum_{j=1}^N |y_j| \quad (y \text{ in cm}) \quad \dots(3.2)
 \end{aligned}$$

$$\text{JRC} = 2.76 + 78.87 \text{ CLA} \quad \dots(3.3)$$

The surface profile (JRC) and joint properties (JCS) obtained from *in-situ* investigation were discussed in detail in Section 4.2.1 and 4.2.2. These results were taken in account in the design and modeling of the filled joint in laboratory assessments.

### **3.3 Sample Preparation**

#### **3.3.1 Infill**

Samples of infill material were scratched out of the filled joint and packed into plastic bags. They were then oven-dried overnight. Foreign substances, such as grass roots were removed from the sample. Fine particles that cling on to larger particles were loosened to minimized amalgamation effect. This was done manually without using any machine or hammer, to prevent potential crushing of the grains. These samples were then sieved to obtain its particle size distribution (PSD), according to BS1377: Part 2 (1990). The entire infill sample tested in laboratory test was reconstituted according to this PSD obtained (shown in Figure 4.3). Apart from PSD, the specific gravity of the infill particle was also investigated.

The details of the PSD and specific gravity of infill material are discussed in Section 4.3.1.

### 3.3.2 Artificial Joint Block

Artificial joint blocks were made from Grade 60 concrete. The mix design of the cast concrete was cement: sand: coarse aggregate (20 mm maximum size) of 1: 1.2: 3; water to cement ratio was 0.34. To increase workability, superplasticizer was added into the cement mix (about 1% of cement). The mix was design in such a way as to provide controllable and reproducible joint block with more regular and uniform surface roughness. To obtain surfaces similar to joint surface in rock, Two types of surface textures were prepared and these were flat and planar surface representing smooth-surfaced joint, and saw-toothed surface representing rough joint surface (see Figure 3.5).

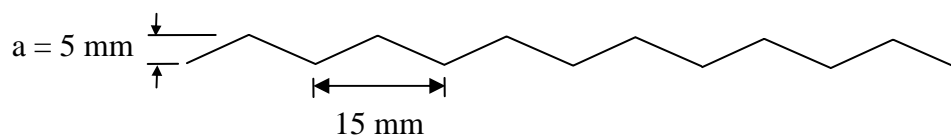


**Figure 3.5:** Schematic diagram of saw-toothed surface

### 3.4 Preliminary Tests

A number of preliminary tests were carried out prior to the main testing programme. They were undertaken to verify the basic behaviours of the infill material that may have interactive effects on the behaviour of the model filled joint. The information obtained from these tests served as guidelines in designing the methods and procedures used in the main testing programmes. Most importantly, this information was essential in designing and fabricating the large shear box

equipment. For example, the amount of dilation and compression that can be expected when the model joint was sheared under specific normal load.

### **3.4.1 Static Compression Test**

This was a non-conventional test where certain procedures were adopted to achieve the required result. The test was termed as static compression test and was carried out to study the compressibility and deformability of infilling material under static load. The effects of infill thickness and magnitude of applied stress were compared against the compressibility of the infill.

Reconstitutive infill samples of certain weight (300, 400 and 500 g) were filled into the compression mould under loose condition (see schematic diagram in Figure 3.6). The thickness of the infill in the mould was measured and the initial infill density was calculated. The relationship between infill density and thickness was investigated. Static normal load (109 kPa, 132 kPa and 155 kPa) was then applied onto the infill material for 24 hours. The settlement of infill was measured. The void ratio of the tested sample (before and after test) was calculated. The reduction of void ratio throughout the test was calculated as the compressibility of the infill.

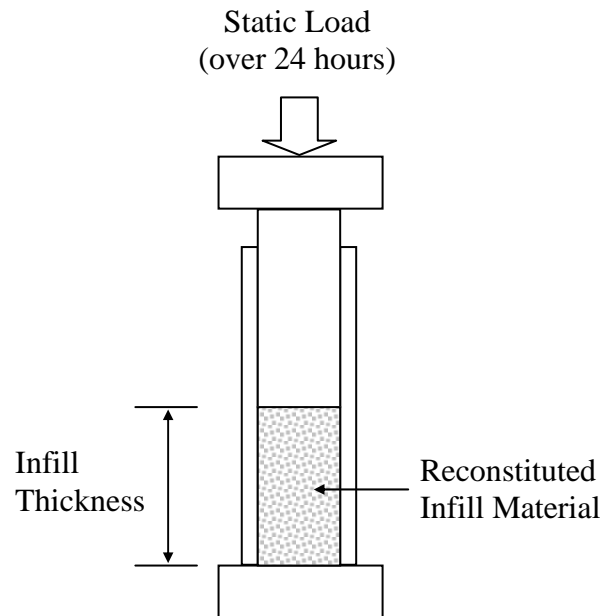


**Figure 3.6:** Schematic diagram of static compression test

### 3.4.2 Uniaxial Compression Test

Uniaxial compression tests (UCT) were carried out on joint model of smaller scale. This test was to verify the effect of discontinuity plane (i.e. joint) on the behaviour of intact rock, as mentioned by (Goodman, 1974). The main characteristics observed in this test were the amount of compression displayed by various types of joint. Data on Uniaxial Compressive Strength (UCS) and the Young's Modulus (E) of joint models were collected.

Normal compressive load was applied at a constant increasing rate (1.5 kN/sec) onto specimen. The specimens tested consisted of intact rock, matched rock joint, mis-matched rock joint and filled joint model (see Figure 3.7 and Figure 3.8). For this investigation, granite core samples of 52 mm diameter (D) were used. The core samples were sawn into two and rejoined, to create an artificial smooth, matched joint. The smooth surfaces of joint blocks were grinded to become rough

and undulated, which were then paired into mis-matched joints. The overall height (H) of the specimen was limited to 104 mm to maintain an H/D ratio of 2.

The infill material used was the reconstitutive sample as discussed in previous section. Infill material was filled in between of joint blocks with smooth surfaces to simulate filled joints.

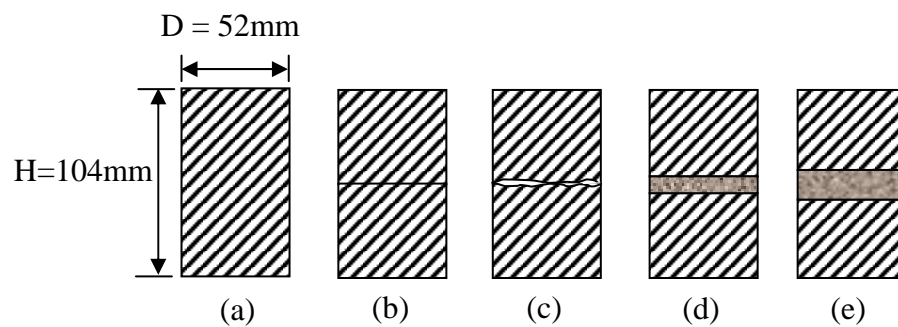


**Figure 3.7:** Model of specimen tested in uniaxial compression test, (a) Intact rock, (b) Matched joint, (c) Mis-matched joint, (d) Filled joint ( $t = 10$  mm) and (e) Filled joint ( $t = 20$  mm)

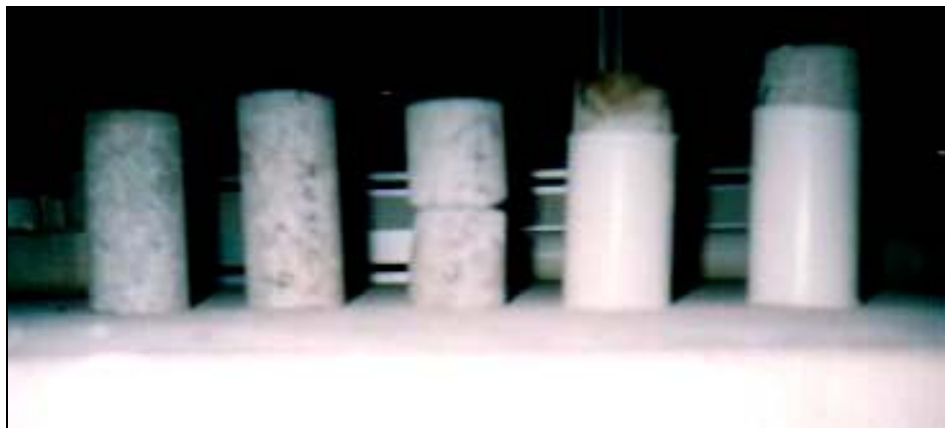


**Figure 3.8:** UCT test specimens

Continuous readings of normal load and vertical displacement were recorded throughout the test, till the failure of the specimen. The stress-strain curve for each specimen tested was plotted to obtain its E and UCS. These results were compared in order to verify the effect of clean joint and infilling to the properties of intact rock.

### 3.4.3 Direct Shear Test on Infill Material

The shear behaviour of the infill material alone was investigated using a small-scale direct shear test apparatus. The test was undertaken by filling the shear box (dimension 100 x 100 x 40 mm) with reconstitutive sample of infill material (see Section 3.3.1) under loose condition.

Two types of loading conditions were imposed on the infill prior to shearing, and these were with preloading and without preloading. In the shear tests with preloading, the sample was subjected to a normal compressive load ( $\sigma_{pre}$ ) of 133 kPa for duration of 30 minutes before shearing. In the shear tests without preloading, shearing was undertaken immediately upon placement of sample into the shear box. These series of loading conditions were undertaken essentially to verify the effect of preloading on the shear behaviour of the infill

For both types loading conditions, direct shear test was conducted at a shearing rate of 0.6 mm/sec as suggested by Brown (1981). Two levels of normal stress were applied during shearing i.e.  $\sigma_{n1} = 133$  kPa and  $\sigma_{n2} = 264$  kPa to simulate granite slope of 5 and 10 m height. Measurement of both vertical and horizontal displacements and the corresponding shear stress were recorded for analysis.



#### **3.4.4 Direct Shear Test on Joint-Infill Boundary**

Small-scale direct shear tests were also carried out to investigate the shearing behaviour between the infill material and the joint block, particularly at the interface between the joint and the infill (joint-infill boundary).

Reconstitutive infill sample and smaller joint blocks (cross-sectional area of 100 x 100 mm) of similar material and surface profiles as mentioned in Section 3.3.2 were used in this series of tests. Figure 3.9 (a) and (b) show the arrangement of concrete block and infill material in the shear box. The joint-infill boundary was arranged as close to the shear plane as possible.

Prior to shearing, the specimen was preloaded with normal stress of 133 kPa for 30 minutes. This was to ensure a more uniform distribution of density within the infill layer, and also a more uniform contact between the infill grain and the joint block surface. Two normal stresses as in Section 3.4.3 were applied during shearing (shear rate = 0.6 mm/sec).

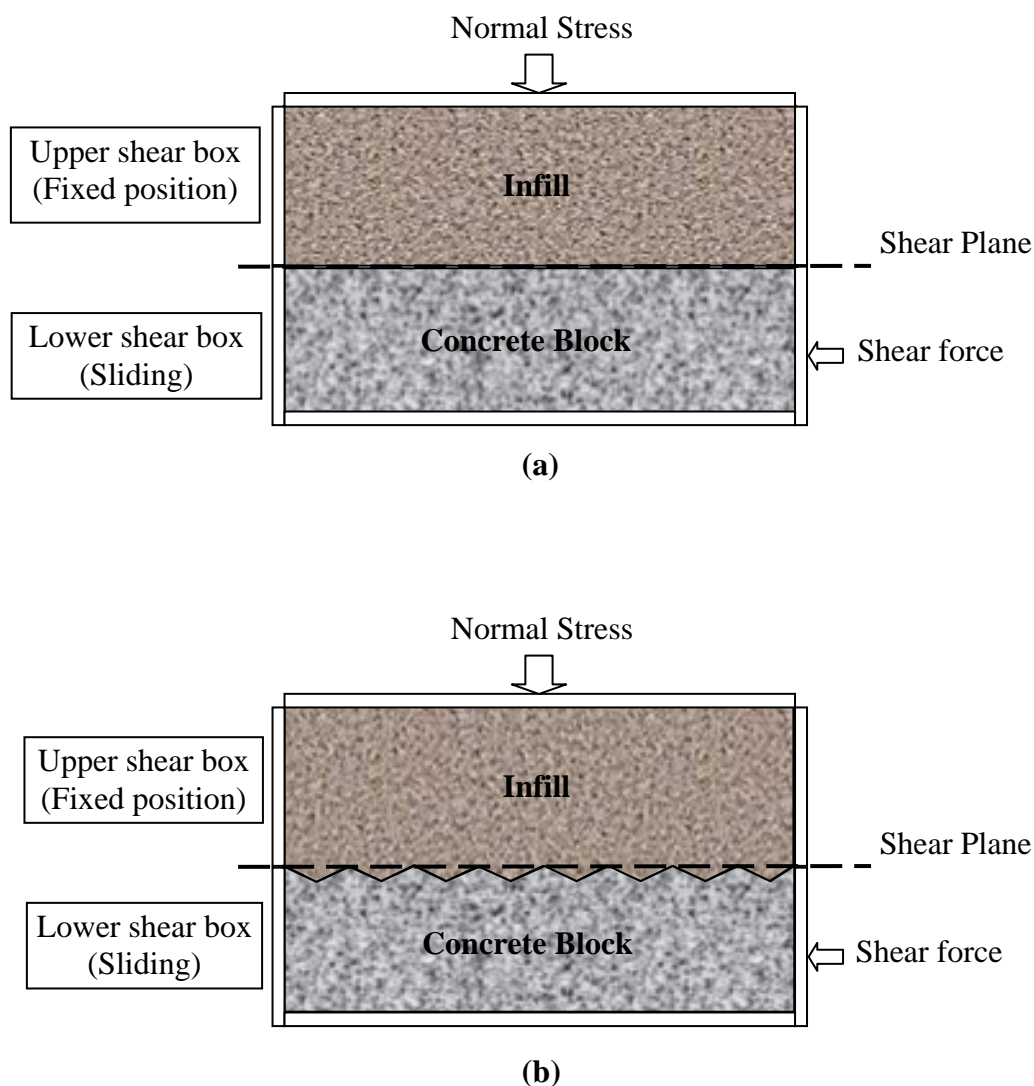


**Figure 3.9:** Direct shear test for the investigation of shear strength of joint-infill boundary for (a) Smooth joint, and (b) Rough joint

### 3.5 Field and Laboratory Test Equipment

In complementing the scope of this study, several important equipments were used, for both field and laboratory assessments. Generally, they include Schmidt Hammer, compression mould, linear variable displacement transducer (LVDT), load cell and direct shear box. Details of several equipments (uniaxial compression

machine, data logger and large shear box apparatus) were described together with their purposes in the following sections.

### 3.5.1 Uniaxial Compression Machine

Uniaxial compression machine namely MaTest 500 (Figure 3.10) was used to apply normal compressive load onto the modeled joint and filled joint during the UCT (see Section 3.4.2). This machine is able to apply compressive load at various rate up to a maximum load of 2000 kN.

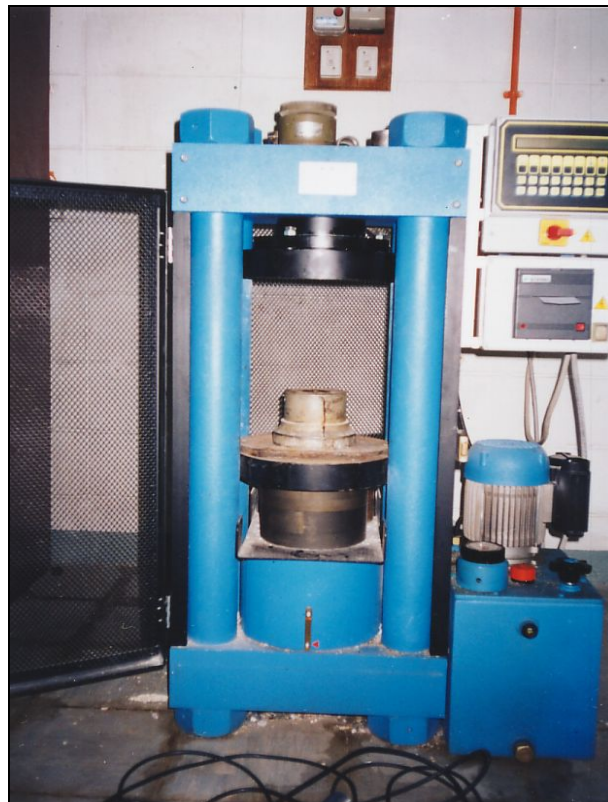


**Figure 3.10:** MaTest 500 compression machine used in UCT

## CHAPTER 4

### RESULT AND ANALYSIS

#### 4.1 Introduction

The results of site investigation and laboratory tests were analysed and presented in this chapter. Appropriate interpretations and inferences were made on the joint behaviours, with possible affecting factors discussed.

#### 4.2 Field Investigation

Figure 4.1 below exhibits the actual filled joint system. The thickness of the infill layer of the joints at the selected site ranged from about 10 cm to 30 cm. The joint surface is estimated to be rough and undulating. A clear and obvious difference in weathering grade is found between the infill layer and the joint block. No banding, i.e. gradual change in weathering grade is observed between the infill layer and the joint block. Consequently, it is believed that the infill was resulted from *in-situ* deposition, rather than differential weathering. Soil particles from the nearby

surface have been washed into the originally open joint aperture to form this filled joint system. This infill material consists of loose granitic residual soil (RS).



**Figure 4.1:** Filled joint system with no banding of weathering grade across the infill and joint blocks

Three major parts of the joint block were recognized. Fresh and intact rock experienced very low degree of weathering. However, the exposed surfaces of the joint block do exhibit slight weathering (SW). A relatively higher weathering effect was observed on the joint surfaces interfacing with the infill (MW to HW). However, the gradual change in weathering grade of the filled joint system is not that significant to be termed as banding effect.

#### 4.2.1 Schmidt Hammer Test

Schmidt hammer or rebound hammer test was carried out *in-situ*. The results obtained from this test are reliable as the surface hardness of the joint tested is greater than 20 MPa (Brown, 1981).

By using Equation 3.1, and the density of granite as  $26 \text{ kN/m}^3$ , the joint compressive strengths (JCS) at different parts of the joint system were calculated and shown in Table 4.1 below. Interpretation of the weathering grade was based on the JCS obtained, with reference to Waltham (2002) (see Appendix D).

**Table 4.1:** JCS at different parts of joint system

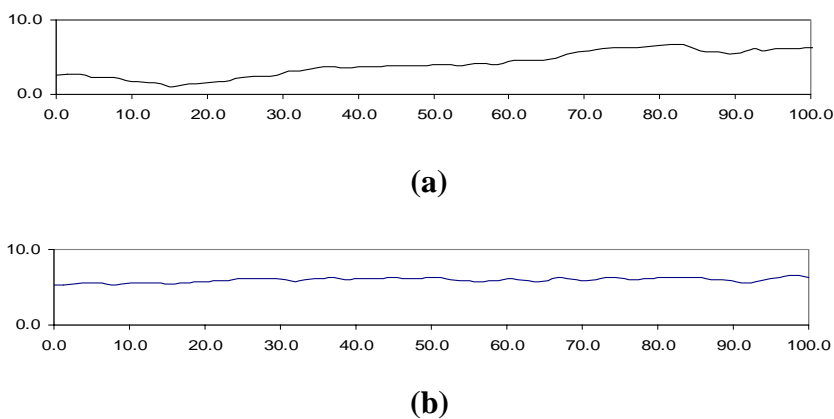
<b>Joint Component</b>	<b>R (average)</b>	<b>R (corrected)</b>	<b>JCS (MPa)</b>	<b>Grade of Weathering</b>
<b>Fresh Rock</b>	55	52.9	<b>166.4</b>	II
<b>Weathered Rock</b>	40	37.3	<b>73.0</b>	III
<b>Joint Surface</b>	24	21.0	<b>30.9</b>	III

Table 4.1 clearly shows that the original intact granite rock is an “extremely strong” rock, with its JCS greater than 150 MPa (Brown, 1981). Broch and Franklin (1972) and McLean and Gribble (1979) categorized rock of this strength as “very strong” rock (see Appendix E). According to Waltham (2002), very slight weathering has affected rock of this range of JCS. However, when exposed to the natural surrounding, the JCS is reduced significantly. For the filled joint studied, weathering has resulted in a loss of about 81 % of JCS at the joint apertures. With continuous weathering on the joint surface, the JCS is expected to decrease with time. Consequently, differential weathering of the joint surface will lead to the increase of infill thickness.

With the understanding on the JCS of the rock joint, suitable concrete strength (UCS) was chosen for the joint block model. Cast concrete block of Grade 60 was used to simulate weathered rock joint of weathering grade III.

#### 4.2.2 Joint Roughness Coefficient

As discussed in Section 3.2, the Joint Roughness Coefficient (JRC) of the joint surface was calculated. The value of JRC measured on different portions of the joint surface varies from 4.7 to 14.1. By comparing the joint surface profile with the profile suggested by Barton (1976, 1978), the joint surface investigated could be described as rough and undulating. Figure 4.2 below shows the profiles of the joint surface displaying the maximum and minimum JRC measured from the field.



**Figure 4.2:** Joint surface profiles (a) JRC = 14.1 and (b) JRC = 4.7

### **4.3 Preliminary Tests**

Preliminary tests are supplementary works carried out to gather a better understanding on the overall behaviour and properties of filled joint. The properties investigated included the basic characteristics of the infill (PSD and specific gravity), shear behaviours of the infill and the joint-infill boundary effect, and the compressive / dilative behaviours of the infill, intact rock and jointed rock samples.

#### **4.3.1 Particle Size Distribution and Specific Gravity**

The mean PSD curve of the infill tested is shown in Figure 4.3 below. The percentage of various particles size that makes up the infill is also listed in Table 4.2 below.



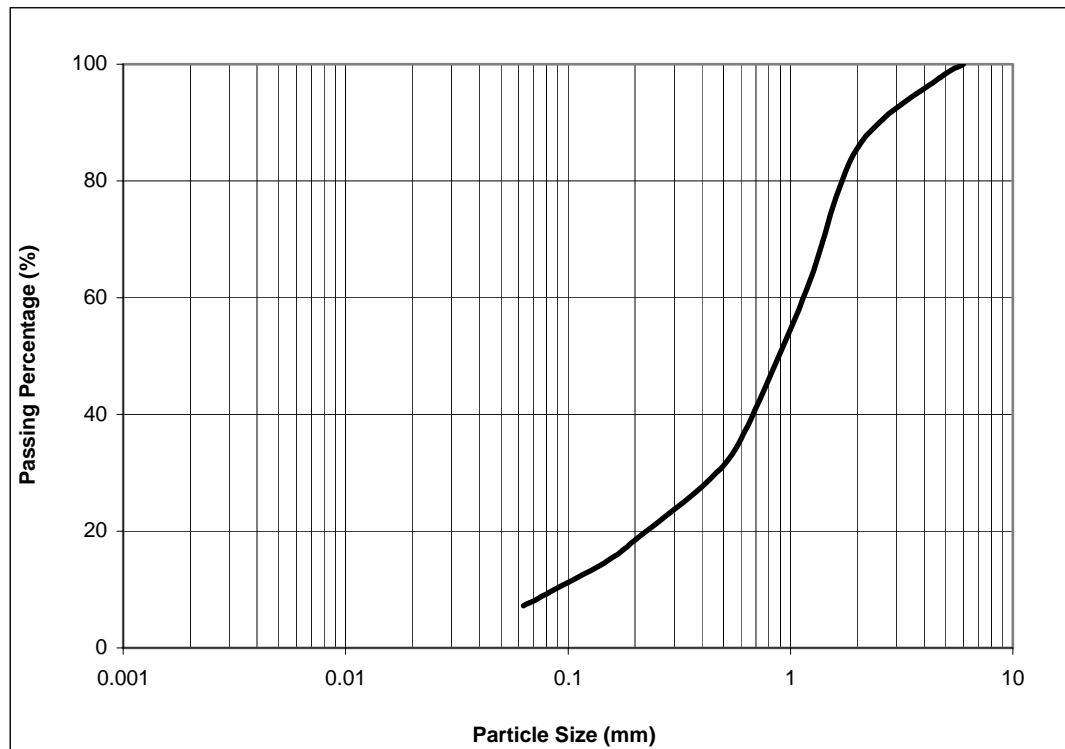


**Figure 4.3:** PSD curve of infill material

**Table 4.2:** Particle size and content of infill sample

Particle size	%
<b>Fine (&lt;0.06 mm)</b>	<b>7</b>
<b>Fine Sand (0.06 – 0.2 mm)</b>	<b>11</b>
<b>Medium Sand (0.2 – 0.6 mm)</b>	<b>18</b>
<b>Coarse Sand (0.6 – 2.0 mm)</b>	<b>50</b>
<b>Fine Gravel (2.0 – 6.0 mm)</b>	<b>14</b>

The infill was graded as Well-Graded Silty Sand. It is evident that a major portion (more than 60%) of the infill consists of medium to fine gravel. Crushing of these coarse and fine gravels is expected to influence the shear strength and shear behaviour of the filled joint model. The various particle sizes may imply that the infill would display variable shear strength, which is believed to be mainly contributed by frictional strength.

Specific gravity of the infill particles was also determined. The average specific gravity for the infill particles of different sizes was found to be about 2.46. Yusof (2003) has done research on the specific gravity of granitic residual soils at 1m – 7m depth, found in peninsular of Malaysia. He suggested that the specific gravity of these materials lies in between 2.50 to 2.74. On the other hand, Abu Bakar (2004) determined the average specific gravity of the granitic residual soils was 2.74. The specific gravity of the infill material tested in this study has been found to be lower than the ranges mentioned. This implies that on the ground surface, the infill material was subjected to more extensive weathering, and that weathering has altered the physical properties of the grains. Figure 4.4 below shows the infill particles separated according to different ranges of particle sizes.



**Figure 4.4:** Infill sample divided according to the grain size

### 4.3.2 Static Compression Test

Compressibility of the infill material (%) was investigated through static compression test. The influence magnitude of normal stress (N) to the compressibility of the infill is shown in Figure 4.5 below.

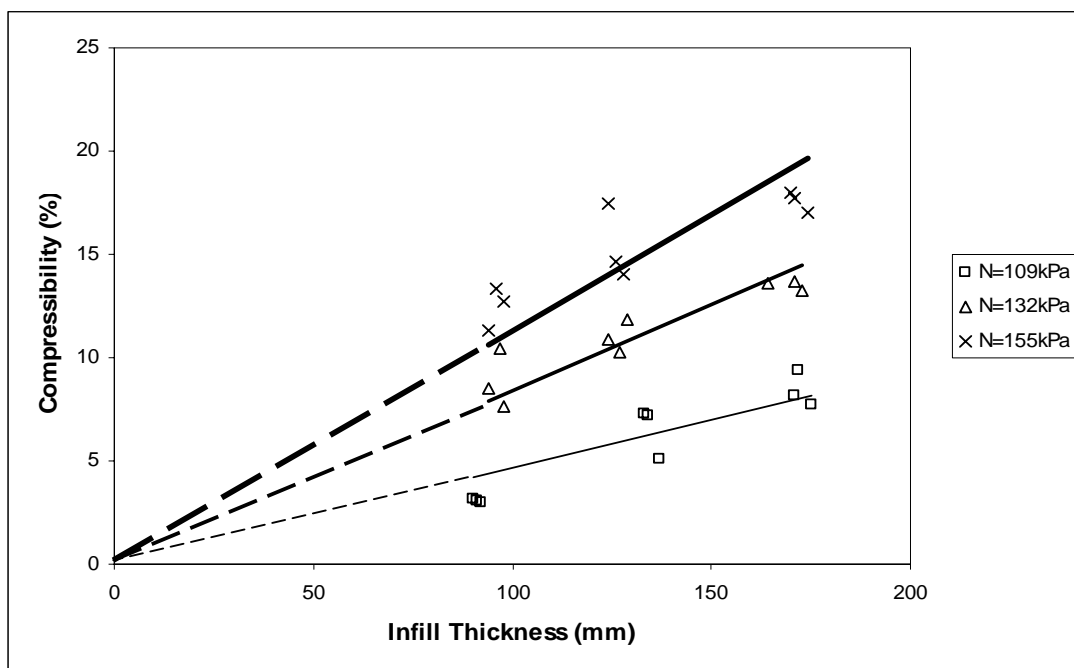


**Figure 4.5:** Compressibility vs. infill thickness graph

To obtain certain thickness of infill, the weight of the infill was limited to 300, 400 and 500 g. The compressibility of infill material of different weight (W) under different normal load is shown in Figure 4.6 below.

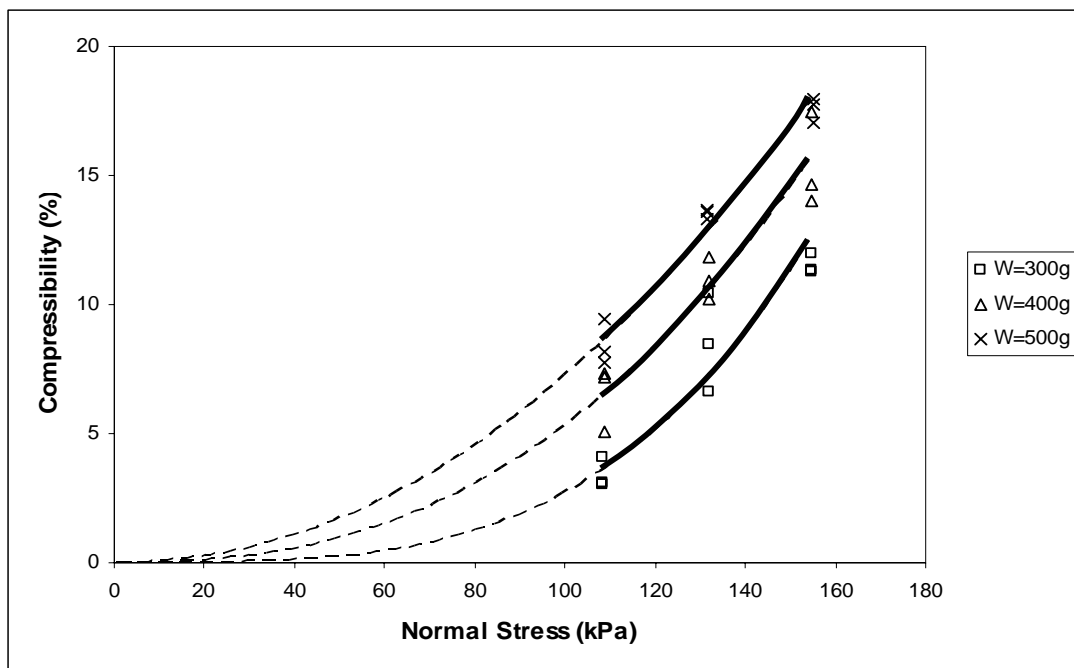


**Figure 4.6:** Compressibility vs. normal stress graph

Through Figure 4.6, it is proven that the infill is more compressible when its thickness is increased. More pores present in thicker infill contribute to a higher compressibility. At higher stress ( $>100$  kPa), compressibility of infill increases almost linearly with the thickness. Similar trends are observed in the relationship between infill compressibility and the magnitude of the normal stress. At various infill thicknesses, higher normal stress results in greater compressibility.

The changes in density of infill material throughout the static compression tests are listed in Table 4.3 below.

**Table 4.3:** Density of infill before and after static compression test

Average Initial Height (mm)	Average Initial Density ( $\text{kg/m}^3$ )	Average Final Density ( $\text{kg/m}^3$ )		
		$\sigma_n = 109\text{kPa}$	$\sigma_n = 132\text{kPa}$	$\sigma_n = 155\text{kPa}$
94.4	1497.1	1569.7	1519.4	1547.0
129.1	1460.4	1438.2	1552.6	1587.7
171.2	1375.5	1415.6	1475.2	1484.0

It is clearly shown that thicker infill tends to be more porous. This explains the occurrence of greater compressibility in thicker infill samples. Similar trend is observed in the post test infill density (with the exception of specimen with 94.4 mm initial height and normal stress of 132 kPa). To reach a certain level of density, thicker infill requires a greater normal load and longer period of compression as compared to thinner infill, although they appear to be more compressible.

The PSD of infill sample after the compaction test is almost similar to that of the original PSD (reconstitutive sample). This indicates that static compaction did not cause any significant amount of crushing. Hence, the compressibility exhibited by the infill is mainly due to the particles rearrangement within the available voids.

### **4.3.3 Uniaxial Compression Test**

Unlike static compression test, uniaxial compression test was carried out with increasing compressive load applied onto joint models. The Uniaxial Compressive Strength (UCS) (the compressive stress at failure), Young's Modulus (E) (tangent modulus obtained at 50% UCS) and the compressional behaviour of the rock specimen were studied. As mentioned, this series of tests was carried out mainly to investigate the effect of various types of joint on the compressibility of rock specimens.

The stress-strain curves of intact rock, matched-joint and mismatched-joint are shown in Figure 4.7, 4.8 and 4.9 respectively below (IR = Intact rock sample; SJ = Smooth matched-joint sample; RJ = Rough mismatched joint sample)

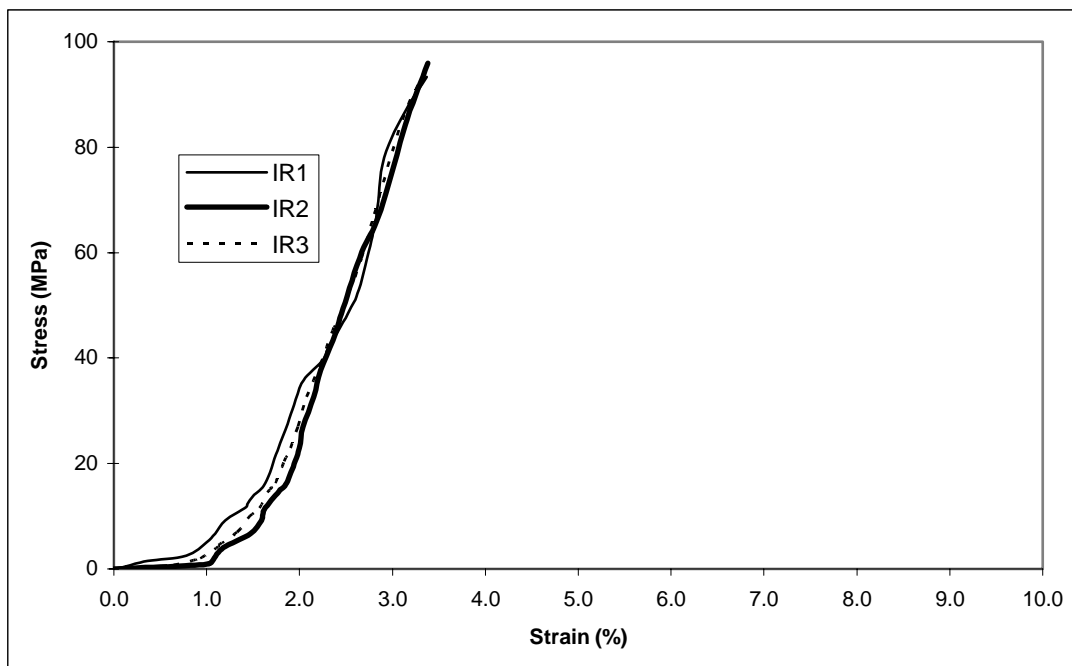


**Figure 4.7:** Stress-strain relationship of intact rocks

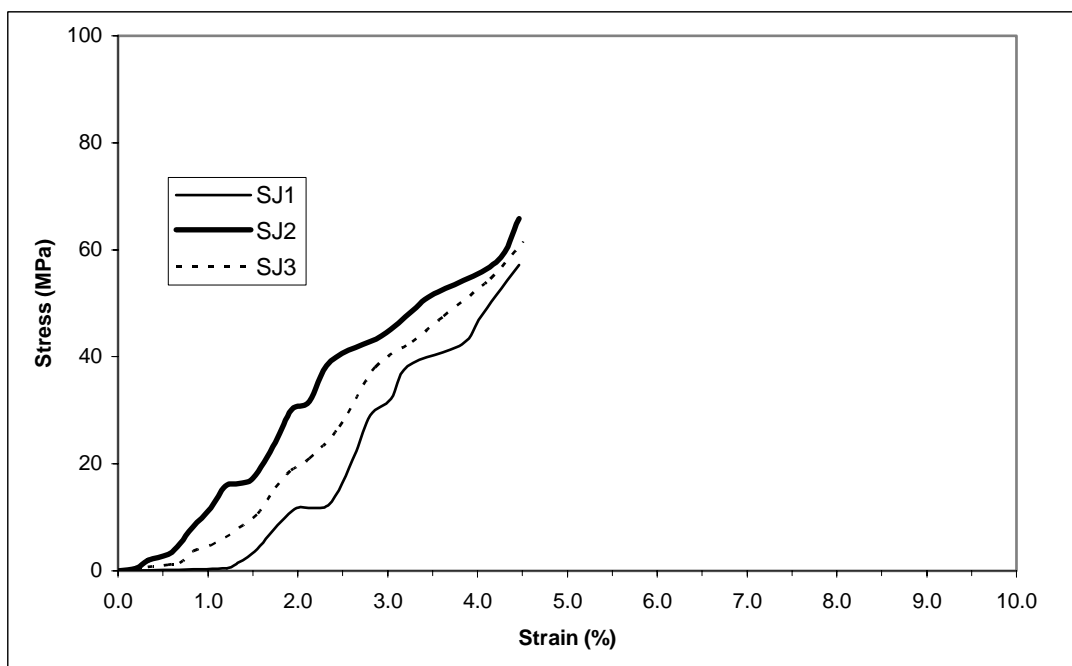


**Figure 4.8:** Stress-strain relationship of matched-joints

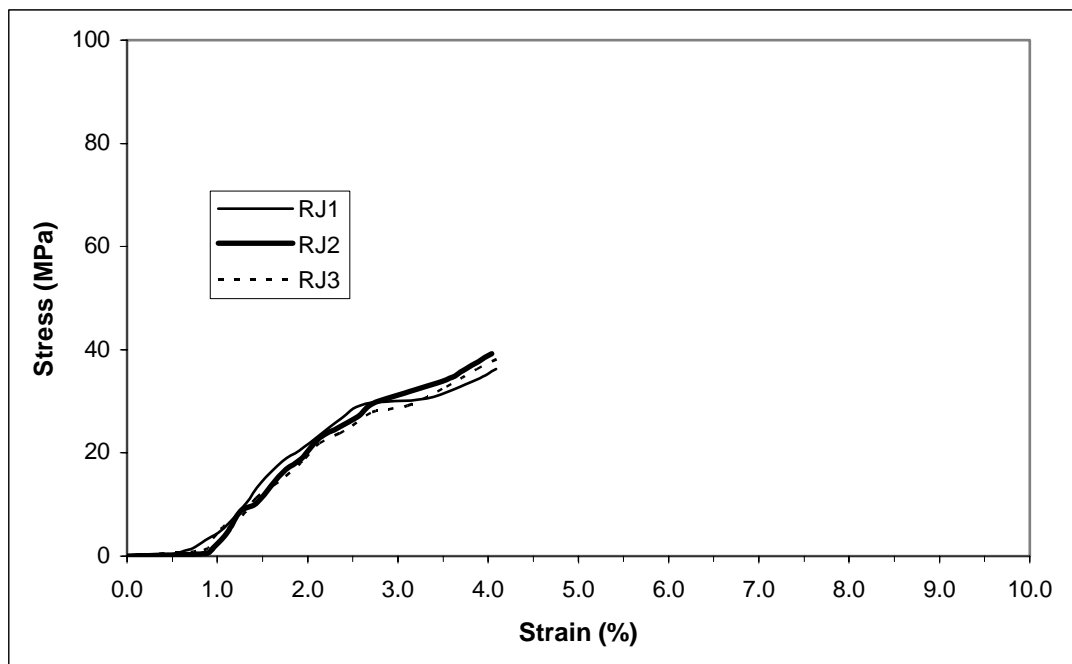


**Figure 4.9:** Stress-strain relationship of mismatched-joints

It is observed that the intact rock specimens (without any fracture plane) could sustain an average maximum compressive stress of 95.1 MPa before failing at 3.4 % strain. For the rock specimens with matched-joint, the average maximum compressive stress was found to be 61.5 MPa, achieved at a strain of 4.5 %. As for the specimens with mismatched-joint, the ultimate compressive strength was determined to be 38 MPa, obtained at 4.1 % strain.

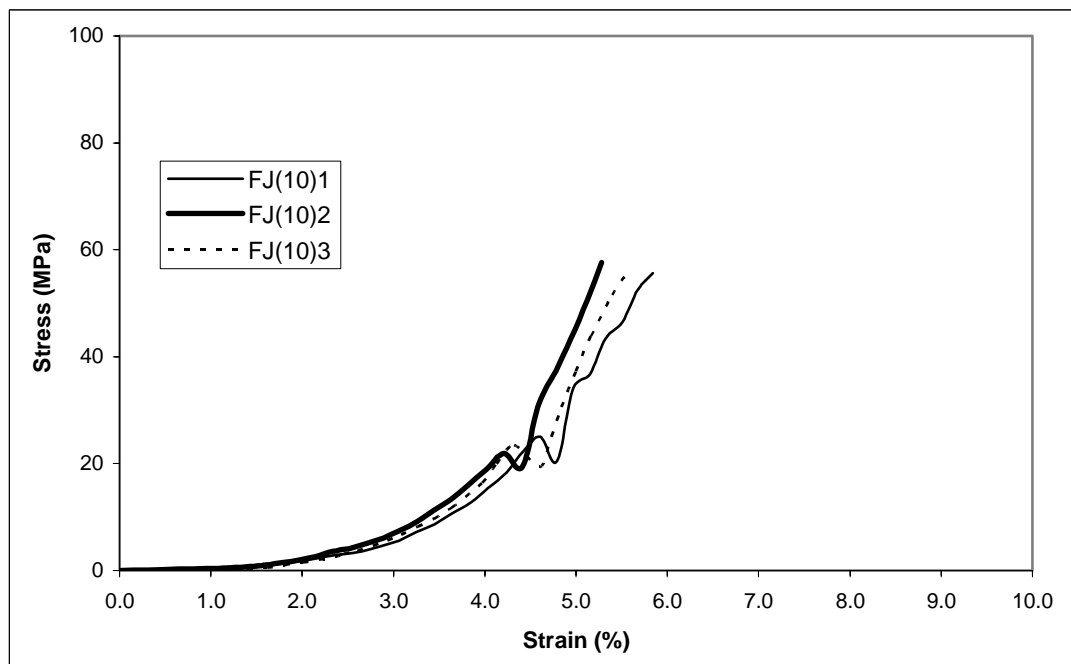
From this series of tests, it is proven that the presence of fracture planes such as joint in rock specimen can significantly affect its deformational behaviour. In jointed specimens, the applied compressive load concentrates on the weaker part of the sample (i.e. joint). The joint surface, therefore, fails at a stress lower than the compressive strength of the intact rock (35 % lower). Worse situation occurs on rock specimens with mismatched-joint. The undulating joint surfaces reduce the contact area between the interfacing joint surfaces, thus increasing the amount of stress at contacts and this leads to the reduction in the compressive strength of the specimens (60 % lower than the intact rock).

Besides reducing the compressive strength of the rock specimens, the presence of joint also leads to an increase in the compressibility of the specimens. Apart from the compression of the intact rock material, the fracturing of the joint surfaces also contributes to additional deformation to the rock specimens. For mismatched-joint, the load concentrated on the contact area between the adjacent rough joint surfaces. The rock material at those areas failed at a much lower stress, prior to the compression of the rock material at the remaining parts of the sample. Therefore, the strain-at-failure for rock with mismatched-joint was smaller than that of the rock with matched-joint.

Figure 4.10 below shows the stress-strain curves for jointed rock specimens, with 10 mm infill (FJ = Filled joint sample; (10) = infill of 10 mm thickness). These curves exhibit two distinctive peaks and are different from the previous curves shown in Figure 4.7, 4.8 and 4.9. The first stage is depicted by a gradual build-up of stress with an increasing strain. It is thought that at this stage the deformation was due to the rearrangement of particle grains in the infill layer. The first peak stress (23.5 MPa stress, 4.4 % strain) was achieved when the stress applied was sufficient to bring about the breakage of the weaker infill material. Less stress was required to facilitate the rearrangement of the newly broken infill grains. As a result, a slight drop of stress was observed after first peak stress.

As the size of the broken infill grains was getting smaller due to breakage, the infill layer became denser when compressed. Contact between grains gradually increased with further compression and this led to a better distribution of the applied stress within the infill material. In this situation, the infill tends to be stronger, hence, the stress-strain curve became steeper. Fracturing of the rock material (i.e. the joint block) did not take place, as the stress applied was insufficient to overcome the ultimate compressive strength of the rock (95.1 MPa). As such the deformation shown in Figure 4.10 was mainly due to the presence of the infill layer which was more compressible than the rock material.

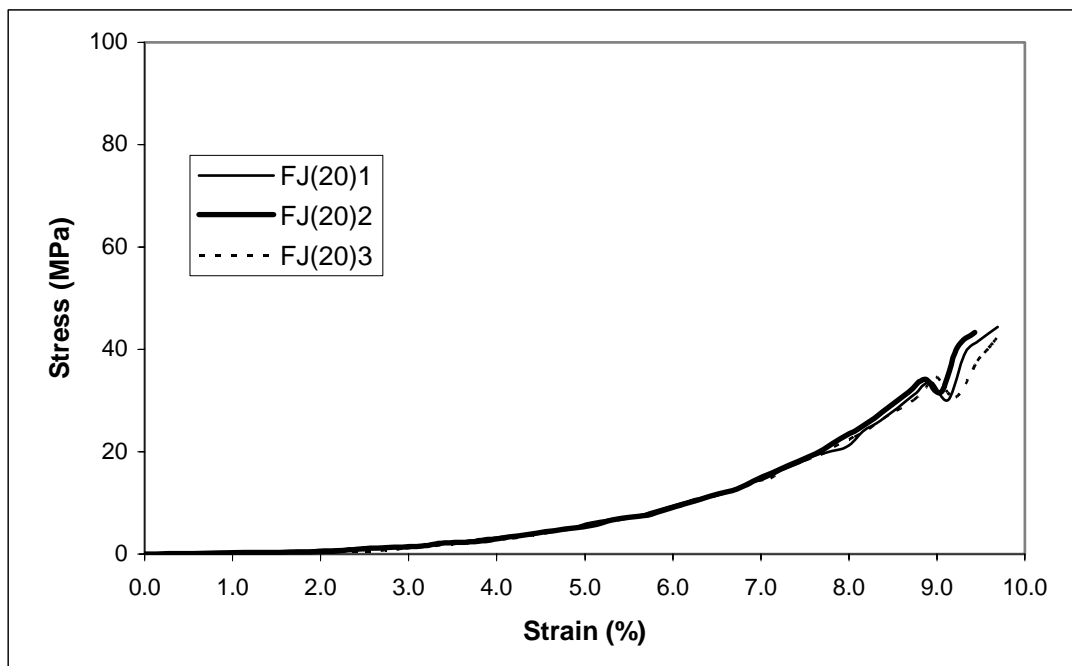




**Figure 4.10:** Stress-strain relationship of filled joint (10 mm infill)

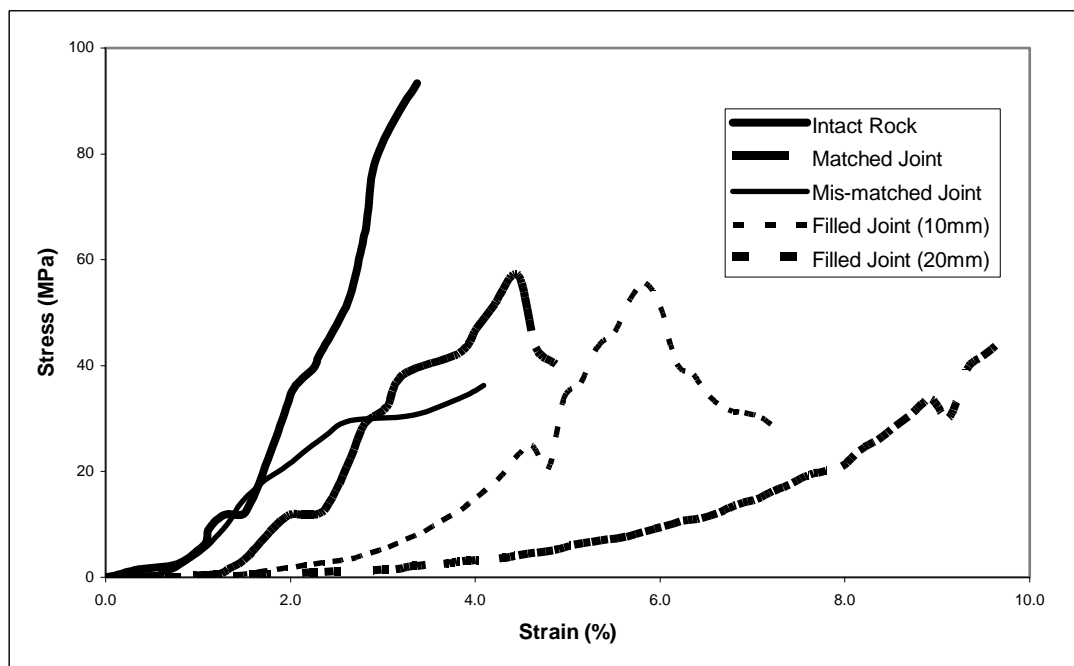
Subsequent peaks could be expected should a higher compressive stress be continuously applied. Beyond the UCS of the rock, a combined failure of the infill and the joint block would prevail. This high stress level would break the infill into even finer grains, which will then be rearranged into an even denser layer. At a very much higher stress (which is not possible to be achieved under laboratory condition) the infill layer could be recrystallised into a solid body due to the process known as secondary mineralization.

Figure 4.11 below shows the stress-strain relationship of rock specimen with joint of 20 mm thick infill (FJ = Filled joint sample; (20) = infill of 20 mm thickness). The curves shown were similar to those of the specimens with 10 mm infill. The first peak stress (34.2 MPa) was achieved at 8.9 % strain. Test results indicate that joint with thicker infill exhibits greater compressibility. Thicker infill layer consists of more voids which directly induce compressibility to the infill layer (as discussed in Section 4.3.2) and also the jointed rock specimen.



**Figure 4.11:** Stress-strain relationship of filled joint (20 mm infill)

Stress-strain curves of different types of samples are shown in Figure 4.12 below. The average UCS (first peak stress for sample with filled joint) and E (at 50 % UCS) values of each specimen are listed in Table 4.4 below.



**Figure 4.12:** Stress-strain relationship of different rock specimens

**Table 4.4:** UCS and E values of rock specimens

Rock Specimen	Average UCS (MPa)	Strain at Failure (%)	Average E (GPa)
Intact Rock	95.1	3.4	4.1
Matched-Joint	61.5	4.5	2.0
Mis-Matched-Joint	38.0	4.1	1.6
Filled Joint (10mm)	56.3	4.4	1.1
Filled Joint (20mm)	43.7	8.9	0.7

The presence of 10 mm infill reduced the UCS of the rock mass by as much as 41 %. The compressibility (i.e. uniaxial strain) of the rock specimen was also increased by 30 %. Worse conditions occurred when the thickness of infill doubled, where there was a reduction of about 54 % UCS of the intact rock. Joint with 20 mm infill was found to be 163 % more compressible than the intact rock. These results are in good agreement with Wittke (1990), who found that an infill layer of 5 mm thickness would induce an additional 50 % compressibility to an intact rock block of 1 m height.

In term of Young's Modulus, a matched-joint reduced the E value of intact rock by half (from 4.1 GPa to 2.0 GPa). Greater reduction in E was found with the presence of mismatched-joint, 10 mm-filled-joint, and 20 mm-filled-joint with respective reduction of 61 %, 73 % and 84 % as compared to intact E value. Joint and infilling are proven to adversely affect the compressibility of a rock body.

Joint surface profile (roughness) is another potential element that would affect the UCS of rock. Surface roughness dictates the contact area of adjacent joint blocks, which subsequently determines the stress concentration. In the tests conducted, the undulation of joint block surface has resulted in the loss of about 60 % UCS.

Figure 4.13 below displays the PSD curves of infill material before and after the UCT. The changes of the constituent of the tested infill particles are clearly shown.

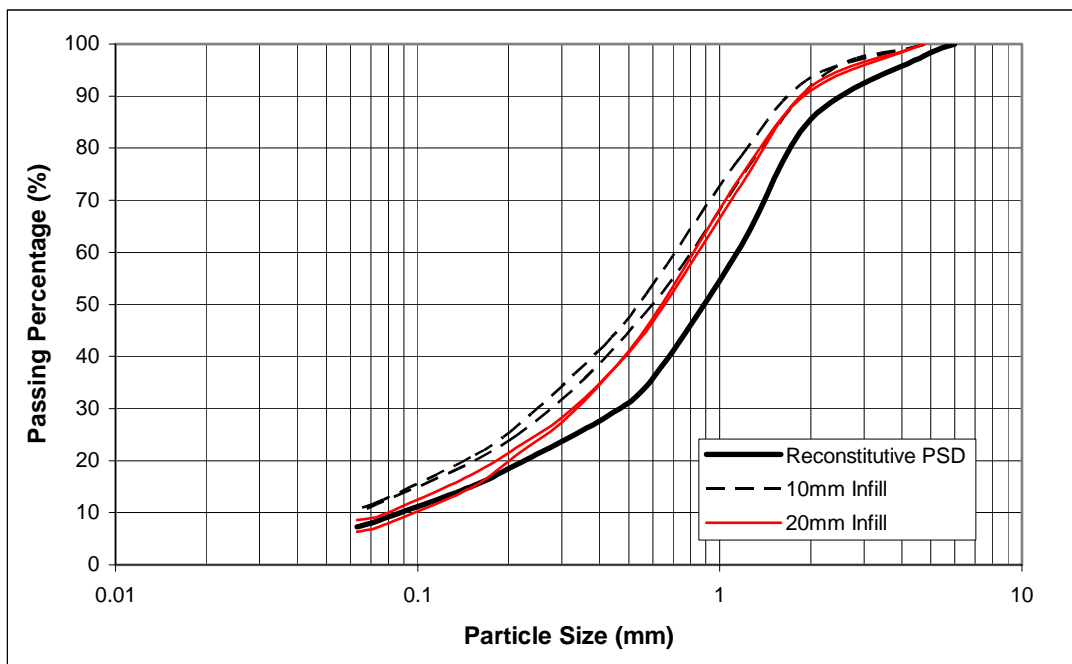


**Figure 4.13:** Particle size distribution of infill material after UCT

It is obvious that the compression of the infilling in between the intact rocks led to the crushing and breakage of infill particle. This is indicated by the shifting of all the PSD curves to the left of the original PSD curve (PSD curve of the reconstitutive infill material). It is apparent that the crushing of the infill grains that contributes to an increase in the compressibility of rock joint particularly, joint with thicker infill.

#### 4.3.4 Direct Shear Test on Infill Material

The shear characteristics of infill material were investigated through direct shear tests carried out on reconstitutive samples of the infill. Comparison was made between shearing of the infill samples with and without preloading.

Figure 4.14(a) and (b) below show the typical shear stress-displacement curves of preloaded infill under 133 kPa and 264 kPa normal stresses (IA = Infill sample tested under normal stress of 133 kPa; IB = Infill sample tested under normal stress of 264 kPa). From the curves, it is clearly shown that the infill samples tested undergone a strain-hardening behaviour, where there is no indication of drop in strength, at least within the horizontal displacement applied. Due to this behaviour, the maximum shear strength of the infill was defined as the shear stress taken at 10 mm shear displacement.

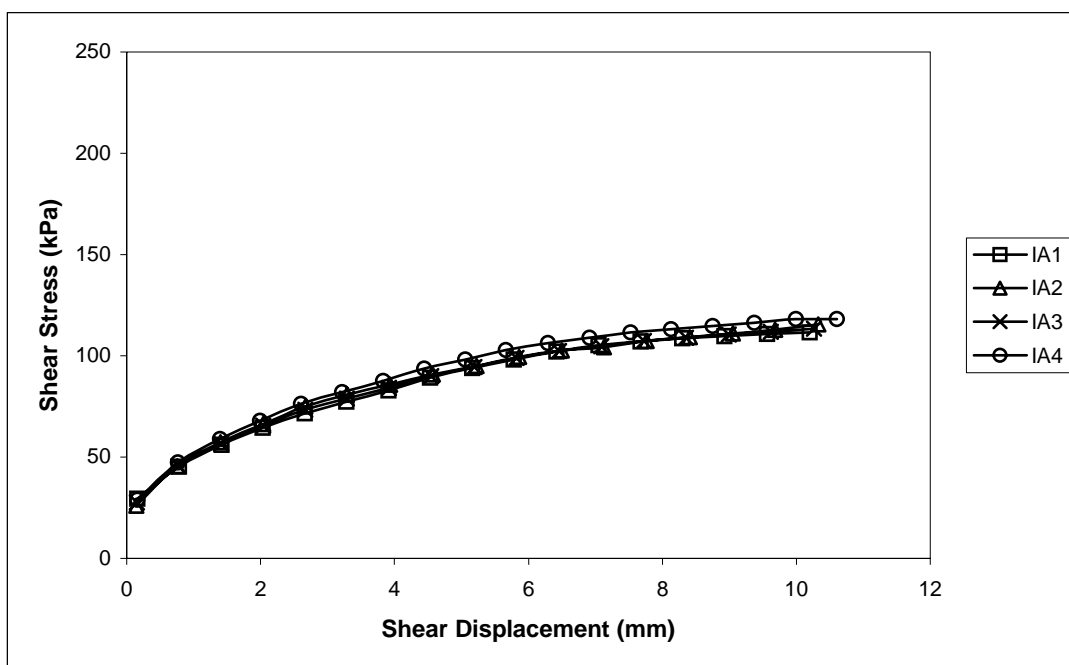
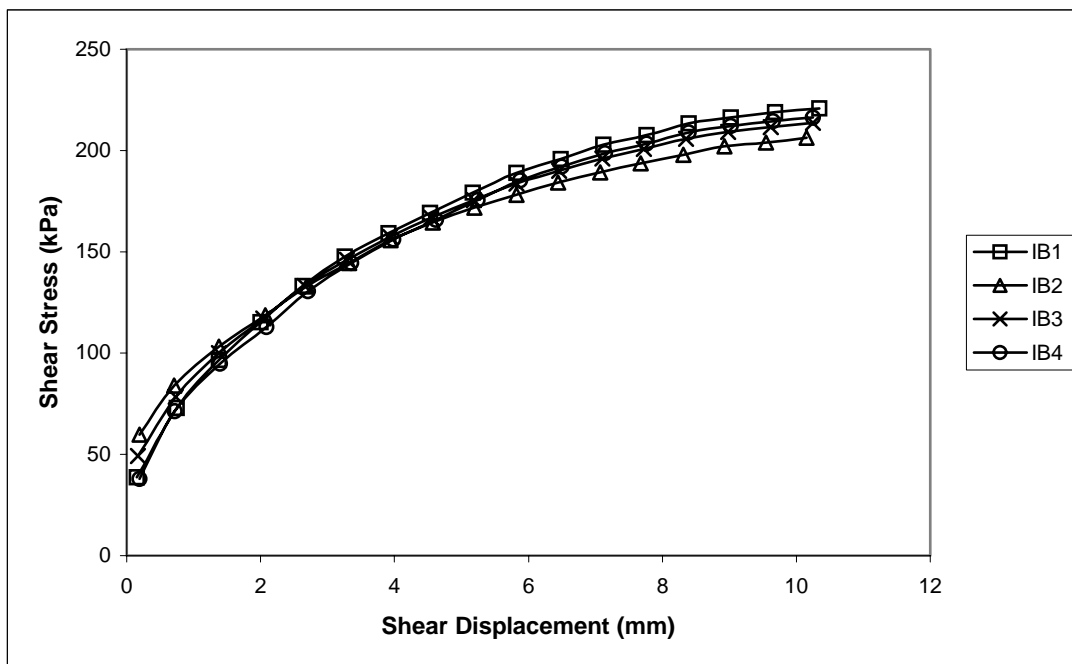


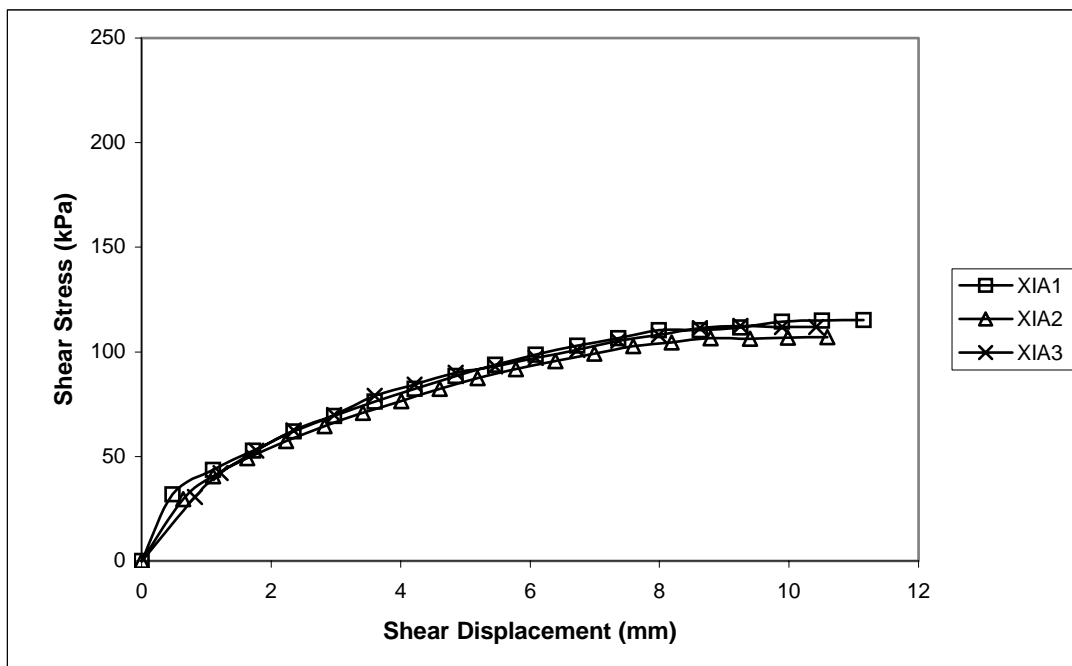
**Figure 4.14:** Shear stress versus displacement, for infill with preloading, under normal stress of (a) 133 kPa, and (b) 264 kPa



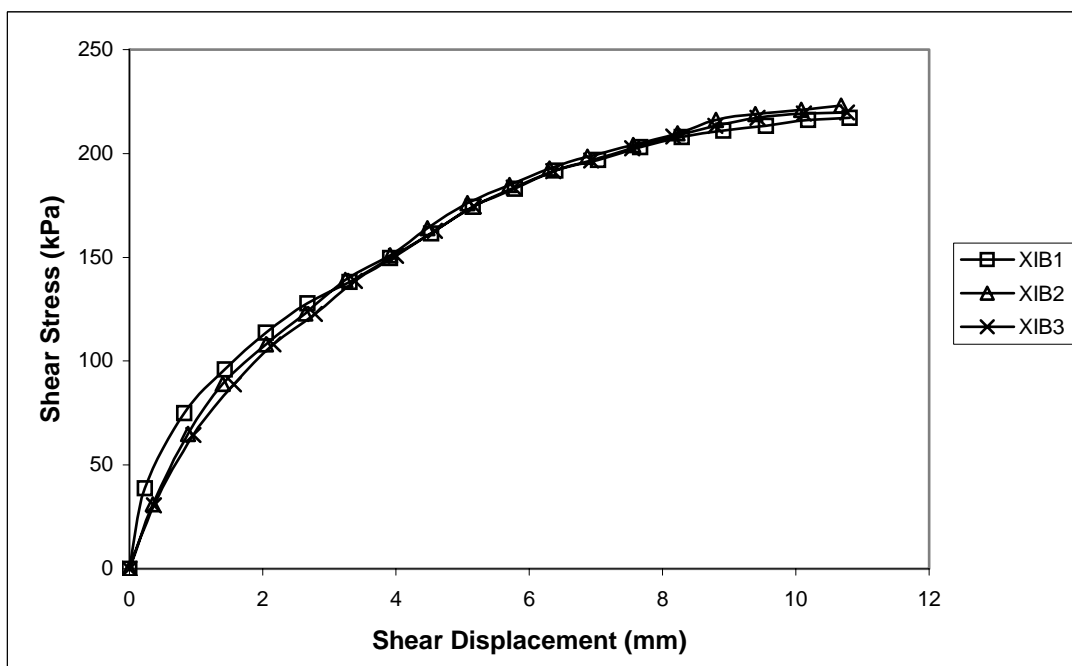
(b)

**Figure 4.14** (continued)

Figure 4.15(a) and (b) below show the shear stress-displacement relationship for infill samples without preloading (XIA = Infill sample tested under normal stress of 133 kPa, without preloading; XIB = Infill sample tested under normal stress of 264 kPa, without preloading). Subsequently, comparison of shear stress-displacement curves of infill samples with and without preloading is shown in Figure 4.16.



(a)



(b)

**Figure 4.15:** Shear stress versus displacement, for infill without preloading, under normal stress of (a) 133 kPa, and (b) 264 kPa

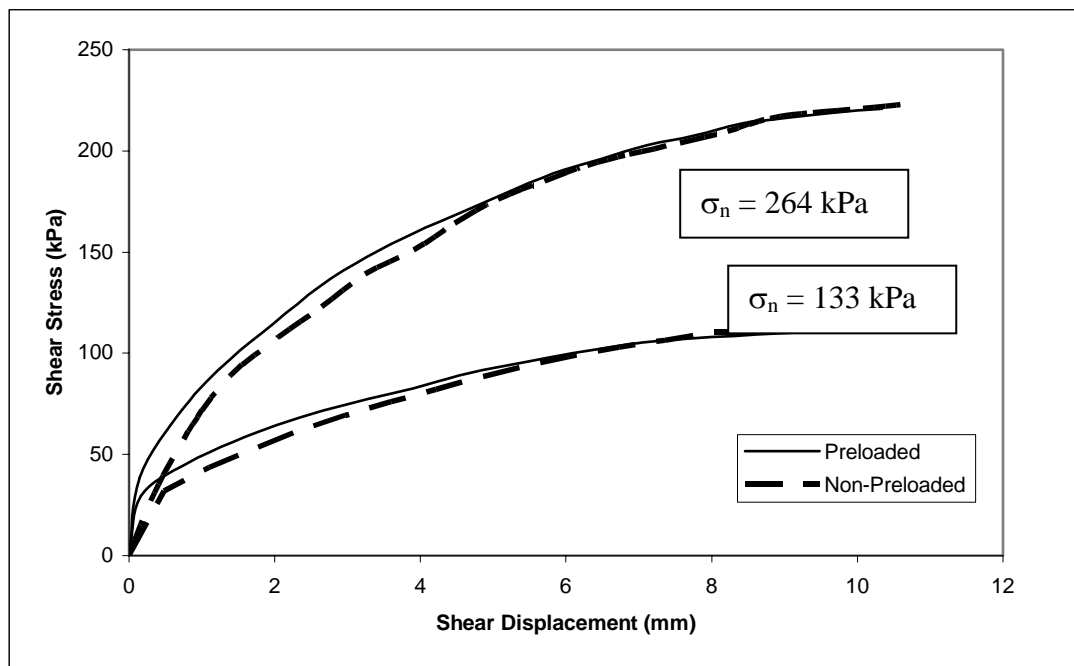


**Figure 4.16:** Shear stress versus displacement, for infill samples with and without preloading

From Figure 4.16, it is found that the shearing of the infill without preloading displayed an almost similar behaviour as those preloaded samples. However, the shear strength of the preloaded samples tend to be slightly higher than the samples without preloading, particularly during the early stage of shearing. Assuming this is not due to sample variability (reconstituted sample), then, this can be explained in terms of the compactness of sample due to pre-loading. Before shearing, sample with pre-loading exhibits a higher state of compactness relative to sample without preloading. As a result, sample with pre-loading shows higher shear strength. However, as shearing progresses, particles rearrangement may increase the state of compactness of samples without preloading, which eventually reaches a similar state of compactness as the preloaded samples. At this stage, shear strength of both types of infill samples will be similar, and this occurs after 6 mm of shear displacement.



Figure 4.17 below depicts the vertical displacement of infill (both with and without preloading) during shearing. From the figure shown, it is obvious that the shear compressibility of the infill without preloading was much greater than that of the preloaded infill. Significant amount of settlement occurred almost immediately upon shearing. For both test conditions, the rate of settlement gradually decreased until about 6mm of shear displacement.

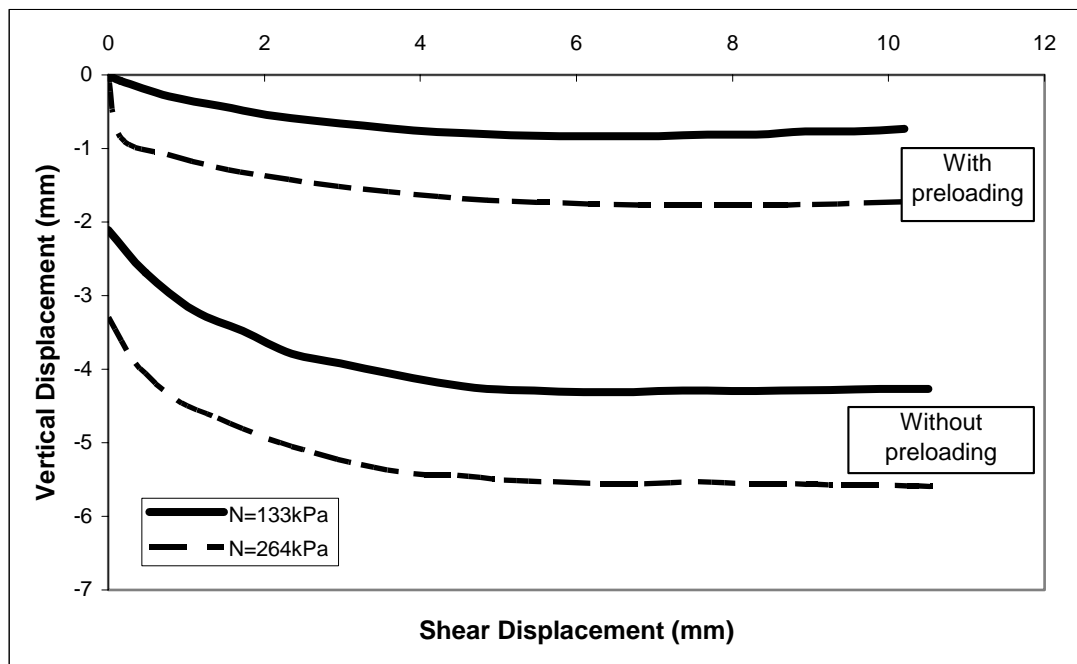


**Figure 4.17:** Normal versus shear displacement, for infill sample with and without preloading

The settlements of infill samples at different stage (preloading and shearing) are listed in Table 4.5 below. The total settlement,  $C_t$  listed is inclusive of the settlement of infill after 30 minutes of preloading (for preloaded samples only) and after 10 mm of shear displacement. The preload compressibility,  $C_p$ , shear compressibility,  $C_s$  and total compressibility,  $C_t$  of the infill sample were calculated based on the initial infill thickness (40 mm approximately). The average compressibility and shear strength of the infill are listed in Table 4.6. The shear compressibility of samples without preloading was found to be greater than samples with preloading. However, the total compressibility of both samples with and

without preloading was almost similar to each other. The shear strengths of samples with and without preloading were almost the same, with a difference of less than 3 %. It implies that the preloading procedure has no significant influence on the shear resistance of the infill. Consequently, it can be deduced that the initial density does not influence shear strength of the infill, but its shear compressibility.

**Table 4.5:** Settlement of infill sample at different stages

	<b>Preload Settlement (mm)</b>	<b>Shear Settlement (mm)</b>	<b>Total Settlement (mm)</b>
IA1	3.7	0.8	4.5
IA2	3.3	0.6	3.9
IA3	3.5	0.7	4.2
IA4	3.5	0.6	4.1
IB1	4.0	1.7	5.7
IB2	3.9	1.7	5.6
IB3	4.0	1.7	5.7
IB4	3.9	1.8	5.8
XIA1	-	4.3	4.3
XIA2	-	4.6	4.6
XIA3	-	4.7	4.7
XIB1	-	5.7	5.7
XIB2	-	5.6	5.6
XIB3	-	5.9	5.9

**Table 4.6:** Shear characteristics of infill with and without preloading

	$\sigma_n$ (kPa)	$C_p$ (%)	$C_s$ (%)	$C_t$ (%)	$\sigma_s$ (kPa)
<b>With Preloading</b>	133	8.8	1.7	10.5	114.1
	264	9.9	4.3	14.2	214.1
<b>Without Preloading</b>	133	-	11.3	11.3	111.2
	264	-	14.3	14.3	218.7

### 4.3.5 Direct Shear Test on Joint-Infill Boundary

Small-scale direct shear test was conducted to investigate the frictional behaviour at soil-rock contact. The shear behaviours for different conditions of joint-infill boundaries (smooth and rough), under different normal stresses, were shown in Figure 4.18 and 4.19 below.

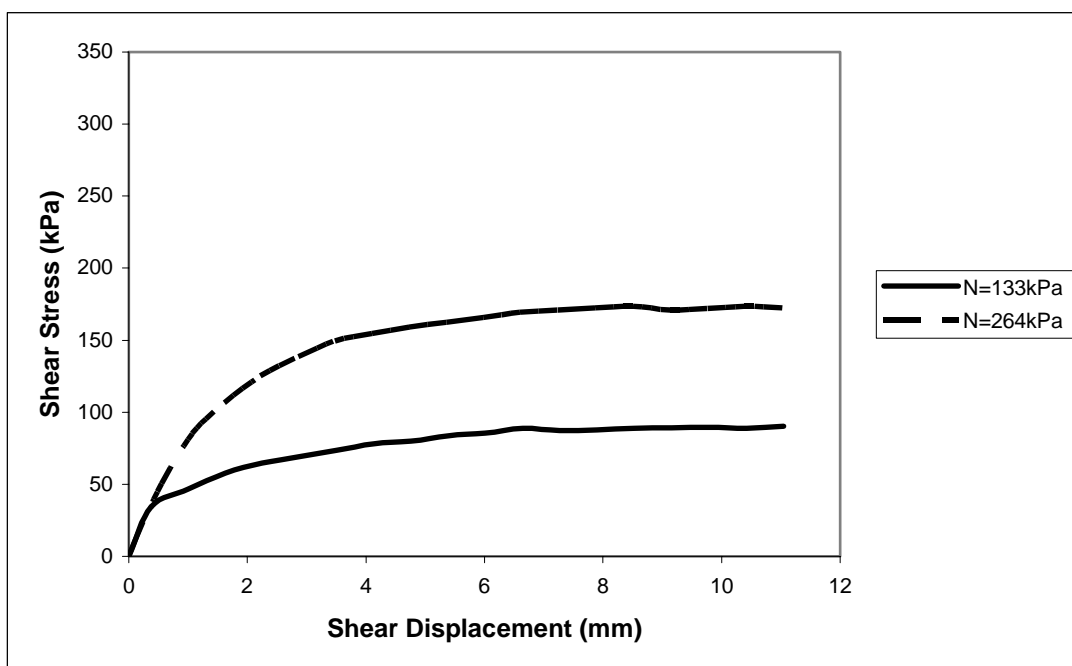


**Figure 4.18:** Shear stress versus displacement, for smooth soil-rock contact

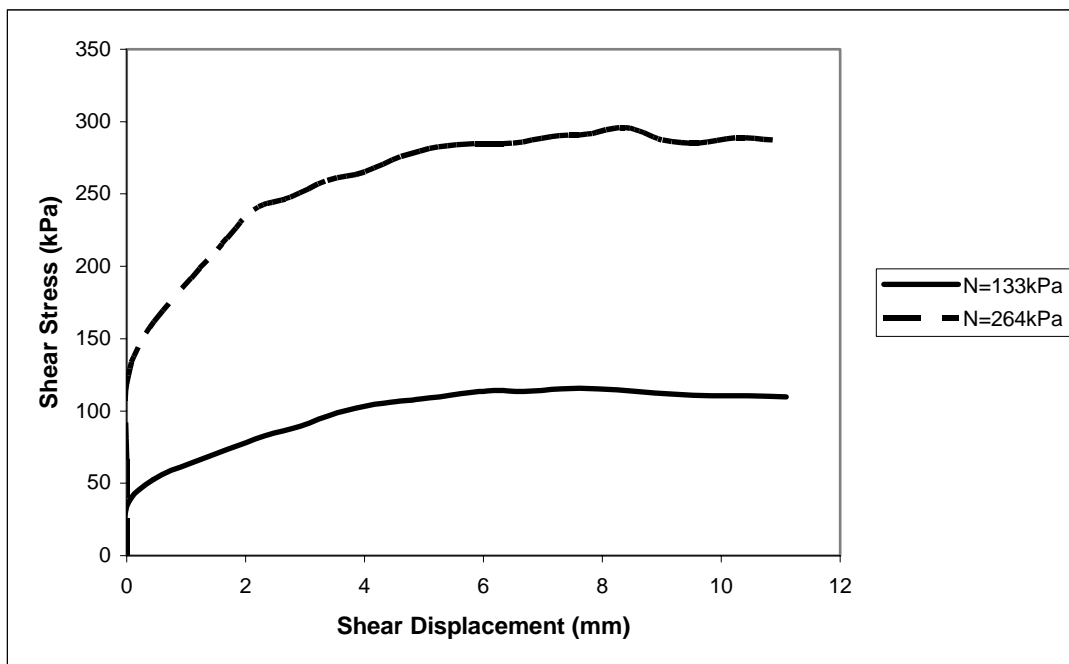


**Figure 4.19:** Shear stress versus displacement, for rough soil-rock contact

From Figure 4.18, it can be seen that planar joint-infill boundary exhibited strain-hardening shear behaviour. At the initial stage of shearing, the shear strength built up rapidly over a small displacement. Following that, the increase in shear stress gradually reduced. The shear stress eventually became almost constant after about 8 mm of displacement, under both different normal stresses.

Similar behaviour was observed for rough joint-infill boundary as shown by the curves in Figure 4.19 above. A sudden build-up of shear stress occurred at the moment when shear stress was applied. The shear stress eventually reached a peak and constant shear stress after 8 mm of shear displacement. It seems that the rough joint surface has imposed some degree of restraining to the infill particles, thus limiting the sliding and rolling of the grains along the rough surface. It is thought that this sudden build-up of shear stress must occur in order for the infill grains to roll upwards against the asperities of the joint surface.

To understand the influence of surface roughness on the frictional behaviour at joint-infill boundary, the shear stresses for smooth and rough soil-rock contact at 10 mm displacement are plotted and compared in Figure 4.20 below.

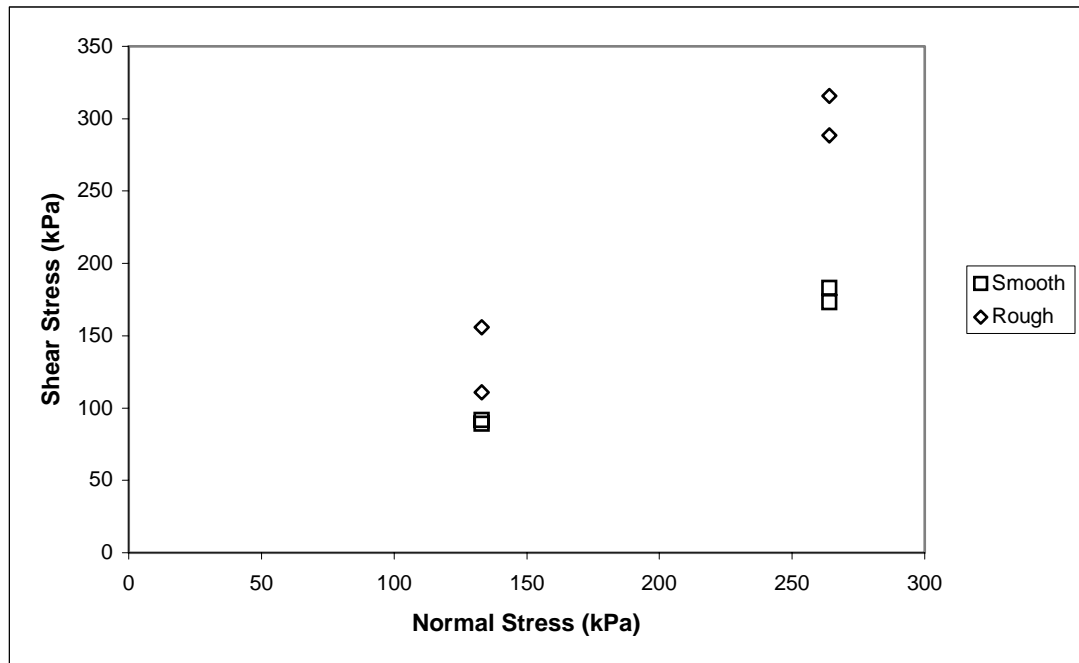


**Figure 4.20:** Shear stress (at 10 mm shear displacement) versus normal shear stress for smooth and rough joint-infill contact

It can be seen that the roughness of the joint surface interfacing the infill materials has a significant influence on the shear behaviour of filled joints. Under similar normal stress, joint block with saw-toothed surface exhibited a greater resistance against sliding and rolling of the infill grains. This effect would be more significant when sheared at higher normal stress. At normal stress of 133 kPa, the shear stress for rough joint-infill interface was about 48 % higher than that of the smooth soil-rock interface. However, when the normal stress was increased to 264 kPa, the difference in shear stress between the two types of soil-rock contact increased to almost 70 %.

Figure 4.21 below shows the normal displacement of the infill when sheared under different conditions of joint-infill contact. For both conditions the normal displacement is negative in value indicating a contraction. When sheared at lower normal stress (133 kPa), the amount of displacement of the infill was almost similar for both smooth and rough joint surfaces. However, at higher normal stress (264 kPa), the displacement of the infill was found to be smaller for the shearing of rough soil-rock contact. This implies that a rough joint surface minimizes the movement of the infill particles. The constraint against rolling and sliding is most probably imposed by the surface topography of rough joint.

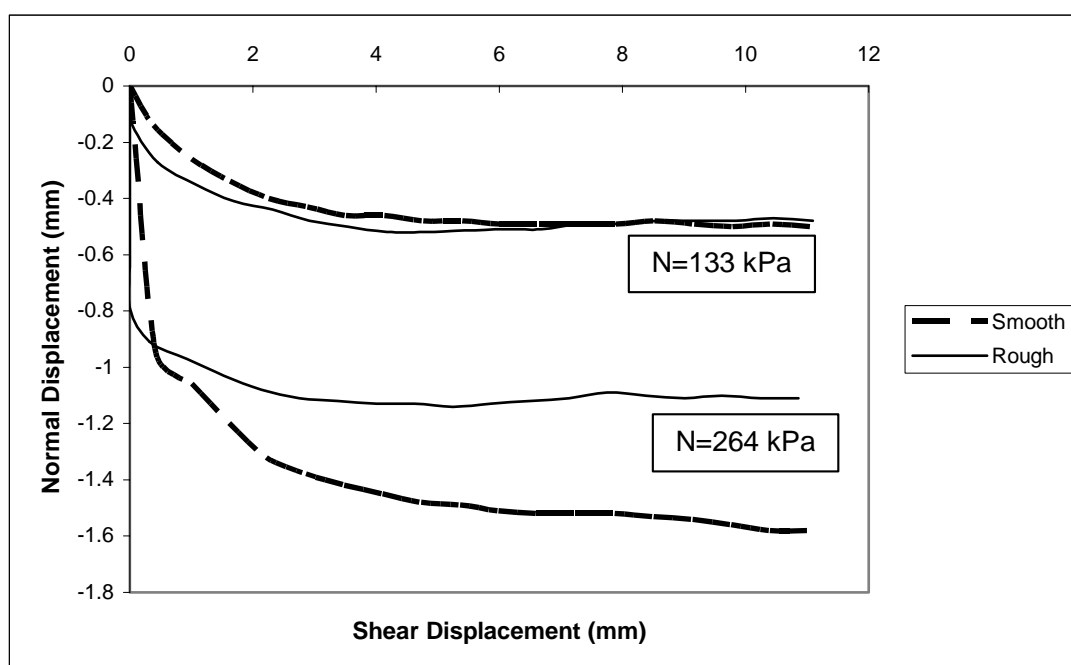


**Figure 4.21:** Normal versus shear displacement, for shearing of different joint-infill boundaries

Comparison was made between the shear resistances of the infill material alone with that of the joint-infill boundary. From Figure 4.15 (a) and (b), the average shear strength of the infill material alone at 10 mm shear displacement was found to be 114 kPa (at  $\sigma_n = 133$  kPa) and 241 kPa (at  $\sigma_n = 264$  kPa). From Figure 4.19, the friction between the infill and the smooth joint surface was determined to be 90 kPa (at  $\sigma_n = 133$  kPa). Similarly, at normal stress of 264 kPa, the shear stress for the

contact between smooth joint and infill was found to be 173 kPa. It proves that a smooth joint surface imposes minimal sliding resistance to the infill particles, and laboratory test data indicates that the resulting shear strength at this boundary condition can be smaller than the shear strength of the infill material alone. In other words, the weakest shearing plane for a filled joint system may not necessarily be within the infill layer. Thus, it can be inferred that the lower limit for the shear strength envelope of a filled joint system can occur along the joint-infill boundary when the interfacing joint surface is relatively smooth, compared to the infill grading.

## **CHAPTER 5**

### **CONCLUSIONS AND RECOMMENDATIONS**

#### **5.1 Introduction**

Filled joint is a common discontinuity plane encountered in excavations of rock mass. Its discrete and unique properties have been the main reasons for its complex behaviour under loading. To comprehend this problem, the typical deformational behaviours of filled joint under shear and normal load must be verified. This research has been successfully carried out to verify and understand the general behaviour of filled joint, through laboratory tests on physical model of filled joint. The effects of the main constitutive components of filled joint on the behaviours of filled joint were also characterised.



## 5.2 Conclusions

Based on the field study on actual filled joints and laboratory tests on model filled joints, several conclusions can be made.

There are several essential components of a filled joint system, together with their influence on the behaviours filled joint have been identified and assessed. These include roughness of the joint surface and, type and thickness of infill material in the joint aperture are thought to be the main controlling components. With regard to shear loading, the magnitude of the applied normal stress was also found to dictate the shear strength and deformational behaviour filled joint.

Laboratory investigations showed that the shear strength of smooth joint filled with granular infill is slightly higher than the shear strength of the infill material alone. It has also been noted that the thickness of the infill does not influence the shear strength of filled joint with smooth joint surface. However, if the thickness of the infill layer is equivalent to a single grain size (i.e. very thin infill), the rolling friction between the infill particles and the joint surface will be even lower than the shear strength of the infill material alone. This leads to the fact that the weakest portion of a filled joint system does not necessarily lie within the infill layer. For smooth joint surface with thin granular infill, the lowest strength lies at the 'infill-joint interface'.

Infill thickness exhibits a significant influence on the compressibility of filled joint system under loading. Thicker infill leads to a larger normal compressibility (and correspondingly a lower compressive strength) of filled joint.

Finally, the characteristics (types) of the infill material and roughness of joint surface are among the main features that control the behaviour of filled joint. The geological and mechanical characteristics of these components must be verified in the field and laboratory in order to predict the joint behaviour. The measurable characteristics include the thickness and grain size of the infill material, and the

roughness of the joint surface. It is thought that these are the components of a filled joint that may be used as classification index for predicting the joint behaviour.

### **5.3 Recommendations**

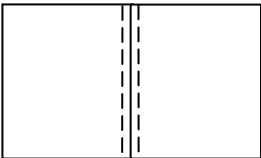
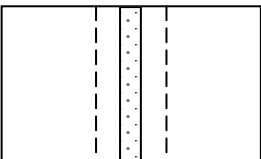
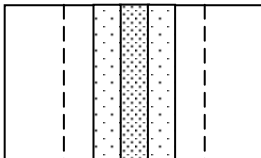
It is thought that further study should be focused on accommodating the *in-situ* conditions of filled joint in laboratory tests. Weathering effect on joint blocks and crushing of the infill particles are among the important elements to be considered in future research. Test procedures, loading configurations (uniaxial and triaxial compression and fatigue loading) and refinement of the model of filled joint should be given due consideration in achieving representative laboratory data.

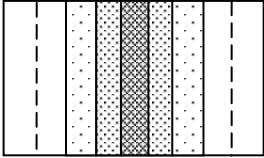
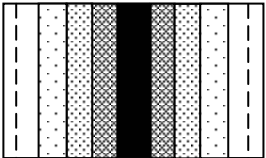
In terms of simulation, a more comprehensive infill condition should be included. The effect of *in-situ* density and moisture content of infill should be taken into consideration.

Investigations should also be carried out to correlate the results from laboratory tests with the actual behaviours of filled joint in the field. More elaborate tests on other types of filled joint, perhaps using clay gouge and expansive clays should be conducted to obtain a comprehensive data on filled joint.

## APPENDIX A

**Probable weathering stages of filled joint in granite (after Mohd Amin and Kassim, 1999a)**

Weathering stages	Material – description and grade	Rock mass – Zone and weathering class
Stage 1 	<p><u>Block</u>: stain margin in total blocks indicates weathering starts to penetrate into the joint wall, but rock material is still intact and sound. <b>Grade I</b>.</p> <p><u>Joint</u>: discolouration on joint surfaces. <b>Grade II</b></p>	<p><b>Zone 1</b>: SW with discolouration on joint surfaces</p>
Stage 2 	<p><u>Block</u>: material closer to the joint is highly discoloured. Grain boundaries start to open but material is no friable. Stain margin penetrates deeper.</p> <p><b>Grade I</b> (if volume % of fresh blocks &gt; discoloured volume)</p> <p><u>Joints</u>: surfaces completely discoloured. Joint beginning to open-up with slight sealing of joint wall material. <b>Grade III</b></p>	<p><b>Zone 1</b>: SW with highly discoloured joint surfaces and in material closer to the joint.</p>
Stage 3 	<p><u>Block</u>: Grade II and III layers occur deeper in the block but less than 50% of the block volume. <b>Grade I</b> (approaching Grade II)</p> <p><u>Joint</u>: previously Grade III layer and joint walls begin to disintegrate to friable material.</p>	<p>Between <b>Zone I</b> and approaching <b>Zone II</b>, with moderately &amp; highly decomposed / disintegrated friable material in the joint aperture (specify volume of infill as % of intact joint block)</p>

	<p>Transition from completely discoloured rock to soil.</p> <p>Increase in “effective” joint width due to presence of infill material sealing of joint wall.</p> <p><b>Grade III or IV</b> (depend on vol. %)</p>	
<p>Stage 4</p> 	<p><b>Block:</b> Layer of Grade II and III cover more than 50% of block volume. Compare vol. % of Grade II and III.</p> <p><b>Grade II</b> (slightly weathered material is dominant)</p> <p><b>Joint:</b> Filled with highly and completely decomposed ‘ disintegrated material Grade IV &amp; V (previously Grade III and IV, respectively) original texture still intact. Grade V (if completely weathered material is dominant)</p>	<p><b>Zone 2:</b> (if vol. % of dominant infill material &lt; than the slightly weathered block), joint is filled with highly and completely decomposed / disintegrated material (specify volume of infill as % of slightly weathered blocks)</p>
<p>Stage 5</p> 	<p><b>Block:</b> Volume of Grade II and III cover more than 50% of block. Probably at this stage, Grade III material is more dominant than Grade II. Blocks almost completely affected by weathering. <b>Grade III.</b></p> <p><b>Joint:</b> Joint aperture is filled with three different grades of material; highly and completely decomposed ‘ disintegrated materials and residual soil (with original texture destroyed).</p> <p><b>Grade V or VI</b> (whichever is dominant)</p>	<p><b>Zone II</b> but approaching <b>Zone III.</b> Joint is filled with completely decomposed / disintegrated materials and residual soil (specify total volume of infill as % of blocks). Note: if volume of infill is greater than block then, the most dominant infill grade material dictates the zone grade.</p>

**APPENDIX B**

Comparison of Uniaxial Compressive and Uniaxial Tensile Strengths of Rocks (Pitts, 1984)

<b>Rock Type</b>	<b>UCS (MN/m<sup>2</sup>)</b>	<b>UTS (MN/m<sup>2</sup>)</b>
Granite	100-250	7-25
Dolerite	200-350	15-35
Basalt	150-300	10-30
Sandstones	20-170	4-25
Mudrocks	10-100	2-10
Limestones	30-250	5-25
Gneisses	50-200	5-20

### APPENDIX C

**Corrections for reducing measured Schmidt hammer rebound (R) when the hammer is not used vertically downwards (After Brown, 1981)**

Rebound, r	Downwards		Upwards		Horizontal x= 0
	x= -90	x= -45	x= +90	x= +45	
10	0	-0.8		-	-3.2
20	0	-0.9	-8.8	-6.9	-3.4
30	0	-0.8	-7.8	-6.2	-3.1
40	0	-0.7	-6.6	-5.3	-2.7
50	0	-0.6	-5.3	-4.3	-2.2
60	0	-0.4	-4	-3.3	-1.7

## APPENDIX D

### Weathering Grade and Rock Properties (after Waltham, 2003)

Grade of Weathering		I	II	III	IV	V
Granite: unconfined compressive strength	MPa	250	150	5-100	2-15	
Triassic sandstone: unconfined compressive strength	MPa	30	15	5	2	<1
Carboniferous sandstone: rock quality designation	%	80	70	50	20	0
Chalk: standard penetration test	N	>35	30	22	17	<15
Chalk: safe bearing pressure	kPa	1000	750	400	200	75
Triassic mudstone: safe bearing pressure	kPa	400	250	150	50	
Triassic mudstone: clay particle fraction	%	10-35		10-35	30-50	

## APPENDIX E

Strength classification based on point load index (Broch and Franklin, 1972)

Strength Classification	Is (MN/m <sup>2</sup> )	Equivalent UCS (MN/m <sup>2</sup> )
Very strong	>6.7	>100
Strong	3.35-6.7	50-100
Moderately strong	0.85-3.35	12.5-50
Moderately weak	0.4-0.85	5-12.5
Weak	0.12-0.4	1.25-5
Very weak rock or hard soil	0.05-0.12	0.6-1.25

Unconfined compressive strength (UCS) of the main rock types (McLean & Gribble, 1979).

Descriptive Terms	UCS (MPa)	Rock Types
<b>Very weak rock.</b>	< 1.25	Some weakly compacted sedimentary rocks, some very highly weathered igneous or metamorphic rocks, boulder-clays.  Some sedimentary rocks, some foliated metamorphic rocks, highly weathered igneous and metamorphic rocks.  Some low-grade metamorphic rocks, marbles, some strongly cemented sandstones (silica cement), some weathered and metamorphic igneous rocks.  Mainly plutonic, hypabyssal and extrusive igneous rocks (medium to coarse grained), sedimentary quartzites, strong slate, gneisses.  Fine-grained igneous rock, metamorphic quartzites, some hornfelses.
<b>Weak rock.</b>	1.25 – 5.0.	
<b>Moderately weak rock</b>	5.0 – 12.5	
<b>Moderately strong rock</b>	12.5 – 50.0	
<b>Strong rock.</b>	50 – 100	
<b>Very strong rock.</b>	100 – 200	
<b>Extremely strong rock.</b>	> 200	



Categorization and description of rock based on its uniaxial compressive strength  
(Brown, 1981)

<b>Grade</b>	<b>Description</b>	<b>Field identification</b>	<b>Approx. range of uniaxial compressive strength (MPa)</b>
R0	Extremely weak rock	Indented by thumbnail	0.25 – 1.0
R1	Very weak rock	Crumbles under firm blows with point of geological hammer, can be peeled by a pocket knife	1.0 – 5.0
R2	Weak rock	Can be peeled by a pocket knife with difficulty, shallow indentations made by firm blow with point of geological hammer	5.0 – 25
R3	Medium strong rock	Cannot be scraped or peeled with a pocket knife, specimen can be fractured with single firm blow of geological hammer	25 - 50
R4	Strong rock	Specimen requires more than one blow of geological hammer to fracture it	50 – 100
R5	Very strong rock	Specimen requires many blows of geological hammer to fracture it	100 – 250
R6	Extremely strong rock	Specimen can only be chipped with geological hammer	> 250

## APPENDIX F

### Data of Rebound Hammer Test

No.	Rebound number		
	Fresh rock	Weathered Rock	On Joint
1	58	51	22
2	41	28	30
3	54	42	14
4	58	37	28
5	60	53	26
6	61	28	18
7	58	34	32
8	41	44	32
9	63	43	18
<b>Average</b>	<b>55</b>	<b>40</b>	<b>24</b>
<b>Corrected</b>	<b>52.9</b>	<b>37.3</b>	<b>21.0</b>

## APPENDIX G

## Calculation of Surface Roughness (S1)

x	y (cm)	y to min level	Y (to scale)	y <sup>2</sup>	y
0.0	0.65	-0.29	-0.22	0.05	0.22
2.0	0.63	-0.31	-0.24	0.06	0.24
4.0	0.60	-0.34	-0.26	0.07	0.26
6.0	0.70	-0.24	-0.18	0.03	0.18
8.0	0.80	-0.14	-0.11	0.01	0.11
10.0	0.81	-0.13	-0.10	0.01	0.10
12.0	0.83	-0.11	-0.08	0.01	0.08
14.0	0.82	-0.12	-0.09	0.01	0.09
16.0	0.83	-0.11	-0.08	0.01	0.08
18.0	0.82	-0.12	-0.09	0.01	0.09
20.0	0.81	-0.13	-0.10	0.01	0.10
22.0	0.80	-0.14	-0.11	0.01	0.11
24.0	0.82	-0.12	-0.09	0.01	0.09
26.0	0.89	-0.05	-0.04	0.00	0.04
28.0	0.88	-0.06	-0.05	0.00	0.05
30.0	0.83	-0.11	-0.08	0.01	0.08
32.0	0.84	-0.10	-0.08	0.01	0.08
34.0	0.82	-0.12	-0.09	0.01	0.09
36.0	0.83	-0.11	-0.08	0.01	0.08
38.0	0.85	-0.09	-0.07	0.00	0.07
40.0	0.82	-0.12	-0.09	0.01	0.09
42.0	0.86	-0.08	-0.06	0.00	0.06
44.0	0.89	-0.05	-0.04	0.00	0.04
46.0	0.90	-0.04	-0.03	0.00	0.03
48.0	0.90	-0.04	-0.03	0.00	0.03
50.0	0.90	-0.04	-0.03	0.00	0.03
52.0	0.92	-0.02	-0.02	0.00	0.02
54.0	0.90	-0.04	-0.03	0.00	0.03
56.0	0.90	-0.04	-0.03	0.00	0.03
58.0	0.95	0.01	0.01	0.00	0.01
60.0	0.99	0.05	0.04	0.00	0.04
62.0	1.00	0.06	0.05	0.00	0.05
64.0	1.01	0.07	0.05	0.00	0.05
66.0	1.01	0.07	0.05	0.00	0.05
68.0	1.00	0.06	0.05	0.00	0.05
70.0	1.05	0.11	0.08	0.01	0.08

72.0	1.10	0.16	0.12	0.02	0.12
74.0	1.09	0.15	0.12	0.01	0.12
76.0	1.08	0.14	0.11	0.01	0.11
78.0	1.08	0.14	0.11	0.01	0.11
80.0	1.05	0.11	0.08	0.01	0.08
82.0	1.00	0.06	0.05	0.00	0.05
84.0	1.00	0.06	0.05	0.00	0.05
86.0	0.95	0.01	0.01	0.00	0.01
88.0	0.98	0.04	0.03	0.00	0.03
90.0	1.00	0.06	0.05	0.00	0.05
92.0	1.00	0.06	0.05	0.00	0.05
94.0	1.00	0.06	0.05	0.00	0.05
96.0	1.03	0.09	0.07	0.00	0.07
98.0	1.03	0.09	0.07	0.00	0.07
100.0	1.10	0.16	0.12	0.02	0.12
102.0	1.10	0.16	0.12	0.02	0.12
104.0	1.09	0.15	0.12	0.01	0.12
106.0	1.07	0.13	0.10	0.01	0.10
108.0	1.04	0.10	0.08	0.01	0.08
110.0	1.04	0.10	0.08	0.01	0.08
112.0	1.12	0.18	0.14	0.02	0.14
114.0	1.10	0.16	0.12	0.02	0.12
116.0	1.07	0.13	0.10	0.01	0.10
118.0	1.08	0.14	0.11	0.01	0.11
120.0	1.03	0.09	0.07	0.00	0.07
122.0	1.00	0.06	0.05	0.00	0.05
124.0	1.00	0.06	0.05	0.00	0.05
126.0	0.99	0.05	0.04	0.00	0.04
128.0	1.02	0.08	0.06	0.00	0.06
130.0	1.01	0.07	0.05	0.00	0.05
132.0	1.00	0.06	0.05	0.00	0.05
	63.1		<b>TOTAL</b>	<b>0.59</b>	<b>5.35</b>
Av.	<b>0.94</b>		<b>CLA</b>		<b>0.08</b>
<b>JRC</b>	<b>= 2.76 + 78.87</b>		<b>CLA</b>		<b>9.1</b>

## Calculation of Surface Roughness (S2)

x	y (cm)	y to min level	y (to scale)	y <sup>2</sup>	y
0.0	1.10	-0.01	-0.01	0.00	0.01
2.0	1.10	-0.01	-0.01	0.00	0.01
4.0	1.09	-0.02	-0.01	0.00	0.01
6.0	1.04	-0.07	-0.05	0.00	0.05
8.0	1.00	-0.11	-0.08	0.01	0.08
10.0	0.99	-0.12	-0.09	0.01	0.09
12.0	1.03	-0.08	-0.06	0.00	0.06
14.0	1.04	-0.07	-0.05	0.00	0.05
16.0	1.05	-0.06	-0.04	0.00	0.04
18.0	1.08	-0.03	-0.02	0.00	0.02
20.0	1.10	-0.01	-0.01	0.00	0.01
22.0	1.10	-0.01	-0.01	0.00	0.01
24.0	1.10	-0.01	-0.01	0.00	0.01
26.0	1.10	-0.01	-0.01	0.00	0.01
28.0	1.10	-0.01	-0.01	0.00	0.01
30.0	1.08	-0.03	-0.02	0.00	0.02
32.0	1.08	-0.03	-0.02	0.00	0.02
34.0	1.10	-0.01	-0.01	0.00	0.01
36.0	1.12	0.01	0.01	0.00	0.01
38.0	1.10	-0.01	-0.01	0.00	0.01
40.0	1.10	-0.01	-0.01	0.00	0.01
42.0	1.10	-0.01	-0.01	0.00	0.01
44.0	1.05	-0.06	-0.04	0.00	0.04
46.0	1.01	-0.10	-0.07	0.01	0.07
48.0	1.01	-0.10	-0.07	0.01	0.07
50.0	1.01	-0.10	-0.07	0.01	0.07
52.0	1.02	-0.09	-0.06	0.00	0.06
54.0	1.00	-0.11	-0.08	0.01	0.08
56.0	1.03	-0.08	-0.06	0.00	0.06
58.0	1.02	-0.09	-0.06	0.00	0.06
60.0	1.00	-0.11	-0.08	0.01	0.08
62.0	1.01	-0.10	-0.07	0.01	0.07
64.0	1.06	-0.05	-0.04	0.00	0.04
66.0	1.10	-0.01	-0.01	0.00	0.01
68.0	1.09	-0.02	-0.01	0.00	0.01
70.0	1.10	-0.01	-0.01	0.00	0.01
72.0	1.09	-0.02	-0.01	0.00	0.01

74.0	1.10	-0.01	-0.01	0.00	0.01
76.0	1.09	-0.02	-0.01	0.00	0.01
78.0	1.13	0.02	0.01	0.00	0.01
80.0	1.15	0.04	0.03	0.00	0.03
82.0	1.20	0.09	0.06	0.00	0.06
84.0	1.18	0.07	0.05	0.00	0.05
86.0	1.18	0.07	0.05	0.00	0.05
88.0	1.18	0.07	0.05	0.00	0.05
90.0	1.18	0.07	0.05	0.00	0.05
92.0	1.19	0.08	0.06	0.00	0.06
94.0	1.20	0.09	0.06	0.00	0.06
96.0	1.20	0.09	0.06	0.00	0.06
98.0	1.22	0.11	0.08	0.01	0.08
100.0	1.20	0.09	0.06	0.00	0.06
102.0	1.20	0.09	0.06	0.00	0.06
104.0	1.20	0.09	0.06	0.00	0.06
106.0	1.19	0.08	0.06	0.00	0.06
108.0	1.15	0.04	0.03	0.00	0.03
110.0	1.16	0.05	0.04	0.00	0.04
112.0	1.19	0.08	0.06	0.00	0.06
114.0	1.20	0.09	0.06	0.00	0.06
116.0	1.20	0.09	0.06	0.00	0.06
118.0	1.17	0.06	0.04	0.00	0.04
120.0	1.12	0.01	0.01	0.00	0.01
122.0	1.13	0.02	0.01	0.00	0.01
124.0	1.11	0.00	0.00	0.00	0.00
126.0	1.10	-0.01	-0.01	0.00	0.01
128.0	1.13	0.02	0.01	0.00	0.01
130.0	1.10	-0.01	-0.01	0.00	0.01
132.0	1.05	-0.06	-0.04	0.00	0.04
134.0	1.11	0.00	0.00	0.00	0.00
136.0	1.09	-0.02	-0.01	0.00	0.01
138.0	1.10	-0.01	-0.01	0.00	0.01
140.0	1.12	0.01	0.01	0.00	0.01
	78.5		<b>TOTAL</b>	<b>0.14</b>	<b>2.54</b>

Av.	1.11	<b>CLA</b>	<b>0.04</b>
	<b>JRC = 2.76 + 78.87 CLA</b>		<b><u>5.6</u></b>

Calculation of Surface Roughness (S3)

x	y (cm)	y to min level	y (to scale)	y <sup>2</sup>	y
0.0	0.88	-0.17	-0.13	0.02	0.13
2.0	0.89	-0.16	-0.12	0.01	0.12
4.0	0.90	-0.15	-0.11	0.01	0.11
6.0	0.90	-0.15	-0.11	0.01	0.11
8.0	0.90	-0.15	-0.11	0.01	0.11
10.0	0.90	-0.15	-0.11	0.01	0.11
12.0	0.91	-0.14	-0.10	0.01	0.10
14.0	0.92	-0.13	-0.10	0.01	0.10
16.0	0.93	-0.12	-0.09	0.01	0.09
18.0	0.94	-0.11	-0.08	0.01	0.08
20.0	0.96	-0.09	-0.07	0.00	0.07
22.0	0.98	-0.07	-0.05	0.00	0.05
24.0	1.00	-0.05	-0.04	0.00	0.04
26.0	1.02	-0.03	-0.02	0.00	0.02
28.0	1.05	0.00	0.00	0.00	0.00
30.0	1.08	0.03	0.02	0.00	0.02
32.0	1.10	0.05	0.04	0.00	0.04
34.0	1.10	0.05	0.04	0.00	0.04
36.0	1.10	0.05	0.04	0.00	0.04
38.0	1.08	0.03	0.02	0.00	0.02
40.0	1.09	0.04	0.03	0.00	0.03
42.0	1.08	0.03	0.02	0.00	0.02
44.0	1.02	-0.03	-0.02	0.00	0.02
46.0	0.99	-0.06	-0.04	0.00	0.04
48.0	1.00	-0.05	-0.04	0.00	0.04
50.0	1.00	-0.05	-0.04	0.00	0.04
52.0	1.01	-0.04	-0.03	0.00	0.03
54.0	1.02	-0.03	-0.02	0.00	0.02
56.0	1.03	-0.02	-0.01	0.00	0.01
58.0	1.06	0.01	0.01	0.00	0.01
60.0	1.07	0.02	0.01	0.00	0.01
62.0	1.08	0.03	0.02	0.00	0.02
64.0	1.07	0.02	0.01	0.00	0.01
66.0	1.09	0.04	0.03	0.00	0.03
68.0	1.10	0.05	0.04	0.00	0.04

70.0	1.10	0.05	0.04	0.00	0.04
72.0	1.10	0.05	0.04	0.00	0.04
74.0	1.10	0.05	0.04	0.00	0.04
76.0	1.10	0.05	0.04	0.00	0.04
78.0	1.10	0.05	0.04	0.00	0.04
80.0	1.10	0.05	0.04	0.00	0.04
82.0	1.00	-0.05	-0.04	0.00	0.04
84.0	1.00	-0.05	-0.04	0.00	0.04
86.0	1.02	-0.03	-0.02	0.00	0.02
88.0	1.00	-0.05	-0.04	0.00	0.04
90.0	1.00	-0.05	-0.04	0.00	0.04
92.0	0.99	-0.06	-0.04	0.00	0.04
94.0	1.00	-0.05	-0.04	0.00	0.04
96.0	0.99	-0.06	-0.04	0.00	0.04
98.0	1.00	-0.05	-0.04	0.00	0.04
100.0	1.01	-0.04	-0.03	0.00	0.03
102.0	1.06	0.01	0.01	0.00	0.01
104.0	1.09	0.04	0.03	0.00	0.03
106.0	1.10	0.05	0.04	0.00	0.04
108.0	1.09	0.04	0.03	0.00	0.03
110.0	1.09	0.04	0.03	0.00	0.03
112.0	1.10	0.05	0.04	0.00	0.04
114.0	1.11	0.06	0.04	0.00	0.04
116.0	1.09	0.04	0.03	0.00	0.03
118.0	1.09	0.04	0.03	0.00	0.03
120.0	1.09	0.04	0.03	0.00	0.03
122.0	1.15	0.10	0.07	0.01	0.07
124.0	1.17	0.12	0.09	0.01	0.09
126.0	1.17	0.12	0.09	0.01	0.09
128.0	1.17	0.12	0.09	0.01	0.09
130.0	1.18	0.13	0.10	0.01	0.10
132.0	1.19	0.14	0.10	0.01	0.10
134.0	1.19	0.14	0.10	0.01	0.10
136.0	1.19	0.14	0.10	0.01	0.10
	72.2		<b>TOTAL</b>	<b>0.24</b>	<b>3.41</b>
Av.	1.05		<b>CLA</b>		<b>0.05</b>
<b>JRC = 2.76 + 78.87 CLA</b>					<b><u>6.7</u></b>

## Calculation of Surface Roughness (S4)

x	y(cm)	y to min level	y (to scale)	y <sub>2</sub>	y
0.0	0.34	-0.19	-0.15	0.02	0.15
2.0	0.35	-0.18	-0.14	0.02	0.14
4.0	0.36	-0.17	-0.13	0.02	0.13
6.0	0.30	-0.23	-0.18	0.03	0.18
8.0	0.30	-0.23	-0.18	0.03	0.18
10.0	0.29	-0.24	-0.18	0.03	0.18
12.0	0.25	-0.28	-0.22	0.05	0.22
14.0	0.22	-0.31	-0.24	0.06	0.24
16.0	0.20	-0.33	-0.25	0.06	0.25
18.0	0.18	-0.35	-0.27	0.07	0.27
20.0	0.13	-0.40	-0.31	0.09	0.31
22.0	0.17	-0.36	-0.28	0.08	0.28
24.0	0.19	-0.34	-0.26	0.07	0.26
26.0	0.21	-0.32	-0.25	0.06	0.25
28.0	0.22	-0.31	-0.24	0.06	0.24
30.0	0.25	-0.28	-0.22	0.05	0.22
32.0	0.30	-0.23	-0.18	0.03	0.18
34.0	0.31	-0.22	-0.17	0.03	0.17
36.0	0.32	-0.21	-0.16	0.03	0.16
38.0	0.33	-0.20	-0.15	0.02	0.15
40.0	0.40	-0.13	-0.10	0.01	0.10
42.0	0.40	-0.13	-0.10	0.01	0.10
44.0	0.45	-0.08	-0.06	0.00	0.06
46.0	0.48	-0.05	-0.04	0.00	0.04
48.0	0.49	-0.04	-0.03	0.00	0.03
50.0	0.47	-0.06	-0.05	0.00	0.05
52.0	0.48	-0.05	-0.04	0.00	0.04
54.0	0.48	-0.05	-0.04	0.00	0.04
56.0	0.49	-0.04	-0.03	0.00	0.03
58.0	0.50	-0.03	-0.02	0.00	0.02
60.0	0.51	-0.02	-0.02	0.00	0.02
62.0	0.51	-0.02	-0.02	0.00	0.02
64.0	0.50	-0.03	-0.02	0.00	0.02
66.0	0.52	-0.01	-0.01	0.00	0.01
68.0	0.52	-0.01	-0.01	0.00	0.01
70.0	0.51	-0.02	-0.02	0.00	0.02

72.0	0.53	0.00	0.00	0.00	0.00
74.0	0.54	0.01	0.01	0.00	0.01
76.0	0.52	-0.01	-0.01	0.00	0.01
78.0	0.58	0.05	0.04	0.00	0.04
80.0	0.59	0.06	0.05	0.00	0.05
82.0	0.59	0.06	0.05	0.00	0.05
84.0	0.59	0.06	0.05	0.00	0.05
86.0	0.63	0.10	0.08	0.01	0.08
88.0	0.70	0.17	0.13	0.02	0.13
90.0	0.75	0.22	0.17	0.03	0.17
92.0	0.76	0.23	0.18	0.03	0.18
94.0	0.80	0.27	0.21	0.04	0.21
96.0	0.81	0.28	0.22	0.05	0.22
98.0	0.82	0.29	0.22	0.05	0.22
100.0	0.82	0.29	0.22	0.05	0.22
102.0	0.83	0.30	0.23	0.05	0.23
104.0	0.86	0.33	0.25	0.06	0.25
106.0	0.88	0.35	0.27	0.07	0.27
108.0	0.88	0.35	0.27	0.07	0.27
110.0	0.80	0.27	0.21	0.04	0.21
112.0	0.75	0.22	0.17	0.03	0.17
114.0	0.74	0.21	0.16	0.03	0.16
116.0	0.71	0.18	0.14	0.02	0.14
118.0	0.72	0.19	0.15	0.02	0.15
120.0	0.79	0.26	0.20	0.04	0.20
122.0	0.77	0.24	0.18	0.03	0.18
124.0	0.79	0.26	0.20	0.04	0.20
126.0	0.80	0.27	0.21	0.04	0.21
128.0	0.80	0.27	0.21	0.04	0.21
130.0	0.81	0.28	0.22	0.05	0.22
132.0	0.82	0.29	0.22	0.05	0.22
	35.71			1.92	9.63
	0.53		CLA		<u>0.14</u>
	<b>JRC = 2.76 + 78.87 CLA</b>				<u><u>14.1</u></u>

## Calculation of Surface Roughness (S5)

x	y (cm)	y to min level	y (to scale)	y <sup>2</sup>	y
0.0	0.05	-0.10	-0.06	0.00	0.06
2.0	0.04	-0.11	-0.07	0.00	0.07
4.0	0.07	-0.08	-0.05	0.00	0.05
6.0	0.08	-0.07	-0.04	0.00	0.04
8.0	0.09	-0.06	-0.04	0.00	0.04
10.0	0.08	-0.07	-0.04	0.00	0.04
12.0	0.05	-0.10	-0.06	0.00	0.06
14.0	0.06	-0.09	-0.06	0.00	0.06
16.0	0.09	-0.06	-0.04	0.00	0.04
18.0	0.09	-0.06	-0.04	0.00	0.04
20.0	0.08	-0.07	-0.04	0.00	0.04
22.0	0.08	-0.07	-0.04	0.00	0.04
24.0	0.07	-0.08	-0.05	0.00	0.05
26.0	0.09	-0.06	-0.04	0.00	0.04
28.0	0.10	-0.05	-0.03	0.00	0.03
30.0	0.11	-0.04	-0.03	0.00	0.03
32.0	0.12	-0.03	-0.02	0.00	0.02
34.0	0.13	-0.02	-0.01	0.00	0.01
36.0	0.13	-0.02	-0.01	0.00	0.01
38.0	0.17	0.02	0.01	0.00	0.01
40.0	0.18	0.03	0.02	0.00	0.02
42.0	0.18	0.03	0.02	0.00	0.02
44.0	0.18	0.03	0.02	0.00	0.02
46.0	0.18	0.03	0.02	0.00	0.02
48.0	0.15	0.00	0.00	0.00	0.00
50.0	0.12	-0.03	-0.02	0.00	0.02
52.0	0.16	0.01	0.01	0.00	0.01
54.0	0.18	0.03	0.02	0.00	0.02
56.0	0.17	0.02	0.01	0.00	0.01
58.0	0.19	0.04	0.03	0.00	0.03
60.0	0.15	0.00	0.00	0.00	0.00
62.0	0.18	0.03	0.02	0.00	0.02
64.0	0.18	0.03	0.02	0.00	0.02
66.0	0.18	0.03	0.02	0.00	0.02
68.0	0.18	0.03	0.02	0.00	0.02
70.0	0.19	0.04	0.03	0.00	0.03
72.0	0.17	0.02	0.01	0.00	0.01
74.0	0.18	0.03	0.02	0.00	0.02
76.0	0.17	0.02	0.01	0.00	0.01
78.0	0.19	0.04	0.03	0.00	0.03
80.0	0.19	0.04	0.03	0.00	0.03
82.0	0.15	0.00	0.00	0.00	0.00
84.0	0.13	-0.02	-0.01	0.00	0.01
86.0	0.13	-0.02	-0.01	0.00	0.01
88.0	0.12	-0.03	-0.02	0.00	0.02
90.0	0.13	-0.02	-0.01	0.00	0.01
92.0	0.13	-0.02	-0.01	0.00	0.01
94.0	0.18	0.03	0.02	0.00	0.02
96.0	0.16	0.01	0.01	0.00	0.01

98.0	0.13	-0.02	-0.01	0.00	0.01
100.0	0.12	-0.03	-0.02	0.00	0.02
102.0	0.14	-0.01	-0.01	0.00	0.01
104.0	0.19	0.04	0.03	0.00	0.03
106.0	0.17	0.02	0.01	0.00	0.01
108.0	0.16	0.01	0.01	0.00	0.01
110.0	0.13	-0.02	-0.01	0.00	0.01
112.0	0.16	0.01	0.01	0.00	0.01
114.0	0.20	0.05	0.03	0.00	0.03
116.0	0.20	0.05	0.03	0.00	0.03
118.0	0.17	0.02	0.01	0.00	0.01
120.0	0.16	0.01	0.01	0.00	0.01
122.0	0.17	0.02	0.01	0.00	0.01
124.0	0.17	0.02	0.01	0.00	0.01
126.0	0.20	0.05	0.03	0.00	0.03
128.0	0.20	0.05	0.03	0.00	0.03
130.0	0.20	0.05	0.03	0.00	0.03
132.0	0.20	0.05	0.03	0.00	0.03
134.0	0.19	0.04	0.03	0.00	0.03
136.0	0.15	0.00	0.00	0.00	0.00
138.0	0.15	0.00	0.00	0.00	0.00
140.0	0.13	-0.02	-0.01	0.00	0.01
142.0	0.10	-0.05	-0.03	0.00	0.03
144.0	0.10	-0.05	-0.03	0.00	0.03
146.0	0.14	-0.01	-0.01	0.00	0.01
148.0	0.18	0.03	0.02	0.00	0.02
150.0	0.21	0.06	0.04	0.00	0.04
152.0	0.25	0.10	0.06	0.00	0.06
154.0	0.24	0.09	0.06	0.00	0.06
156.0	0.20	0.05	0.03	0.00	0.03

$$0.15 \quad \text{CLA} \quad 0.02$$

$$\text{JRC} = 2.76 + 78.87 \text{ CLA} = 4.7$$

## APPENDIX H

### Specific Gravity of Infill Particles

Specimen Reference		1	2	3
Pycnometer number	bottle	1694	1900	1388
	cover	1881	1674	1257
Mass of bottle+soil+water	$m_3$	85.512	85.565	79.827
Mass of bottle+soil	$m_2$	38.715	41.209	33.379
Mass of bottle full of water	$m_4$	79.900	79.646	75.888
Mass of bottle	$m_1$	29.539	31.363	26.387
Mass of soil	$m_2-m_1$	9.176	9.846	6.992
Mass of water in full bottle	$m_4-m_1$	50.361	48.283	49.501
Mass of water used	$m_3-m_2$	46.797	44.356	46.448
Volume of soil particles	$(m_4-m_1)-(m_3-m_2)$	3.564	3.927	3.053
Particle density	$(m_2-m_1)/[(m_4-m_1)-(m_3-m_2)]$	2.575	2.507	2.290

Specimen Reference		4	5	6
Pycnometer number	bottle	1808	1862	1855
	cover	1808	1862	1855
Mass of bottle+soil+water	$m_3$	85.246	83.682	86.958
Mass of bottle+soil	$m_2$	38.468	38.147	41.221
Mass of bottle full of water	$m_4$	79.512	78.381	82.130
Mass of bottle	$m_1$	29.081	29.393	32.551
Mass of soil	$m_2-m_1$	9.387	8.754	8.670
Mass of water in full bottle	$m_4-m_1$	50.431	48.988	49.579
Mass of water used	$m_3-m_2$	46.778	45.535	45.737
Volume of soil particles	$(m_4-m_1)-(m_3-m_2)$	3.653	3.453	3.842
Particle density	$(m_2-m_1)/[(m_4-m_1)-(m_3-m_2)]$	2.570	2.535	2.257



Specimen Reference		7	8	9	10
Pycnometer number	bottle	1459	34	1567	1426
	cover	1459	2784	1648	1426
Mass of bottle+soil+water	$m_3$	154.251	165.614	151.916	155.482
Mass of bottle+soil	$m_2$	66.481	76.480	64.925	66.131
Mass of bottle full of water	$m_4$	136.250	147.882	134.274	137.496
Mass of bottle	$m_1$	36.514	46.502	34.938	36.193
Mass of soil	$m_2-m_1$	29.967	29.978	29.987	29.938
Mass of water in full bottle	$m_4-m_1$	99.736	101.380	99.336	101.303
Mass of water used	$m_3-m_2$	87.770	89.134	86.991	89.351
Volume of soil particles	$(m_4-m_1)-(m_3-m_2)$	11.966	12.246	12.345	11.952
Particle density	$(m_2-m_1)/[(m_4-m_1)-(m_3-m_2)]$	2.504	2.448	2.429	2.505

Averaged Specific Density = **2.46**

## APPENDIX I

### Result of Static Compression Test

	<b>SC1</b>	<b>SC2</b>	<b>SC3</b>	<b>SC4</b>	<b>SC5</b>	<b>SC6</b>
Normal Load (kg)	20	20	20	20	20	20
Normal Stress (kPa)	108.41	108.41	108.41	108.91	108.91	108.91
Sample Weight (g)	300	300	300	400	400	400
Initial Height (mm)	91	92	90	134	137	133
Final Height (mm)	90	91	89	130	134	129
Initial Volume (m <sup>3</sup> )	0.193	0.195	0.191	0.285	0.290	0.282
Final Volume (m <sup>3</sup> )	0.191	0.193	0.189	0.276	0.285	0.274
Initial Void Ratio	0.552	0.570	0.535	0.715	0.753	0.702
Final Void Ratio	0.535	0.552	0.52	0.66	0.71	0.65
<b>Compressibility (%)</b>	<b>3.09</b>	<b>3.00</b>	<b>3.19</b>	<b>7.16</b>	<b>5.10</b>	<b>7.29</b>

	<b>SC7</b>	<b>SC8</b>	<b>SC9</b>	<b>SC10</b>	<b>SC11</b>	<b>SC12</b>
Normal Load (kg)	25	25	25	25	25	25
Normal Stress (kPa)	132.00	132.00	132.00	132.00	132.00	132.00
Sample Weight (g)	300	300	300	400	400.00	400.00
Initial Height (mm)	97	94	98	124	129	127
Final Height (mm)	93	91	95	119	123	122
Initial Volume (m <sup>3</sup> )	0.206	0.200	0.208	0.263	0.274	0.270
Final Volume (m <sup>3</sup> )	0.198	0.194	0.202	0.253	0.261	0.259
Initial Void Ratio	0.655	0.604	0.672	0.587	0.651	0.625
Final Void Ratio	0.587	0.552	0.621	0.523	0.57	0.56
<b>Compressibility (%)</b>	<b>10.42</b>	<b>8.48</b>	<b>7.62</b>	<b>10.91</b>	<b>11.80</b>	<b>10.24</b>

	<b>SC13</b>	<b>SC14</b>	<b>SC15</b>	<b>SC16</b>	<b>SC17</b>	<b>SC18</b>
Normal Load (kg)	25	25	25	25	25	25
Normal Stress (kPa)	132.00	132.00	132.00	131.5	131.50	131.50
Sample Weight (g)	400	400	400	500.00	500.00	500
Initial Height (mm)	124	129	127	164	171	173
Final Height (mm)	119	123	122	155	161	163
Initial Volume (m3)	0.263	0.274	0.270	0.348	0.363	0.367
Final Volume (m3)	0.253	0.261	0.259	0.329	0.342	0.346
Initial Void Ratio	0.587	0.651	0.625	0.679	0.750	0.771
Final Void Ratio	0.523	0.574	0.561	0.597	0.658	0.679
<b>Compressibility (%)</b>	<b>10.91</b>	<b>11.80</b>	<b>10.24</b>	<b>13.57</b>	<b>13.64</b>	<b>13.28</b>

	<b>SC19</b>	<b>SC20</b>	<b>SC21</b>	<b>SC22</b>	<b>SC23</b>	<b>SC24</b>
Normal Load (kg)	30	30	30	30	30	30
Normal Stress (kPa)	154.60	154.60	154.60	154.60	154.60	154.60
Sample Weight (g)	300	300	300	400	400.00	400.00
Initial Height (mm)	98	96	94	124	128	126
Final Height (mm)	93	91	90	116	121	119
Initial Volume (m3)	0.208	0.204	0.200	0.263	0.272	0.268
Final Volume (m3)	0.198	0.193	0.191	0.246	0.257	0.253
Initial Void Ratio	0.672	0.638	0.604	0.587	0.638	0.612
Final Void Ratio	0.587	0.552	0.535	0.484	0.548	0.523
<b>Compressibility (%)</b>	<b>12.70</b>	<b>13.37</b>	<b>11.30</b>	<b>17.45</b>	<b>14.04</b>	<b>14.63</b>

	<b>SC25</b>	<b>SC26</b>	<b>SC27</b>
Normal Load (kg)	30	30	30
Normal Stress (kPa)	155.10	155.10	155.10
Sample Weight (g)	500.00	500.00	500.00
Initial Height (mm)	171	170	174
Final Height (mm)	158	157	161
Initial Volume (m3)	0.363	0.361	0.370
Final Volume (m3)	0.336	0.333	0.342
Initial Void Ratio	0.750	0.740	0.781
Final Void Ratio	0.617	0.607	0.648
<b>Compressibility (%)</b>	<b>17.73</b>	<b>17.98</b>	<b>17.04</b>

## APPENDIX J

Data of Preliminary Test (Direct Shear Test on Preloaded Infill Material Alone)

(Notation: I = Infill material alone; A =  $\sigma_n=133\text{kPa}$ ; B =  $\sigma_n=264\text{kPa}$ )

IA1

Shear Displ (mm)	Shear Load (N)	Normal Displ (mm)
0.00	0	0.00
0.16	294	-0.08
0.78	453	-0.29
1.42	561	-0.42
2.03	645	-0.54
2.66	717	-0.62
3.28	774	-0.69
3.91	828	-0.75
4.53	891	-0.79
5.16	939	-0.82
5.78	981	-0.83
6.42	1020	-0.83
7.05	1053	-0.83
7.68	1071	-0.81
8.30	1086	-0.81
8.93	1098	-0.77
9.56	1107	-0.77
10.20	1116	-0.73
10.82	1113	-0.71
11.45	1104	-0.70
12.09	1098	-0.67
12.71	1068	-0.67
13.35	1062	-0.66

IA2

Shear Displ (mm)	Shear Load (N)	Normal Displ (mm)
0.00	0	0.00
0.14	261	-0.03
0.76	456	-0.20
1.40	573	-0.34
2.04	663	-0.45
2.67	750	-0.53
3.29	807	-0.59
3.93	858	-0.63
4.57	909	-0.65
5.22	951	-0.66
5.86	996	-0.67
6.50	1026	-0.66
7.13	1041	-0.67
7.76	1074	-0.65
8.41	1092	-0.64
9.05	1110	-0.63
9.68	1128	-0.61
10.33	1155	-0.60
10.95	1161	-0.59
11.59	1161	-0.58
12.23	1164	-0.57
12.87	1173	-0.55

IA3

Shear Displ (mm)	Shear Load (N)	Normal Displ (mm)
0	0	0.00
0.15	278	-0.05
0.77	455	-0.25
1.41	567	-0.38
2.04	654	-0.50
2.67	734	-0.58
3.29	791	-0.64
3.92	843	-0.69
4.55	900	-0.72
5.19	945	-0.74
5.82	989	-0.75
6.46	1023	-0.75
7.09	1047	-0.75
7.72	1073	-0.73
8.36	1089	-0.73
8.99	1104	-0.70
9.62	1118	-0.69
10.27	1136	-0.67
10.89	1137	-0.65
11.52	1133	-0.64
12.16	1131	-0.62
12.79	1121	-0.61

IA4

Shear Displ (mm)	Shear Load (N)	Normal Displ (mm)
0.00	0	0.00
0.16	289	-0.03
0.76	473	-0.21
1.39	590	-0.36
1.99	680	-0.48
2.61	763	-0.56
3.21	822	-0.63
3.83	877	-0.67
4.44	936	-0.69
5.06	983	-0.70
5.66	1028	-0.71
6.29	1064	-0.70
6.91	1089	-0.71
7.53	1115	-0.69
8.13	1133	-0.68
8.75	1148	-0.67
9.37	1162	-0.65
10.00	1181	-0.64
10.60	1182	-0.63
11.22	1178	-0.61
11.85	1176	-0.60
12.46	1165	-0.58

IB1

Shear Displ (mm)	Shear Load (N)	Normal Displ (mm)
0.00	0	0.00
0.15	387	-0.85
0.75	729	-1.08
1.38	966	-1.25
2.00	1152	-1.37
2.63	1332	-1.47
3.26	1476	-1.55
3.91	1593	-1.62
4.53	1692	-1.68
5.17	1791	-1.72
5.82	1890	-1.74
6.48	1959	-1.76
7.12	2028	-1.77
7.76	2076	-1.77
8.39	2133	-1.77
9.02	2163	-1.76
9.68	2190	-1.74
10.34	2208	-1.72
10.98	2223	-1.70
11.63	2223	-1.68
12.26	2214	-1.67
12.89	2190	-1.65

IB2

Shear Displ (mm)	Shear Load (N)	Normal Displ (mm)
0.00	0	0.00
0.19	597	-0.78
0.71	840	-0.97
1.38	1032	-1.15
2.07	1188	-1.31
2.68	1329	-1.40
3.32	1446	-1.49
3.94	1557	-1.54
4.57	1644	-1.60
5.19	1719	-1.65
5.82	1782	-1.67
6.44	1842	-1.69
7.07	1893	-1.70
7.68	1938	-1.69
8.31	1980	-1.69
8.93	2022	-1.69
9.55	2040	-1.69
10.15	2064	-1.66
10.78	2085	-1.65
11.41	2100	-1.60
12.02	2118	-1.58

IB3

Shear Displ (mm)	Shear Load (N)	Normal Displ (mm)
0.00	0	0.00
0.17	492	-0.81
0.73	785	-1.02
1.38	999	-1.20
2.04	1170	-1.34
2.66	1331	-1.44
3.29	1461	-1.52
3.93	1575	-1.58
4.55	1668	-1.64
5.18	1755	-1.69
5.82	1836	-1.70
6.46	1901	-1.73
7.10	1961	-1.74
7.72	2007	-1.73
8.35	2057	-1.73
8.98	2093	-1.73
9.62	2115	-1.72
10.25	2136	-1.69
10.88	2154	-1.67
11.52	2162	-1.64
12.14	2166	-1.62
12.89	2190	-1.62

IB4

Shear Displ (mm)	Shear Load (N)	Normal Displ (mm)
0.00	0	0.00
0.19	379	-0.87
0.72	714	-1.09
1.39	947	-1.28
2.09	1129	-1.43
2.71	1306	-1.54
3.35	1446	-1.63
3.98	1561	-1.69
4.62	1658	-1.75
5.24	1755	-1.81
5.88	1852	-1.82
6.50	1920	-1.85
7.14	1987	-1.86
7.76	2034	-1.85
8.39	2090	-1.85
9.02	2120	-1.85
9.65	2146	-1.84
10.25	2164	-1.81
10.89	2179	-1.79
11.52	2179	-1.75
12.14	2170	-1.73
12.84	2146	-1.73

## APPENDIX K

Data of Preliminary Test (Direct Shear Test on Non-Preloaded Infill Material Alone)

(Notation: X = Non-preloaded; I = Infill material alone; A =  $\sigma_n = 133\text{kPa}$ ; B =  $\sigma_n = 264\text{kPa}$ )

XIA1

Shear Displ (mm)	Shear Load (N)	Normal Displ (mm)
0.00	0	0
0.00	0	-2.11
0.48	318	-2.69
1.10	435	-3.2
1.72	528	-3.48
2.35	618	-3.79
2.97	693	-3.92
3.60	762	-4.06
4.22	822	-4.18
4.85	885	-4.27
5.46	939	-4.29
6.09	987	-4.31
6.73	1029	-4.31
7.36	1065	-4.29
7.99	1104	-4.3
8.62	1104	-4.29
9.25	1116	-4.28
9.89	1143	-4.27
10.51	1149	-4.27
11.15	1152	-4.28

XIA2

Shear Displ (mm)	Shear Load (N)	Normal Displ (mm)
0.00	0	0.00
0.00	0	-2.28
0.64	296	-2.88
1.10	404	-3.39
1.63	491	-3.71
2.23	575	-4.04
2.82	644	-4.22
3.42	708	-4.38
4.01	764	-4.47
4.61	823	-4.55
5.19	873	-4.61
5.79	918	-4.63
6.39	957	-4.64
6.99	990	-4.65
7.59	1027	-4.63
8.19	1046	-4.63
8.79	1064	-4.64
9.40	1063	-4.61
9.98	1068	-4.61
10.59	1071	-4.60



XIA3

Shear Displ (mm)	Shear Load (N)	Normal Displ (mm)
0.00	0	0.00
0.00	3	-2.04
0.82	307	-3.22
1.22	420	-3.63
1.77	527	-4.00
2.35	624	-4.22
2.97	698	-4.47
3.60	789	-4.6
4.22	844	-4.65
4.85	899	-4.68
5.46	929	-4.71
6.09	972	-4.80
6.73	1009	-4.84
7.36	1052	-4.78
7.99	1080	-4.80
8.62	1113	-4.78
9.25	1125	-4.75
9.89	1120	-4.72
10.42	1120	-4.69

XIB1

Shear Displ (mm)	Shear Load (N)	Normal Displ (mm)
0.00	0	-0.01
0.00	2	-3.00
0.23	387	-3.87
0.82	750	-4.56
1.43	960	-4.91
2.05	1137	-5.16
2.67	1278	-5.37
3.30	1380	-5.51
3.91	1497	-5.58
4.53	1614	-5.65
5.15	1743	-5.70
5.78	1830	-5.72
6.39	1917	-5.72
7.03	1968	-5.70
7.66	2031	-5.72
8.29	2079	-5.75
8.91	2109	-5.75
9.55	2133	-5.78
10.18	2160	-5.72
10.81	2172	-5.75
11.45	2187	-4.69
12.08	2178	-4.67

XIB2

Shear Displ (mm)	Shear Load (N)	Normal Displ (mm)
0.00	0	-0.00
0.00	0	-3.30
0.35	310	-3.92
0.88	650	-4.42
1.40	890	-4.67
2.05	1080	-4.95
2.64	1230	-5.14
3.24	1390	-5.30
3.91	1510	-5.42
4.47	1640	-5.44
5.07	1760	-5.51
5.70	1849	-5.53
6.30	1928	-5.56
6.87	1984	-5.56
7.56	2040	-5.53
8.22	2098	-5.56
8.80	2160	-5.56
9.39	2190	-5.58
10.08	2210	-5.58
10.68	2230	-5.60
11.45	2209	-4.71
12.08	2215	-4.69

XIB3

Shear Displ (mm)	Shear Load (N)	Normal Displ (mm)
0.00	0	-0.00
0.00	5	-3.59
0.37	305	-4.18
0.96	645	-4.83
1.57	888	-5.16
2.16	1081	-5.37
2.78	1228	-5.67
3.38	1387	-5.72
4.00	1506	-5.78
4.58	1628	-5.80
5.17	1745	-5.86
5.77	1835	-5.83
6.36	1914	-5.86
6.93	1967	-5.91
7.54	2025	-5.89
8.16	2082	-5.89
8.79	2134	-5.86
9.42	2172	-5.83
10.12	2191	-5.89
10.77	2198	-5.86
11.45	2192	-4.71
12.08	2194	-4.69

## APPENDIX L

Data of Preliminary Test (Direct Shear Test on Smooth Joint-Infill Boundary)

(Notation: SSRC = Smooth Soil Rock Contact; A =  $\sigma_n=133\text{kPa}$ ; B =  $\sigma_n=264\text{kPa}$ )

### SSRCA1

Shear Displ (mm)	Shear Load (N)	Normal Displ (mm)
0.00	0	0
0.38	345	-0.14
1.00	465	-0.26
1.63	576	-0.34
2.25	648	-0.4
2.88	693	-0.43
3.51	735	-0.46
4.13	780	-0.46
4.76	798	-0.48
5.39	837	-0.48
6.01	855	-0.49
6.65	888	-0.49
7.27	873	-0.49
7.9	876	-0.49
8.52	888	-0.48
9.16	891	-0.49
9.79	894	-0.5
10.43	888	-0.49
11.05	903	-0.5

### SSRCA2

Shear Displ (mm)	Shear Load (N)	Normal Displ (mm)
0.00	0	0.00
0.47	384	-0.10
1.08	510	-0.23
1.70	609	-0.31
2.33	693	-0.36
2.96	765	-0.39
3.59	843	-0.42
4.21	876	-0.44
4.84	879	-0.45
5.46	894	-0.46
6.09	882	-0.47
6.72	882	-0.48
7.36	888	-0.46
7.98	888	-0.48
8.60	891	-0.49
9.23	891	-0.49
9.86	915	-0.50
10.51	924	-0.50
11.14	936	-0.50

SSRCB1

Shear Displ (mm)	Shear Load (N)	Normal Displ (mm)
0.00	0	0.00
0.42	396	-0.95
1.00	810	-1.06
1.61	1065	-1.20
2.22	1251	-1.32
2.86	1383	-1.38
3.48	1494	-1.42
4.10	1545	-1.45
4.73	1590	-1.48
5.36	1623	-1.49
5.98	1656	-1.51
6.60	1695	-1.52
7.24	1710	-1.52
7.87	1725	-1.52
8.50	1734	-1.53
9.13	1710	-1.54
9.77	1722	-1.56
10.39	1737	-1.58
11.03	1725	-1.58

SSRCB2

Shear Displ (mm)	Shear Load (N)	Normal Displ (mm)
0.00	0	0.00
0.32	276	-0.61
0.47	753	-0.76
1.08	999	-0.89
1.70	1158	-1.00
2.31	1293	-1.08
2.92	1413	-1.13
3.55	1488	-1.17
4.18	1569	-1.23
4.80	1605	-1.24
5.43	1635	-1.26
6.06	1653	-1.26
6.68	1686	-1.28
7.31	1695	-1.29
7.94	1728	-1.32
8.56	1773	-1.32
9.20	1788	-1.33
9.83	1803	-1.34
10.47	1836	-1.35

## APPENDIX M

Data of Preliminary Test (Direct Shear Test on Rough Joint-Infill Boundary)

(Notation: RSRC = Rough Soil Rock Contact; A =  $\sigma_n=133\text{kPa}$ ; B =  $\sigma_n=264\text{kPa}$ )

RSRCA1

Shear Displ (mm)	Shear Load (N)	Normal Displ (mm)
0.00	0	0.00
0.00	342	-0.12
0.45	528	-0.27
1.07	636	-0.35
1.69	735	-0.41
2.32	828	-0.44
2.92	894	-0.48
3.54	987	-0.5
4.17	1047	-0.52
4.81	1074	-0.52
6.06	1137	-0.51
6.68	1134	-0.51
7.3	1152	-0.49
7.93	1155	-0.49
8.57	1134	-0.48
9.2	1116	-0.48
9.84	1104	-0.48
10.45	1104	-0.47
11.09	1098	-0.48

RSRCA2

Shear Displ (mm)	Shear Load (N)	Normal Displ (mm)
0.00	0	0.00
0.00	291	-0.12
0.00	486	-0.27
0.00	621	-0.38
0.63	768	-0.46
1.25	900	-0.50
1.86	909	-0.53
2.49	936	-0.55
3.11	1002	-0.55
3.74	1047	-0.54
4.37	1146	-0.52
4.99	1125	-0.52
5.61	1164	-0.51
6.24	1182	-0.50
6.86	1188	-0.49
7.49	1200	-0.48
8.13	1200	-0.47
8.76	1182	-0.45
10.01	1173	-0.43
10.64	1134	-0.43

RSRCB1

Shear Displ (mm)	Shear Load (N)	Normal Displ (mm)
0.00	0	0.00
0.00	498	-0.61
0.00	894	-0.79
0.32	1152	-0.91
0.93	1383	-0.97
1.53	1590	-1.03
2.14	1794	-1.08
2.75	1857	-1.11
3.38	1944	-1.12
4.01	1989	-1.13
4.62	2070	-1.13
5.25	2118	-1.14
5.86	2136	-1.13
6.50	2139	-1.12
7.13	2172	-1.11
7.75	2187	-1.09
8.38	2220	-1.10
9.01	2154	-1.11
9.61	2139	-1.10
10.24	2166	-1.11
10.86	2154	-1.11

RSRCB2

Shear Displ (mm)	Shear Load (N)	Normal Displ (mm)
0.00	0	0.00
0.29	465	-0.64
0.88	828	-0.81
1.49	1095	-0.94
2.12	1326	-1.02
2.73	1491	-1.09
3.37	1617	-1.15
3.97	1818	-1.19
4.61	1911	-1.22
5.22	2016	-1.25
5.86	2076	-1.26
6.48	2133	-1.27
7.11	2184	-1.28
7.72	2250	-1.29
8.36	2283	-1.30
9.01	2313	-1.30
9.64	2334	-1.28
10.26	2376	-1.28
10.89	2370	-1.26

## REFERENCES

- Aora, V. K. and Trivedi, A. (1992). Effect of Kaolin Gouge on Strength of Jointed Rocks. *Proceedings of Asian Regional Symposium on Rocks Slopes*. 7-11 December 1992. New Delhi, India: pp 21-25.
- Awang, H. (2000). *Uniaxial Deformation of Unfilled And Filled Joint*. Master Degree Report: Universiti of Teknologi Malaysia.
- Bandis, S. C., Lumsden, A. C. and Barton, N. R. (1983). Fundamental of Rock Joint Deformation. *International Journal of Rock Mechanics and Mining Sciences & Geomechanical Abstracts*. Vol. 20, No. 6: pp. 249-268.
- Barton, N. (1974). A Review of the Shear Strength of Filled Discontinuities in Rock. Publication No. 105. Oslo: Norwegian Geotechnical Institute.
- Barton, N. (1976). The Shear Strength of Rock and Rock Joints. *International Journal of Rock Mechanics and Mining Sciences & Geomechanical Abstracts*. Vol. 13: pp. 255-279
- Barton, N. (1978). Suggested Methods for the Quantitative Description of Discontinuities in Rock Masses. *International Journal of Rock Mechanics and Mining Sciences & Geomechanical Abstracts*. Vol. 15: pp. 319-368.
- Barton, N. and Choubey, V. (1977). The Shear Strength of Rock Joints in Theory and Practice. *Rock Mechanics*. Vol. 10: 1-54.

- Beavis, F. C. (1992). *Engineering Geology*. Komoo, I. and Jamaluddin, T. A. (trans). Kuala Lumpur, Malaysia: Dewan Bahasa dan Pustaka, Kementerian Pendidikan Malaysia.
- Bell, F. G. (1983). *Fundamentals of Engineering Geology*. UK: Butterworths.
- Blyth, F. G. H. and de Freitas, M. H. (1984). *A Geology for Engineers*. London, UK: Edward Arnold Ltd.
- Bolton, M. D. (1979). *A Guide to Soil Mechanics*. London, U. K.: Macmillan Press Ltd.
- Brady, B. H. G. and Brown, E. T. (1985). *Rock Mechanics For Underground Mining*. U.K.: George Allen & Unwin (Publishers) Ltd.
- Brekke, T.L. and Howard, T.R. (1972). Stability Problems Caused by Seams and Faults. *Proc. North Am. Rapid Excavation & Tunneling Conference*. Vol. I. New York. pp. 25-41.
- British Standards Institution (1990). *British Standard Methods of Test for Soils for Civil Engineering Purpose, Part 2: Classification Tests*. London: BS1377.
- Broch, E. and Franklin, J. A. (1972). The Point-Load Strength Test. *International Journal of Rock Mechanics and Mining Sciences*. 9(6). pp. 669-693.
- Brown, E. T. ed. (1981). *Rock Characterization Testing & Monitoring – ISRM Suggested Methods*. U.K.: Pergamon Press.
- Cheng, L. and Evett, J. B. (1987). *Soils and Foundations*. 2<sup>nd</sup> edition. Englewood Cliffs, N. J., USA: Prentice-Hall, Inc.
- Chernyshev, S. N. and Dearman, W. R. (1991). *Rock Fractures*. Butterworth, Malaysia: Heinemann Ltd.



- Cheung, C. K., Greenway, D. R. and Massey, J. B. (1988). Direct Shear Testing of a Completely Decomposed Granite. *Proc. 2<sup>nd</sup>. Int. Conf. Geomechanics in Tropical Soils*. Singapore. Pp. 109-118.
- Coop, M. R. (1993). The Behaviour of Granular Soils at Elevated Stress. *Predictive Soil Mechanics*. London: Thomas Telford.
- Daly, R. A., Manger, G. E. and Clark, S. P. (1966). Density of Rocks. In: Clark, S. P. ed. *Handbook of Physical Constants*. Geol. Soc. Am. Mem. Vol. 97. pp.19-26.
- da Pinto, A. and Muralha, J. (1995). Scale Effects in the Determination of Mechanical Properties of Jointed Rock. In: Myer, L. R., Cook, N. G. W., Goodman, R. E. and Tsang, C. F. eds. *Fractured and Jointed Rock Masses*. Balkema, Netherlands. pp. 479 – 485.
- de Toledo, P. E. C. and de Freitas, M. H. (1993). Laboratory Testing and Parameters Controlling The Shear Strength of Filled Rock Joints. *Geotechnique*. Vol 43: 1,1-19.
- de Toledo, P. E. C. and de Freitas, M. H. (1995). The Peak Shear Strength of Filled Joints. *Proceedings of International Symposium on Fractured and Jointed Rock Masses*. Balkema, Rotterdam.
- Dunlap, W.A. (1966). *Deformation Characteristics of Granular Materials Subjected to Rapid, Repetitive Loading*. USA: Texas A&M University. Doctoral thesis.
- Farmer, I. W. and Attewell, P. B. (1973). The Effect of Particle Strength on the Compression of Crushed Aggregate. *Rock Mechanics*. Vol. 5: pp. 237-248.
- Feda, J. (1971). The Effect of Grain Crushing on The Peak Angle of Internal Friction of a Sand. *Proc. 4<sup>th</sup> Conf. On Soil Mechanics*. Budapest. pp. 79-93.
- Feda, J. (2002). Notes on The Effect of Grain Crushing on The Granular Soil Behaviour. *Engineering Geology*. Vol. 63. pp. 93-98.

- Franklin, J. A. and Dusseault, M. B. (1989). *Rock Engineering*. USA: McGraw-Hill.
- Ge, X. (1991). The Study of the Swelling Properties of the Altered Granite by Means of Large Scale Field Tests for Underground Excavations of the Largest Pumped Storage Power Station in China. In: Balasubramaniam *et al.* eds. *Developments in Geotechnical Aspects of Embankments, Excavations and Buried Structures*. Balkema, Netherlands. Pp. 183 – 195.
- Goodman, R. E. (1974). *Methods of Geological Engineering in Discontinuous Rock*. St. Paul: West Publication Company.
- Hardin, B. O. (1985). Crushing of Soil Particles. *Journal of Geotechnical Engineering Div.* ASCE. Vol 111. Part 10. pp. 1177 – 1192.
- Haynes, J.H. (1966). Effect of Repeated Loading on Gravel and Crushed Stone Base Course Materials used in AASHO Road Test. *Joint Research Project*. N. 15. India: Purdue University.
- Holubec, I. and D'Appolonia, E. (1973). Effect of Particle Shape on the Engineering Properties of Granular Soils. *Evaluation of Relative Density and Its Role in Geotechnical Projects Involving Cohesionless Soils, ASTM STP 523*. USA: American Society for Testing and Materials.
- Jafari, M. K., Amini Hosseini, K., Pellet, F., Boulon, M. and Buzzi, O. (2003). Evaluation of Shear Strength of Rock Joints Subjected to Cyclic Loading. *Soil Dynamics and Earthquake Engineering*. Vol. 23. pp. 619-630.
- Kanji, M.A. (1974). Unconventional Laboratory Tests For The Determination of The Shear Strength of Soil-Rock Contacts. *Proceedings of the Congress of the International Society for Rock Mechanics*. Vol. 2: Part A. pp. 241-247.
- Kassim, A. (1996). *Engineering Properties of Undisturbed Highly Weathered Malaysian Granite*. Universiti Teknologi Malaysia: M. Sc. Thesis.

- Kenney, T. C. (1967). The Influence of Mineral Composition on the Residual Strength of Natural Soils. *Geotechnical Conf. on Shear Strength of Natural Soils and Rocks*. Oslo. Vol. 1. pp. 123-129.
- Khan, I. N. and Saran, S. (2005). A Study of The Phenomenon of Soil-Reinforcement Interaction. *The Journal of The Institution of Engineers, Malaysia*. Vol. 66, No. 2. pp. 38 – 45.
- Koerner, R.M. (1970). Effect of Particle Characteristics on Soil Strength. *Journal of the Soil Mechanics and Foundations Division*. Vol. 96. pp. 1221-1234.
- Kutter, H. K. and Rauttenberg, A. (1979). The Residual Shear Strength of Filled Joints in Rocks. *Proceedings of 4<sup>th</sup> Symposium of ISRM*. Montreux: pp. 1:221-227.
- Ladanyi, N. K. and Archambault, G. (1977). Shear Strength and Deformability of Filled Indented Joints. *Proceedings of 1<sup>st</sup> International Symposium on the Geotechnics of Structural Complex Formations*. Capri: pp. 317-326.
- Lama, R. D. (1978). Influence of Clay Filling on Shear Behaviour of Joints. *Proceedings of 3<sup>rd</sup> Congress of International Association of Engineering Geology*. Madrid: Vol. 2. pp 27-34.
- Lama, R. D. and Vutukuri, V. S. (1978). *Handbook on Mechanical Properties of Rocks – Testing Techniques and Results*. Vol. IV. Clasuthal, Germany: Trans Tech Publication.
- Lee, H. S., Park, Y. J. Cho, T. F. and You, K. H. (2001). Influence of Asperity Degradation on the Mechanical Behaviour of Rough Rock Joints Under Cyclic Shear Loading. *International Journal of Rock Mechanics & Mining Sciences*. Vol. 38. pp. 967-980.
- McLean, A.C. and Gribble, C.D. (1979). *Geology for Civil Engineers*. London: George Allen & Unwin (Publishers) Ltd.

- Miller, R. P. (1965). *Engineering Classification and Index Properties for Intact Rock*. University of Illinois: Ph.D. Thesis
- Miura, N., Hidekazu, M. and Yasufuku, N. (1984). Stress-Strain Characteristics of Sand in a Particle-Crushign Region. *Soils and Foundations*. Japanese Soc. of Soil Mechanics and Foundation Engineering. Vol. 24, No. 1. pp 77 – 89.
- Miura, N. and O-Hara, S. (1979). Particle-crushing of a Decomposed Granite Soil Under Shear Stresses. *Soils and Foundations*. Japanese Soc. Of Soil Mechanics and Foundation Engineering. Vol. 19, No. 3. pp 1 – 14.
- Mohd Amin, M. F. and Awang, H. (2002). Compressibility and Young's Modulus of a Filled Joint Under Uniaxial Compression. *Annual Geological Conference*. 26-27 May 2002. Kelantan, Malaysia: Geological Society of Malaysia. pp 323-328.
- Mohd Amin, M. F. and Kassim, A. (1999a). Description and Classification of Filled Joint in Granite- An Approach. *Annual Geological Conference*. Desaru, Johor, Malaysia: Geological Society of Malaysia.
- Mohd Amin, M. F. and Kassim, A. (1999b). Mechanics of Rock Joint Filled With Weak, Granular Material. *Civil and Environmental Enginnering Conference, New Frontiers and Challenges*. 8-12 November 1999. Bangkok, Thailand: pp VII-53 – VII-62.
- Mohd Amin, M. F., Kassim, A. and Mustaffar, M. (2000). *A Systematic Classification of Filled Joint in Granite*. Geotechnique and Transportation Department, Faculty of Civil Engineering, University Technology of Malaysia: RMC Report, Vote 71319.
- Ong, T. S. (2000). *Compressibility, Strength and Stress-Strain Behaviour of Feldspar Mineral Grain Under Uniaxial Load*. B. Eng. Thesis. Universiti of Teknologi Malaysia.

- Onitsuka, K. and Yoshitake, S. (1990). Engineering Properties of Decomposed Granite Soils as Backfill Materials. *Residual Soils in Japan*. Japanese Soc. of Soil Mechanics and Foundation Engineering. pp. 97 – 104.
- Papaliangas, T., Hencher, S. R., Lumsden, A. C. and Manolopoulou, S. (1993). The Effect of Frictional Fill Thickness on the Shear Strength of Rock Discontinuities. *International Journal of Rock Mechanics and Mining Sciences & Geomechanical Abstracts*. Vol. 30, No. 2: pp. 81-91.
- Papaliangas, T., Lumsden, A. C., Hencher, S. R. and Manolopoulou, S. (1990). Shear Strength of Modelled Filled Rock Joints. *Proceedings of International Symposium on Rock Joints*. Balkema, Rotterdam.
- Patton, F. D. (1966). *Multiple Modes of Shear Failure in Rock and Related Materials*. University of Illinois: PhD. Thesis.
- Pereira, J. P. (1990). Mechanics of Filled Discontinuities. *Proceedings of International Conference on Mechanics of Jointed and Faulted Rock*. Balkema, Rotterdam.
- Phien-wej, N., Shrestha, U. B. and Ching. (1991). Strength and Displacements of Model Infilled Rock Joints. *Developments in Geotechnical Aaspects of Embankments, Excavation and Buried Structures*. Balkema, Rotterdam.
- Phien-Wej, N., Shrestha, U. B. and Rantucci, G. (1990). Effect of Infill Thickness on Shear Behaviour of Rock Joints. *Proceedings of International Symposium on Rock Joints*. Loen, Norway: pp. 289-294.
- Pitts, J. (1984). *A Manual Geology for Civil Engineers*. Singapore: World Scientific Publishing. pp. 19-72.
- Price, N. J. (1966). *Fault and Joint Development in Brittle and Semi-Brittle Rock*. UK: Pergamon Press.

- Sinha, U. N. and Singh, B. (2000). Testing of Rock Joints Filled With Gouge Using A Triaxial Apparatus. *International Journal of Rock Mechanics and Mining Sciences*. Vol 37: pp 963-981.
- Tse, R. and Cruden, D. M. (1979). Estimating Joint Roughness Coefficients. *International Journal of Rock Mechanics and Mining Sciences & Geomechanical Abstracts*. Vol. 16: pp. 303-307.
- Tulinov, R. and Molokov, L. (1971). Role on Joint Filling Material in Shear Strength of Rocks. *ISRM Symposium*. Nancy: Paper II-24.
- Waltham, T. (2002). *Foundation of Engineering Geology*. 2<sup>nd</sup> Ed. London, U.K.: Spon Press.
- Wan Mohd Kamil, W. A. (2002). *Laboratory study on the physical model of a filled joint under compression*. M. Sc. Thesis. Universiti Teknologi Malaysia.
- Wittke, W. (1990). Joint Hydraulics. *Mechanics of Jointed and Faulted Rock. Proceedings of The International Conference*. Balkema, Rotterdam. 59
- Yusof, M. F. (2003). *Engineering Characteristics of Granitic Residual Soils in Peninsular of Malaysia*. M. Sc. Thesis. Universiti Teknologi Malaysia.
- Yuzo, O. and Ryunoshin, Y. (1995). Laboratory Investigation of Scale Effect in Mechanical Behaviour of Rock Joint. In: Myer, L. R., Cook, N. G. W., Goodman, R. E. and Tsang, C. F. eds. *Fractured and Jointed Rock Masses*. Balkema, Netherlands. pp. 465 – 470